

Master Thesis in Geosciences

The Lillehammer Submarine Fan Complex

Maren Kristin Møllerup Skaten



UNIVERSITY OF OSLO

FACULTY OF MATHEMATICS AND NATURAL SCIENCES

The Lillehammer Submarine Fan Complex

Maren Kristin Møllerup Skaten



Master Thesis in Geosciences
Discipline: Petroleum Geology and Geophysics
Department of Geosciences
Faculty of Mathematics and Natural Sciences

UNIVERSITY OF OSLO

13.01.2006

© Maren Kristin Møllerup Skaten, 2006

Tutor(s): Johan Petter Nystuen and Leif Jacob Gelius

This work is published digitally through DUO – Digitale Utgivelser ved UiO

<http://www.duo.uio.no>

It is also catalogued in BIBSYS (<http://www.bibsys.no/english>)

All rights reserved. No part of this publication may be reproduced or transmitted, in any form or by any means, without permission.

Abstract

The Lillehammer Submarine Fan Complex is a mixed mud/sand rich turbidite fan system. The fan complex was deposited in the Neoproterozoic Hedmark rift basin from west towards east extending at least 50 km from the basin margin.

A detailed sedimentary study of outcrops in the Lillehammer area is performed with the aim of analyzing the depositional environment as an analogue for subsurface turbidite systems. Seven sedimentary logs cover a nearly 1000 meter thick stratigraphic section. Seven facies have been organized into seven facies associations, representing architectural elements including basin plain-thin bedded turbidites, basin plain-hemipelagic shale, lobe, lobe-channel, basin floor channel infill, major channel and channel-levee. The Lillehammer Submarine Fan Complex represents two or three fan systems, separated by hemipelagic black shale or thick unit of homogenous shale that may indicate rise in relative sea level. The overall system is progradational and represents an outer and middle to inner fan environment. The main factors controlling the development of the Lillehammer Submarine Fan Complex are thought to be tectonic activity at the basin margin and sediment influx.

Comparison of the Lillehammer Submarine Fan Complex with the Upper Cretaceous fans in the Vøring Basin reveals a good geometrical resemblance despite large differences in sandstone petrography and clay matrix content. The petrographic more impure and clay-rich sandstones of the Lillehammer Submarine Fan Complex, as compared with those in the Vøring Basin, is interpreted to be related to differences in provenance and basin structure.

Synthetic seismograms were performed for a 400 meter thick logged section to discuss the differences in seismic resolution under 1500 meter of overload and 3500 meter of overload. Only half of the seismic events are shown in the deepest model compared to the shallow model. Reflections associated with most interfaces are recognizable, but difficult to distinguish from each other. The shallow model reveals good seismic resolution of two fans separated by a thick layer of homogenous shale. The same model under a thicker overload does not have the same obvious trends, but is recognizable when you know what to expect.

Acknowledgement

First I would like to thank my primary supervisor, Johan Petter Nystuen, for his excellent guiding, help and support in the field and during the process of writing this master thesis. Thanks also to my supervisor Leif Jacob Gelius for help and support of the modelling and writing of the synthetic seismic chapter.

I would also like to thank Isabelle Lecomte for support with the Norsar 2D Ray Modelling program, Ivar Midtkandal for helpful advice in Adobe Illustrator, Knut Bjørlykke for valuable remarks and discussions, Øyvind Marcussen for help with velocity parameters and Ane Rasmussen for revising the reference list.

I thank my family and friends for all support during my study. A special thanks to my friends at the Department of Geosciences, University of Oslo for courage and support during the master!

Oslo, January 2006

Maren Kristin Møllerup Skaten

Content

1 Introduction	1
2 Methods and data	2
2.1 Introduction	2
2.2 Fieldwork and interpretation	2
2.3 Modelling	5
3 Geological framework	6
3.1 Introduction- Geological framework	6
3.2 Structural evolution of the Hedmark Basin	7
3.3 Stratigraphy and sedimentary history of the Hedmark Basin	9
3.4 The Brøttum Formation	14
4 Sediment gravity flow processes	15
4.1 Introduction- Sediment gravity flow processes	15
4.2 Classification of sediment gravity flows	16
4.3.1 Turbidity currents	18
4.3.2 Deposits of turbidity currents	21
4.4.1 Debris flows	23
4.4.2 Deposits of debris flows	24
4.5 Deep-water massive sand and sandstone	25
5 Petrography	26
5.1 Introduction	26
5.2 Description- sandstone lithology	26
5.3 Description- siltstone and shale lithology	27
5.4 Interpretation	28
6 Facies	30
6.1 Introduction- Facies	30
6.2 Facies recorded in the Brøttum Formation	31
6.3 Facies A1: Black shale	32
6.4 Facies B: Siltstone	33
6.4.1 Facies B1: Structureless siltstone	33
6.4.2 Facies B2: Laminated siltstone	36
6.5 Facies C: Sandstone	38
6.5.1 Facies C1: Normal graded sandstone	38
6.5.2 Facies C2: Inverse graded sandstone	43
6.5.3 Facies C3: Non graded sandstone	43
6.6 Shale clasts in facies C1 and C3 sandstone beds- Discussion	45

7 Facies associations	48
7.1 Introduction- Facies associations	48
7.2 Facies association 1: Basin plain	49
7.2.1 Facies association 1.1: Basin plain- thin bedded turbidites	49
7.2.2 Facies association 1.2:Basin plain- hemipelagic shale	52
7.3 Facies association 2: Depositional lobe	53
7.3.1 Facies association 2.1: Lobe	53
7.3.2 Facies association 2.2 Lobe-channel	55
7.4 Facies association 3.1: Basin floor channel infill	57
7.5 Facies association 4.1: Major channel	58
7.6 Facies association 5.1: Channel-levee	61
8 Depositional environment	64
8.1 Introduction	64
8.2 Classification systems	64
8.3 Model of the Lillehammer Submarine Fan Complex	67
8.4 Comparison with the Cretaceous Vøring Basin- On the Mid Norway Shelf	73
9 Seismic modelling	78
9.1 Introduction	78
9.2 Petrophysical data	78
9.3 Methods	87
9.4 Synthetic seismograms	88
10 Discussion	97
11 Conclusion	99
References	100
Appendix	109

1 Introduction

Exploration of deep-marine turbidite deposits and basic understanding of deep-marine sedimentary systems have become increasingly important in the petroleum industry during the last ten years. To improve the understanding of the large-scale system-fans, it is important to get a correct picture of stacking pattern of architectural elements, sandstone thickness, sand/shale ratio, geometry and dimension of sandstone and shale units, and how these elements vary in different basin settings and provenance. Although individual depositional systems tend to be highly variable in geometry, size and internal character from one basin to another, the same main architectural elements can commonly be recognized. Thus, field analogues are assumed to provide information about subsurface deep-marine turbidite reservoirs, particularly about the architectural variability that should be taken care of in reservoir modeling.

The present study is built on the Neoproterozoic Brøttum Formation in the Lillehammer area, the Lillehammer Submarine Fan Complex. The deep-marine system represents a well defined prograding fan complex deposited laterally from west towards east in the Hedmark rift basin.

The aim of the study was to gather field data on facies, bed thicknesses and architecture to analyze facies associations, depositional environment and controlling factors of the system. Synthetic seismograms were generated based on one of the logged sections in order to study how seismic signals would appear in a rock succession of the same stratigraphy and lithological composition under different burial depths.

2 Methods and data

2.1 Introduction

The thesis is based on fieldwork from the Brøttum Formation in the Lillehammer area, where sections are logged and interpreted in terms of facies, facies association and depositional environment. One of the logged sections are further evaluated in synthetic seismic made in the Norsar 2D Ray Modelling program.

2.2 Fieldwork and interpretation

Fieldwork was carried out during one month in May-June 2005 in the Lillehammer area. Description of facies, facies association and depositional environment is based on logged outcrops from 7 different road sections (figure 2.2.1). The outcrops are generally good, but particularly the Dampsagvegen section is partly covered with vegetation. The Brøttum Formation is folded and the beds are mainly vertical in the logged sections where the youngest beds are facing south-east. However, in the top of the Messenlivegen and the Åsmarkvegen 3 section the beds tend to flat out. The sections are located in the southern flank of a large anticlinal structure. Dip and strike measurements are shown on map in figure 2.2.2.

Characteristic features of each lithological unit are measured; these are bed thickness, grain size, grading, sedimentary structures, palaeocurrent direction, colour, geometry of beds and strike/dip. Due to easily recognizable facies groups in the logged sections Marcov-chain analysis has been assessed to be unnecessary in interpreting the facies associations.

Rock samples of the Brøttum Formation were collected from different types of facies and grain size lithologies. The samples where used to make thin sections and a brief outline is given of major petrographic properties of the three main lithologies.

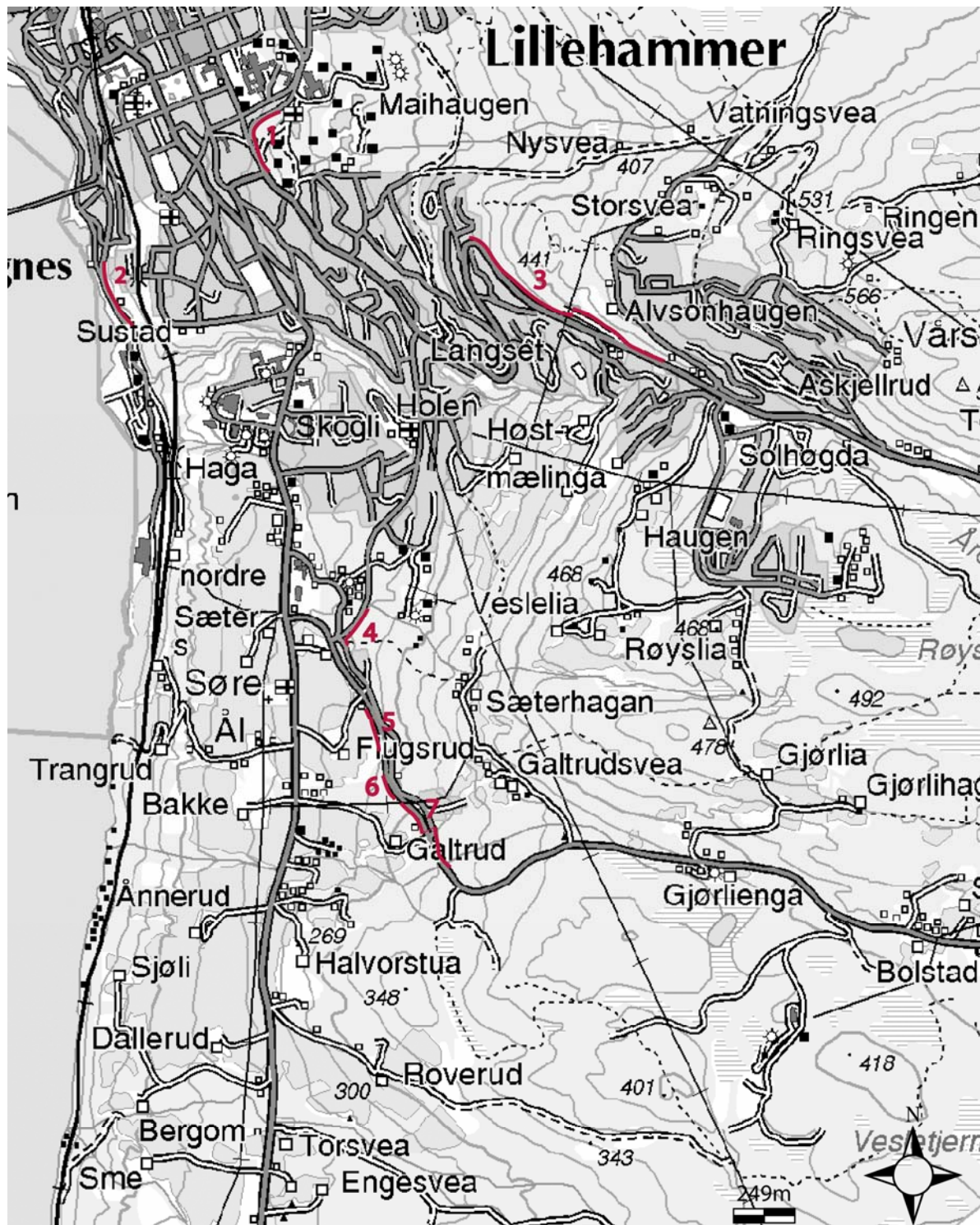


Figure 2.2.1 Logged sections in the Lillehammer area. Nr. 1= Maihaugvegen section, Nr. 2 = Dampsagvegen section, Nr. 3 = Messenlivegen section, Nr. 4 = Fredrik Colletts veg section, Nr. 5 = Åsmarkvegen 1 section, Nr. 6 = Åsmarkvegen 2 section and Nr. 7 = Åsmarkvegen 3 section.

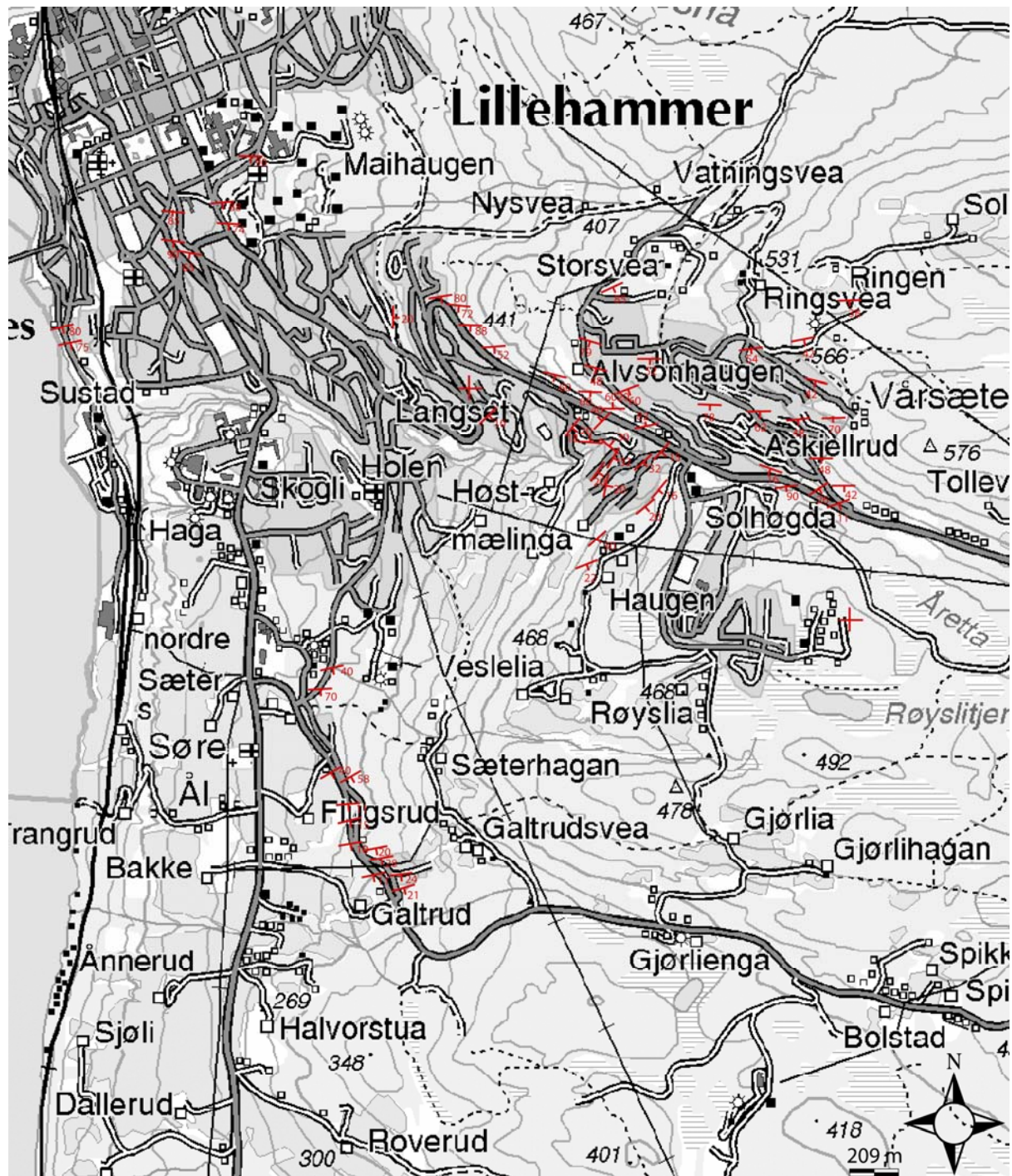


Figure 2.2.2 Measured strike and dip in the Lillehammer area. The average strike is 83° . The dip varies about 80° in the northern parts. Northern dips are generally larger than for the measured dips in the southern part.

2.3 Modelling

Norsar 2D Ray Modelling were used to make synthetic seismic from a nearly 400 meter long logged succession in the Messenlivegen locality (figure 2.2.1).

The aim of the modelling is to study the seismic resolution of a turbidite system in two different cases where it is buried under 1500 meter and 3500 meter of overload, respectively. Parameters required for a seismic modelling is found from general porosity curves published in M.R. Gilles (1997), Diagenesis: A quantitative perspective, and p-velocity-depth curves based on studies from the Mesozoic and Cenozoic sediments from the Norwegian shelf (Storvoll *et al.* 2005). S-velocities are calculated form a standard ratio from p-velocities.

Two geometrical models with respective properties were built and ray tracing was preformed with normal incidence path with respect to selected interface. The synthetic seismograms where made with a Berlage wavelet puls.

Seismic resolution and differences are discussed in chapter 9.

3 Geological framework

3.1 Introduction - Geological framework

The Brøttum Formation represents one of several formations in the Hedmark Group deposited during Neoproterozoic time in the Hedmark Basin, previously called the Sparagmite Basin (Kumpulainen & Nystuen, 1985).

The term ‘sparagmite’ was introduced by Esmark (1829) for the dominant, coarse-grained feldspatic sandstone type in the bedrock of eastern South Norway. The word is derived from the Greek word *sparagma*, meaning fragment. The old term is now mostly applied only for the outcrop area for these rocks in southern Norway and Härjedalen in Sweden, the Sparagmite Region (Bockelie & Nystuen, 1985), figure 3.1.1.

The Hedmark Group mainly occurs in the Osen-Røa Nappe Complex in the Lower Allochthon of the Caledonian thrust sheets in the Sparagmite Region of southeastern Norway (figure 3.1.1). The allochthonous Neoproterozoic sedimentary succession is here preserved in a graben structure bounded by several N-S running major faults of the Rendalen, Osen-Slemdalen, Engerdalen and other faults. The subsidence of the tectonostratigraphic record probably occurred in Permian time when the Oslo Rift was formed (Nystuen, 1987).

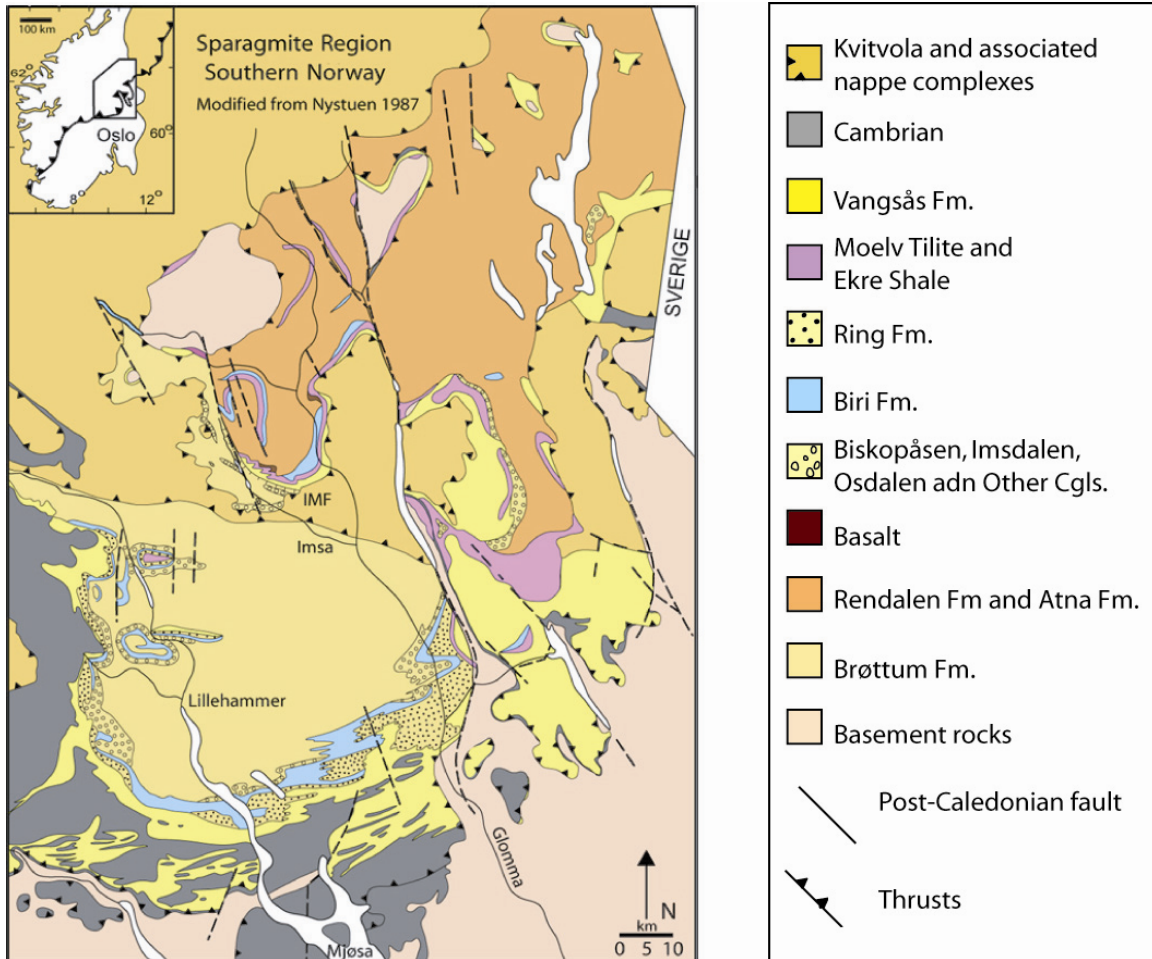


Figure 3.1.1 Geological map of the Sparagmite Region, Southern Norway. Modified from Nystuen (1987).

3.2 Structural evolution of the Hedmark Basin

The Hedmark Basin developed as a rift basin on the northwestern margin of Baltica in late Riphean time about 750 Ma (e.g. Gale & Roberts, 1974; Gee, 1975; Kumpulainen & Nystuen, 1985; Siedlecka *et al.*, 2004). The evolution of the northwestern Baltoscandian basins is believed to be related to the break-up of the supercontinent Rodinia (e.g. Siedlecka *et al.*, 2004) prior to the development of the Iapetus Ocean. New data indicate that Baltica was geographically inverted during the Neoproterozoic time (Torsvik *et al.*, 1991; Harz & Torsvik, 2002) relative to its orientation during the Caledonian orogeny, which indicates that Baltica was facing the Siberian plate during the break-up. The northwestern margin of Neoproterozoic Baltica was strongly tectonically deformed

during the compression and extensional stages of the Caledonian development in late Silurian time (Bockelie & Nystuen, 1985).

The amount of Caledonian displacement was debated for decades, and the parautochthonous basin model was for a long time the accepted model for explaining the tectonic position of the basin in southern Norway. Schiøtz (1902) suggested that the “sparagmite succession” was bounded during depositional time by the Rendalen, Osen and Engerdalen faults in the east (Figure 3.1.1) and some presumed faults west of the basin. This model was later further evolved by Holtedahl (1920, 1921), Skjeseth (1963), Ramberg & Englund (1969), Englund (1969), Bjørlykke (1974) and Bjørlykke *et al.* (1976). However, Oftedahl (1943) suggested an overthrust model for the thick basin-derived Hedmark Group, calculating the amount of displacement to have been at least in the order of 140 kilometers. An allochthonous position for the succession was supported by later stratigraphic and structural geological studies that demonstrated that the Hedmark Group was thrust over younger Cambrian strata (Nystuen, 1981, 1983; Sæther & Nystuen, 1981; Bockelie & Nystuen, 1985). This implies that the Hedmark Basin succession had been displaced out of its original location at a site north-west from its present position. The proposed distance of tectonic transport varies from some few tens of kilometers to 200-400 km (Gee, 1975, 1978; Nystuen, 1981, 1982), but analyses of structural restoration suggest that it has been transported at least 130-140 km relative to the autochthonous Lower Cambrian beds at the nappe front (Nystuen, 1981; Morley, 1986). Figure 3.2.1 illustrates a reconstructed position of the Hedmark Basin, assuming a Caledonian translation of 230 km for the southern basin margin (Kumpulainen & Nystuen, 1985).

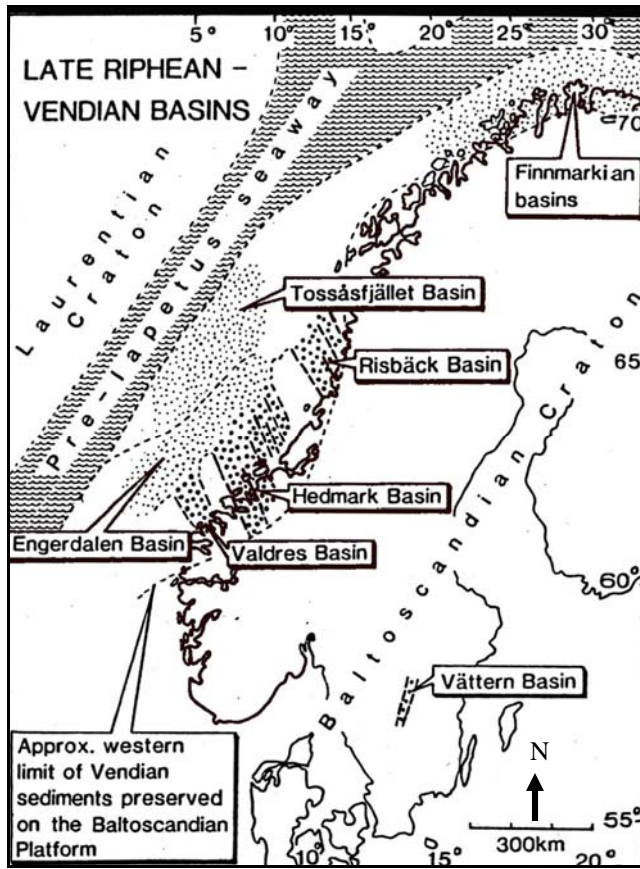


Figure 3.2.1 Paleogeographic reconstructions of the Baltoscandian basins. The Hedmark Basin as a graben basin NW of present location of the outcrop area of the Hedmark Group From Nystuen (1987).

As a result, the southeastern parts of the Scandinavian Caledonides comprises a stack of southeastward –transported thrust nappes, and are classified in the following order, as: Parautochthon, Lower Allochthon, Middle Allochthon, Upper Allochthon and Uppermost Allochthon (Roberts & Gee, 1985). The allochthonous hypothesis has been reviewed and discussed by Nystuen (1981).

3.3 Stratigraphy and sedimentary history of the Hedmark Basin

The sedimentary successions of late Proterozoic age in Caledonian thrust sheets in South Norway comprise the Hedmark, Engerdalen, Valdres and the Melsenn Groups, in addition to other less well defined rock successions (Bockelie & Nystuen, 1985; Kumpulainen & Nystuen, 1985). The rock successions are located in several nappe

complexes, as the Osen-Røa Nappe Complex including the Synfjell Nappe, and the Valdres and Kvivola Nappe Complexes (Nystuen & Siedlecka, 1988). The Valdres and Kvivola thrust sheets are located in the Middle Allochthon whereas the Osen-Røa Nappe Complex together with the Synfjell Nappe is located within the Lower Allochthon.

The Hedmark Group, located in the Osen-Røa Nappe Complex, comprises formations deposited in a western and an eastern depositional province (figure 3.3.1), separated by the Imsdalen Fault which is suggested to be of synsedimentary origin (Sæther & Nystuen, 1981).

The Hedmark Basin is interpreted to have been a wide rift basin complex with 200-300 km in the east-west direction, and the axis running NNW-SSE in the length of some hundreds of kilometers. The Hedmark Group comprises a total thickness of at least 4000 meters of sediments and is overlain by approximately 2000 meter of younger Cambrian-Silurian strata (Bockelie & Nystuen, 1985). Recent studies (Stalsberg 2004) suggest that the total thickness of the Hedmark Group may have been in the order of 6000 meters or more.

The structural-sedimentary evolution of the Hedmark Basin can be divided into seven different stages (Nystuen 1987). (1) Pre-rift sedimentation and initial formation of the main graben; (2) Rifting and basin expansion; (3) Rifting, volcanism and basin submergence; (4) Rifting, sub-basin formation and emergence; (5) Late rifting and glaciation; (6) Late rifting, waning sub-basin activity and regional subsidence; (7) Post-rifting and regional subsidence. These stages are reflected in the sedimentary successions of the Hedmark Basin. It is suggested that these evolutionary stages formed during three major thermal-mechanical phases of one rift episode.

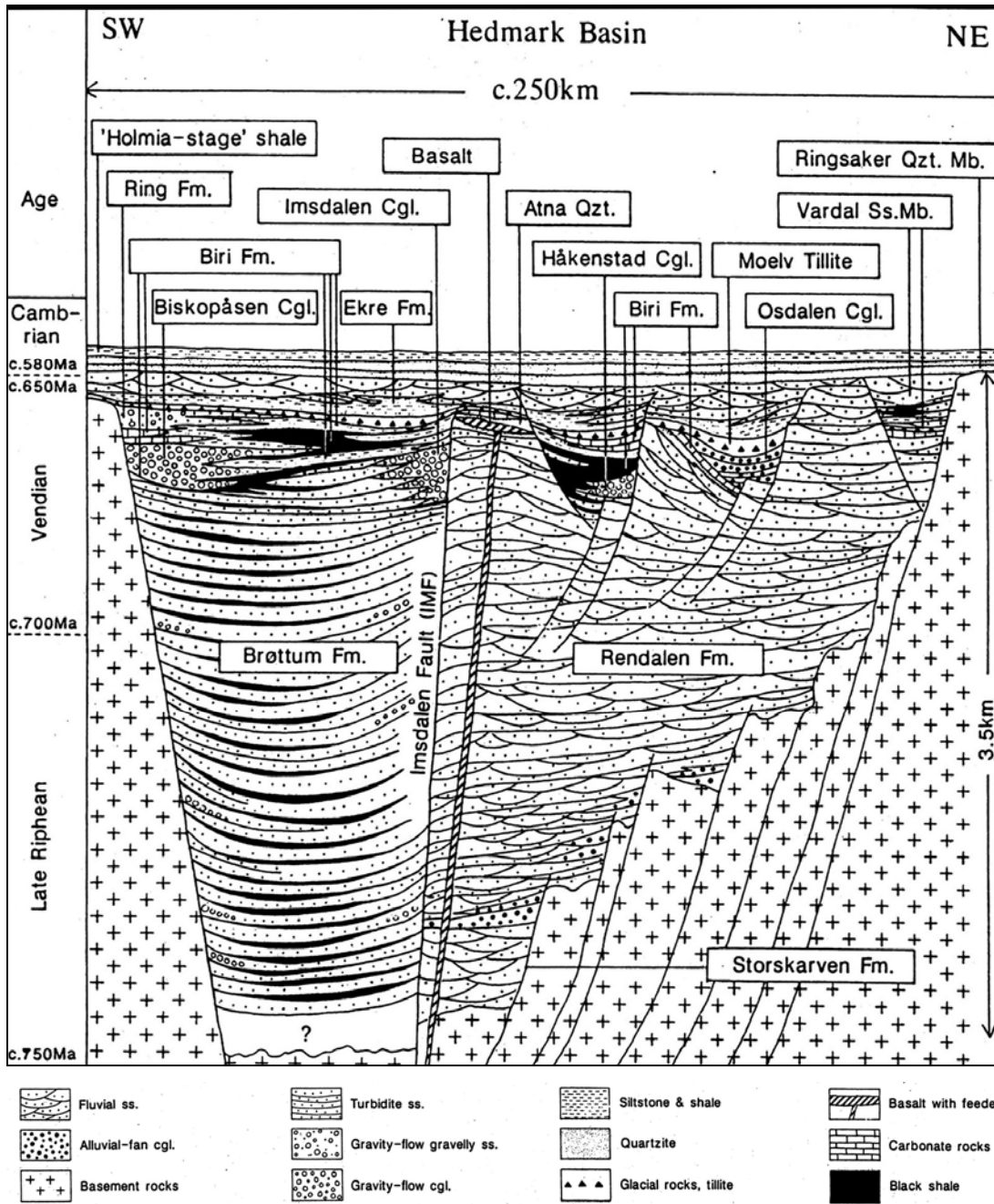


Figure 3.3.1 A schematic SW-NE section through the Hedmark Basin illustrating the western and eastern depositional provinces. From Nystuen (1987).

The lithostratigraphy of the Hedmark Group in the western depositional province of the Hedmark Basin is shown in fig 3.3.2.

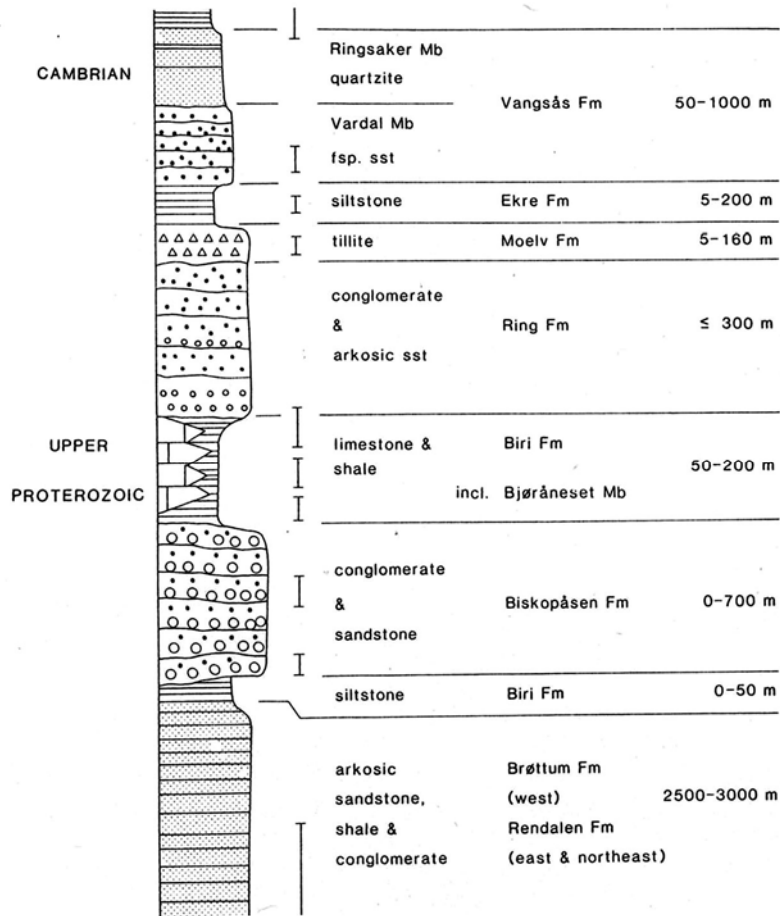


Figure 3.3.2 Stratigraphic section through the Hedmark Group in the Mjøsa area. From Vidal & Nystuen (1990a).

A formal lithostratigraphy of the Late Proterozoic to Cambrian succession in the Hedmark Basin has been developed during the 1960's to 1980's (Skjeseth, 1963; Bjørlykke *et al.*, 1967; Nystuen, 1967, 1981, 1982).

The fluvial Rendalen Formation in the eastern part of the basin and the shallow-marine Atna Formation in the north is equivalent to the deep marine Brøttum Formation in the western depositional province. In the northern parts there are also present sediments that predate the Rendalen Formation, this is the fluvial Storskarven Formation, interpreted as representing a prerift stage of the Hedmark Basin (Nystuen, 1987). The Atna Formation in the eastern province is a transgressive shallow marine quartzite (Nystuen, 1982). The peak rifting period of the Hedmark Basin is expressed by tholeiitic basalt flows present

beneath the Moelv Tillite, probably close to the stratigraphic position of the Atna Formation (Sæther & Nystuen, 1981).

The Brøttum Formation is the main depositional unit in the western depositional province. The marine turbidite succession is succeeded by the Biskopåsen Formation that forms several submarine conglomerate fans (Nystuen, 1987; Vidal & Nystuen, 1990a; Holme, 2002). The Biri Formation is represented in both depositional provinces and reflects a marine transgression with black shale and carbonate rich sediments. A regressive fan-delta induced by renewed faulting in the late synrift stage is represented by the Ring Formation. The coarse-grained sediments preserved in this formation are interpreted to have formed by submarine gravity flow deposits (Nystuen, 1987; Kunz, 2002).

The Moelv Tillite overlies a regional erosional unconformity and comprises submarine and subglacial till and marine debris flow deposits from the Varangerian glaciation. The Ekre Formation succeeds conformably the upper laminated part of the Moelv Tillite. It is interpreted to be a postglacial marine deposit (Vidal & Nystuen 1990a). The Vangsås Formation is the youngest unit in the Hedmark Group and includes the lower Vardal Sandstone Member and the transgressive shallow marine Ringsaker Quartzite Member. The formation represents a late rift phase and the following thermal subsidence in late Vendian to early Cambrian times (Vidal & Nystuen, 1990b).

The Cambro-Silurian succession is introduced with a minor unconformity on top of the Ringsaker Quartzite Member. The uppermost member of the Hedmark Group is overlain by grayish green shale containing macro- and microfossils of the Lower Cambrian 'Holmia stage' (Skjeseth, 1963; Vidal, 1981; Vidal & Nystuen, 1990b).

3.4 The Brøttum Formation

The at least 4000 meters thick Brøttum Formation (Stalsberg 2004) in the western depositional province (figure 3.1.1 and 3.3.1) is thought to be the oldest unit in the Hedmark Group. It represents a sand rich submarine fan system deposited by turbidity currents that covers at least 6000 km². The climate during the deposition was probably warm as the Brøttum formation is succeeded by carbonates, and the high amount of sandstones within the formation suggests a humid climate.

In the northern district (the upper part of the formation) the formation is characterized by coarse-grained sandstones, some cross bedded and conglomerates (Stalsberg 2004; Stalsberg & Nystuen, 2004). In the lower part of the formation, in the Lillehammer area, the formation consist of alternating dark grey sandstones and dark grey to black siltstones and shales, with some conglomerates. Graded beds are common with a gradual transition from sand to the overlying silt and shales.

The finer sediments and absence of cross bedded sandstones indicates a deeper water environment than in the northern parts (Bjørlykke *et al.*, 1967; Englund, 1972).

It is suggested that the basin received detritus both from the west and the east during the deposition of the Brøttum Formation (Englund, 1972).

Acritarchs of early Vendian age recorded from the Brøttum Formation in the Maihugvegen section in Lillehammer show that a marine environment prevailed in the depositional basin (Vidal, 1981; Vidal & Nystuen, 1990a). Further, the thickness of the formation and its relative homogeneous character implies a relatively stable depositional environment (Englund, 1966).

4 Sediment gravity flow processes

4.1 Introduction- Sediment gravity flow processes

Sediment gravity flow processes comprise a range of processes that erode, transport and deposit sediments in deepwater environments (fig 4.1.1). These are important factors in construction of submarine fans comprising canyons, channel-levee systems and distal depositional lobes (Normark, 1970; Normark & Piper, 1972; Mutti, 1992). A sediment gravity flow can be defined as a mixture of fluid and sediment in which the fluid is driven by the grains acting on gravity (Middleton & Hampton, 1973).

Processes	Characteristics	Deposits
Resedimentation		
Rock fall		Olistolith Avalanche deposit
Creep		Creep deposit
Slide		Slide
Slump		Slump
Debris flow		Debrisite
Fluidized flow		Grain flow
Liquified flow		Fluidized flow Liquified flow
Turbidity current (high/low density)		Turbidite (coarse, medium and fine grained)
Semi-permanent bottom currents		
Internal tides and waves		Normal current deposit
Canyon currents		
Bottom currents		Contourite
Deep surface currents		
Surface currents and pelagic settling		
Flocculation		Pelagite
Pelletization		Hemipelagite
Authigenic processes		
FeMn nodules, lamination, pavements and umbers		Chemogenic deposit

Decrease in concentration
Increase in state of internal disaggregation

Figure 4.1.1 Sediment gravity flow processes and their deposits working in the deep sea environment. Modified from Stow 1994.

The term sediment gravity flow was first introduced by Middleton & Hampton (1973) but is also referred to as gravity flows, sediment flows, density flows and mass flows by several other authors.

The only currents that can transport large volumes of coarse-grained material over relatively long distances from an original shallow environment to a deeper water environment are turbidity currents and debris flows (e.g. Stow & Johansson, 2000).

4.2 Classification of sediment gravity flows

Different parameters have been used by different authors to classify sediment gravity processes: (1) Sediment concentration, Bagnold (1962); (2) rheology, Dott (1963); (3) fluid turbulence, Sanders (1965); (4) sediment-support mechanisms, Middleton & Hampton (1973); (5) combination of rheology and sediment-support mechanism, Lowe (1982), and (6) combination of physical flow properties and sediment-support mechanism, Mulder & Alexander (2001). This has led to inconsistent terminology of the same process which causes problems in understanding these flows and their respective deposits.

Sediment concentration by volume directly influences the other factors, but there are no specific threshold values for the various types of sediment gravity flows. This is caused by differences in grain size and concentration of clay minerals in the sediments that have an effect on the sediment concentration (Shanmugam, 1996). Classifications based on sediment-support mechanism (matrix strength, dispersive grain pressure, escaping pore fluid, and fluid turbulence) also induce contradictions when more than one support mechanism can operate simultaneously in one specific flow. Transport mechanism will also only represent the sediment under transport, and at present there are no criteria to recognize transport mechanism from the ancient depositional record. Furthermore, the flow state designating the flows as laminar or turbulent can change during the flow due to a change in sediment concentration or gradient of the basin slope. As a result, classification based on flow state alone will give the same ambiguous outcome. The only parameter that may cause

least unclear classification when defining the various types of flows is rheology, this result in two broad groups of flows.

A sediment gravity flow can either be Newtonian or non-Newtonian. Figure 4.2.1 illustrates that the Newtonian fluid has a linear stress-strain relationship under deformation. A non-Newtonian fluid is called Bingham plastic (Shanmugam, 1997), in this situation there is a critical value of shear stress to be crossed before any deformation can take place, after that there is linear deformation. A common classification scheme is to use both rheology and sediment-support mechanism.

Sediment gravity flows indicating a Newtonian rheology is the *turbidity currents* (e.g. Dott, 1963; Lowe, 1979; Nardin *et al.*, 1979; Shanmugam & Moiola, 1995; Shanmugam, 2000; Gani, 2004) that are characteristic as regard their turbulent state of flow. A flow with non-Newtonian rheology is named *plastic flows* or *debris flows with a laminar type of flow* (Dott, 1963; Johnson, 1970; Lowe, 1979; Shanmugam, 2000).

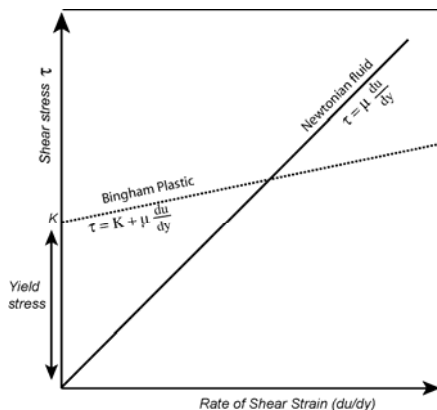


Figure 4.2.1 Classification of sediment gravity flows based on rheology. K =Yield stress, μ = Dynamic viscosity, τ = Shear stress and du/dy = strain rate. From Shanmugam, 1997.

The rheology of a sediment-water mixture in a flow is controlled mainly by sediment concentration and to a lesser extent by grain size and the physical and chemical properties of transported particles (Pierson & Costa, 1987). The boundary between Newtonian and plastic flows (debris flow) occurs at about 20-25% by volume concentration (Middleton, 1967, 1993).

Different qualifications have been used to classify and define different processes or products; as a result the same process can be named differently according to different authors (cf. Shanmugam, 1996), hence, the uses of terms like gravity flow, density flow, and high-density flow for the same process. Several authors have tried to review these problems (e.g. Shanmugam, 1997, 2000; Mulder & Alexander, 2001; Dasgupta, 2003; Gani, 2004).

However, the main problem is sediment gravity flows that contain characteristics matching both turbidity currents and debris flows. These flows have been given a variety of names like high density currents, traction carpet, sandy debris flow, slurry flows and concentrated density flows (e.g. Shanmugam, 2000; Mulder & Alexander, 2001; Kneller & Buckee, 2000). Classifying sediment gravity flows into one category is further made difficult due to flow transformation sometime during its life cycle.

Only the end members turbidity currents and debris flow will be further discussed in the text below.

4.3.1 Turbidity currents

With emphasis on sediment-support mechanism and rheology, the turbidity current is defined as a sediment-gravity flow with Newtonian rheology and turbulent state from which deposition occurs through unhindered settling of individual grains from suspension (Shanmugam, 1997, 2000).

There are several definitions of turbidity currents based on other criteria (e.g. Postma et al., 1988; Kneller, 1995), but the widely accepted definition is based on flows in which the sediment is supported mainly by the upward component of fluid turbulence (Sanders, 1965; Middleton & Hampton, 1973; Lowe, 1979; Simpson, 1997). Fluid turbulence produces a frictional flow with no cohesiveness and is mainly sustained by friction developed at the boundary between the flow and underlying basin floor and ambient fluid (Middleton & Hampton, 1973; Stow & Johansson, 2000). Moreover, only rheology and sediment-support

mechanism is preserved in the deposits and can be used in interpretation of depositional processes.

For Newtonian fluids, the criterion for initiation of turbulence is the *Reynolds Number*, Re , greater than 2000, describing the ratio between inertia and viscous forces.

Bagnold (1962) demonstrated that turbulent, gravity-driven currents could be maintained only for very-low-volume concentrations ($C < 9\%$), this separates the turbidity flows *sensu stricto* from other sediment gravity flows. Accurate application of the Bagnold limit may be difficult in the field and at present, it is only possible to interpret that deposits are from flows in which fluid turbulence was the dominant particle-support mechanism, (turbidity currents *sensu lato*) based on grain size and sedimentary structures (Mulder & Alexander, 2001).

A turbidite current can be initiated of several mechanisms (Normark & Piper, 1991) including sediment failures, flow transformation, storms, earthquakes and pyroclastic flows at river mouths.

Mulder & Alexander (2001) classified sediment gravity flows according to their dominant grain-support mechanism (fig 4.3.1). According to this classification there are three types of turbidity currents; Surge type, surge-like and quasi-steady depending on their flow behavior. There are a continuum between concentrated density flows and turbidity flows, as a result of progressive entrainment and dilution of a denser flow the proportion of total particle support by fluid turbulence will increase. Four different types of flows are illustrating the processes that are neither cohesive nor turbulent and falling between the end members creating terminological confusion in the literature.

Following Mulder & Alexander (2001) *surge-like turbidity currents* have a short duration, and consist of a well defined head, body and tail, surges are very short-duration flows and consist of an isolated flow head. These flows are most probably triggered by flow transformation through erosion and acceleration from a flow type with a higher sediment concentration.

Quasi-steady *hyperpycnal turbidity currents* form where a river discharges into a basin having a lower bulk density than the hyperpycnal effluent. These flows have a dominating flow body and can last from hours to months following the basin floor, and are therefore called quasi-steady.

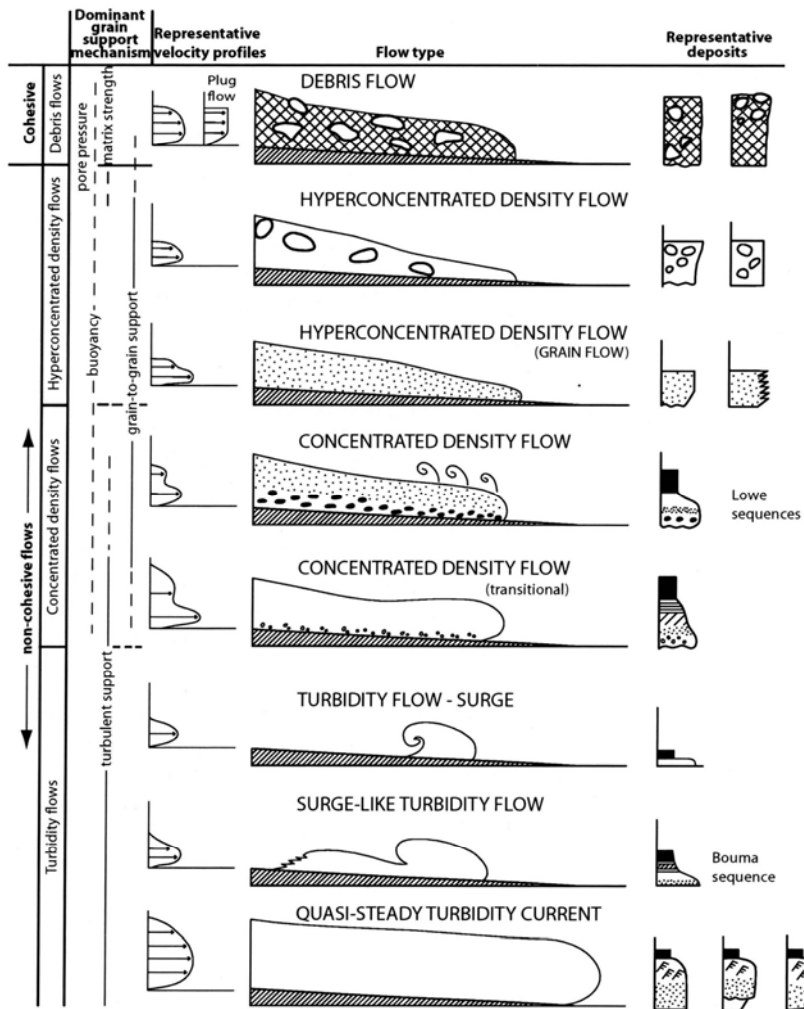


Figure 4.3.1 Classification scheme for sediment gravity flows, illustrating dominant grain support, velocity profiles, and representative deposits. Modified from Mulder & Alexander, 2001.

Turbidity currents are frictional flows which mean they have no matrix strength. Their behavior is directly related to the proportion of water and sediments, which can vary in time and space during the run-out. A single turbidity current goes through different stages and will erode during a waxing period (Vallance & Scott, 1997) and deposit when the current is no longer accelerating (Hsu, 1989). From experiments, it is expected that erosion can take

place at the head at the same time as deposition takes place from the body or tail of the same current (Middleton & Hampton, 1976).

The sediment concentration and particle size of turbidity currents influence the characteristic of the deposits, this has led to the concepts of high- and low-density turbidity currents (Lowe, 1982).

Lowe (1982) named flows with high sediment concentration and high competence to transport coarse sand and gravel 'high-density turbidity currents'. These sequences are also called Lowe sequences. Low-density turbidity currents in which the sediment is supported mainly by the upward component of fluid turbulence tend to have low competence and cannot transport coarse sand and gravel over any significant distances except on steep slopes (Mulder & Alexander, 2001).

Other authors have used the same term, but dissimilar definitions. Kuene (1950) defined the high-density turbidity current based on rapid deposition and flow density, whereas Postma *et al.* (1988) based the definition on the driving force. This has led to a situation where there are no standard criteria to recognize high-density turbidity currents.

Shanmugam (1996) claimed that the basal layer (basal traction carpet) of a high-density turbidity current are plastic and laminar, not turbidity currents *sensu* Middleton & Hampton (1973), and reclassified the deposits as 'sandy debris flows'. However, Sandy debris flows are frictional while debris flows have internal shear strength. Mulder and Alexander (2001) made an attempt to overcome the confusion and reinterpreted the coarse deposits as a product of 'hyperconcentrated density flows'.

4.3.2 Deposits of turbidity currents

Deposits of turbidity currents are called turbidites. Depositions from turbidity currents occur through sediment fallout from suspension (Kuenen & Migliorini, 1950; Dott, 1963). As a result, grains with the highest fall velocities will settle first.

According to Dott (1963) is normal grading (upward decline in grain size) the most reliable criterion to interpret fluidal rheology and suspension deposition of turbidity currents. If

normal grading appears together with features like floating clasts it will indicate a cohesive flow and thereby not turbidity current.

Kuenen & Migliorini (1950) was the first to propose normal grading as a characteristic property of turbidite sandstone beds, workers as Bouma (1962) adopted this concept later; Harms & Fahnstock (1965) proposed normal grading and massive, structureless bedding. Kneller (1995) made a time-space matrix for turbidity currents and their deposits illustrating changes in space (accumulative, uniform, depletive) and time (steady, waxing). According to this scheme a turbidite current can theoretically deposit normal grading, inverse grading and massive sands. This can explain many variations observed in turbidite deposits.

The Bouma sequence (Bouma, 1962) was established to describe deposits of turbidity currents (fig 4.3.2), this has later become one of the most widely used and abused terminology for field description of sands and sandstones interpreted to be of deep-water origin. The traditional interpretation is that the entire sequence is deposited from a single turbidite flow (Bouma, 1962; Walker, 1965; Mutti & Ricci Lucchi, 1972; Middleton & Hampton, 1973, 1976). However, many authors have pointed out that the complete sequence, or parts of the Bouma Sequence, can be explained by other processes than true turbidity currents (e.g. Hsu, 1989; Shanmugam, 1997). In addition, the Bouma Sequence was made primarily for sandy turbidity currents. Stow & Shanmugam (1980) reclassify fine-grained *low-density turbidites* where the lowermost division T₀ correspond to Bouma T_c division, and the uppermost division T₈ correspond to the pelagic deposition of Bouma T_e division. Lowe (1982) made a corresponding classification scheme for coarse-grained *high-density turbidites* ranging from R₁-R₃ and S₁-S₃ (Lowe Sequences). The S₃ division corresponds to the Bouma T_a division.

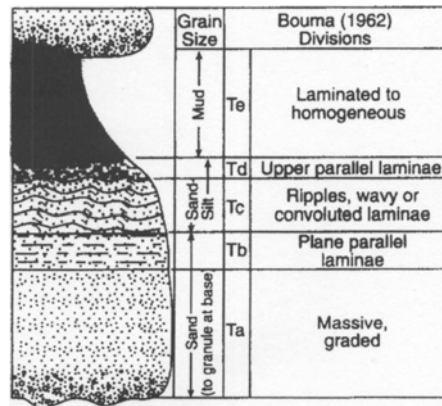


Figure 4.3.2 The Bouma Sequence illustrating the Ta, Tb, Tc, Td and Te divisions. From Shanmugam 1997.

4.4.1 Debris flows

A debris flow is defined as a sediment-gravity flow with Bingham plastic rheology (Johnson, 1970) and laminar state (Johnson, 1970; Carter, 1975) from which deposition occurs through freezing *en masse* (Lowe, 1982). Sediment-support mechanism includes matrix strength, dispersive pressure and buoyant lift (Middleton & Hampton, 1973; Middleton, 1993).

Sediment concentration is generally high (Coussot and Meunier, 1996). Due to multiple sediment-support mechanisms, debris flows are capable to transport sediment particles of all sizes.

Cohesion between the sediment particles provides matrix strength in the flow (Nardin et al., 1979; Lowe, 1982), which resists penetration of ambient water and makes the flow stay together as a massive plug. As a result, the debris flow can develop hydroplaning (Mohrig et al., 1999). Thin layers of water may be capped under the water-sediment mixture and reduce the resistance between the flow and the sea-bottom. This leads to little erosion on the floor (Pickering et al., 1989) and triggers the flow to travel several hundred of kilometers at high speed (Gee et al., 1999). The long run-out-distance of debris flows has been explained by a two-phase flow with a relatively impermeable upper layer overpressuring a lower, less cohesive layer (Gee et al., 1999). Figure 4.3.1 illustrates the

flow body of an ideal debris flow showing a massive plug compared to turbidite currents with a defined flow head.

A flow transformation to other less denser flows may occur due to mixing and dilution at the head entrainment at the upper body or by passage through a hydraulic jump (Hampton, 1972).

4.4.2 Deposits of debris flow

The main process for debris-flow deposition is freezing or *en masse* deposition of the flow or parts of the flow (Lowe, 1982; Postma, 1986). When the force related to the shear resistance of the flow becomes equal to the force due to gravity, the flow stops. This is cohesive freezing.

The yield strength and low water content allows morphological features such as levees, flow snouts and surface features to be preserved after the flow stops resulting in close accordance between thickness of the deposits and the thickness of the flow during motion. Any changes occur after deposition as a result of erosion, consolidation and compaction (Hiscott & James, 1985). *En masse* deposition explains the large variation in grain size, particle shape and composition in debris flows and why the deposits are extremely varied and chaotic.

Debris-flow deposits are characteristically very poorly sorted and may have few signs of internal structures. Fabrics that develop can have a-axis patterns that are parallel to flow or random, with imbrications that dip either up or down flow (Harms, 1974).

4.5 Deep-water massive sand and sandstone

Very thick bedded (>1m), essentially structureless sand and sandstone, are commonly found associated with other deep-water sediments like turbidites. Several authors have reviewed the deep-water massive sand problem and concluded that the processes of flow initiation, transport and deposition are varied and complex (e.g. Kneller, 1995; Stow & Johansson, 2000).

The classical hypothesis for explaining structureless sandstone deposits was a high-density turbidity current (Lowe, 1982). This was widely accepted for a long time, but was later challenged by the hypothesis of a sandy debris-flow mechanism (Shanmugam, 1996). Other hypothesis proposed is post-depositional diapirism and intrusions (Surlyk & Noe-Nygaard, 1998).

One important characteristic of massive sand and sandstone beds is the presence of shale clasts. These vary considerably in terms of size, shape, abundance and position in the bed. Johansson & Stow (1995) recognized eleven different types each of which yields information about the sandstone bed like post-depositional liquification, high energy erosion or low energy erosion.

Other features of these sands are water-escape structures of various types that may yield critical information. A number of processes may also operate following primary deposition and destroy the original nature of originally structured deposits. These include erosion, bioturbation, remobilization and liquefaction.

A series of single massive sandstone beds can be amalgamated into a massive sandstone unit or body. Such units comprise, typically, from two to eight beds (Stow & Johansson, 2000). The boundaries between beds vary from distinct and sharp to completely gradational amalgamation contacts. In addition, the basal contact may be slightly too deeply erosive into the underlying sands or muds.

Stow and Johansson (2000) observed some diagnostic features for massive sand beds. The thickest massive sand beds tend to show a more uniform mean grain size and relatively small clast than beds under 2,5m. This is interpreted as a result of bed amalgamation.

From previous work on ancient successions, there are at least three main interpretations of the depositional settings in which massive sand and sandstone occur. These are: (1) the slope-apron fully-lobe system (Surlyk, 1987), (2) the delta-fed ramp system (Heller & Dickinson, 1985) and (3) the sand-rich submarine fan system (e.g. Armstrong *et al.*, 1987; Carman & Young, 1981; Link & Nilsen, 1980). The key controls on their occurrence are tectonic activity and clean sand supply, whereas sea-level is less critical (Johansson & Stow, 1998)

5 Petrography

5.1 Introduction

Thin sections have been prepared from 11 samples of different representative lithologies from the Brøttum Formation in Lillehammer. Table of position in logs representing the samples are included in the Appendix. Though the petrography of the Brøttum Formation has not been defined as part of this master thesis, a brief outline is given in this chapter of major petrographic properties of the three main lithologies.

5.2 Description - sandstone lithology

Eight samples were collected from sandstone beds. The samples represent different grain size distribution, from fine-grained to coarse-grained sandstone. All sandstone samples are quartz- and feldspar-rich with little clay content between framework grains. The clay mineral matrix is estimated to comprise 2-5 % of the total composition; however, in some of the most clay-rich sandstone samples the matrix content may be as high as 10-15 %. Though the clay mineral content is low, clay minerals tend to envelope many of the clastic framework minerals. The sorting of the framework minerals quartz and feldspar is generally poor to very poor. The most coarse-grained sandstone samples are dominated by angular to sub-rounded quartz and feldspar grains, whereas medium to fine-grained sandstone samples are characterized more by angular to rounded and angular to well-rounded clastic grain population.

Quartz comprises about 80 to 90 % of the clastic framework minerals. The quartz grains include monocrystalline as well as polycrystalline types. Some quartz grains display undulating extinction in polarized light, whereas other grains display distinct extinction. Such unstrained and strained quartz grains occur side by side in the same sample and thus suggest that the strained and unstrained properties are inherited

from the hinterland source rocks, and not a property obtained during Caledonian thrusting and folding. Angular grains may be highly irregular in shape with several corners and embayments, or they can be wedge-shaped. Most quartz grains appear to have preserved original clastic grain morphology. Post-depositional dissolution along grain-to-grain contacts and precipitation of secondary quartz overgrowth has taken place to a moderate extent.

The *feldspar* content is estimated to be in the order of 15 to 20% of the framework mineral population. The feldspars comprise plagioclase with albite twins and alkali feldspar with microcline twins and perthites of various types. The feldspar grains may be totally fresh and unaltered, whereas others, also in the same thin section, can be strongly altered to a mixture of sericite and calcite.

Other observed clastic minerals are thin muscovite flakes, zircons, sphene, and opaque heavy minerals. The phyllosilicate matrix consists of a mixture of colourless clay minerals and minerals with a greenish colour.

Figure 5.2.1 illustrate examples of sandstone sampled from the Brøttum Formation. The grains are angular to well rounded, thus indicating sediment derived both from reworked sand or sandstone and first-generation debris from crystalline granitic bedrock.

5.3 Description - siltstone and shale lithology

Three of the eleven thin section samples are from siltstone and shale lithologies. The siltstone sample is poorly sorted with a certain amount of very fine sand grains, but dominated by the silt fraction (figure 5.2). The grains are angular to subrounded. Other minerals observed in the silt lithology are small clastic muscovite flakes. Some silt laminae up to a thickness of some few millimetres are graded with lower erosional contact to underlying shale with minute flame structures at the base of the graded silt laminae, illustrated in figure 5.3.1.

The thin sections of the black shale reveal a black homogeneous matrix of clay fraction and organic matter (amorphous bitumen or coal) without any silt and sand grains. Calcite occurs as minute calcite grains scattered throughout the shale and cube-shaped pyrite crystals are common.

5.4 Interpretation

The clastic mineral content of the sandstone beds demonstrate that the clastic debris has been derived from crystalline source rocks of granitic composition, as granites, granodiorites or quartz diorites, or/and granitic gneisses. The unstrained quartz grains are likely sourced from undeformed igneous rocks, whereas the highly strained quartz grains may represent a deformed source rock, as gneiss. The predominance of angular to subrounded clastic framework grains indicates that most of the sand population of the Brøttum Formation was deposited as first-generation debris with relative short total distance of transport. However, the presence of some well-rounded quartz grains in the fine sand fraction suggests that older sand or sandstone deposits with texturally mature sand grains also have been reworked and contributed to the Brøttum Formation sand debris.

There is a distinct difference between mudstone formed as siltstone and those formed as black shale with a very high content of organic matter. This latter lithology is interpreted to be represents real hemipelagic mud, originated from the settling of fine clay particles through the water column, together with organic debris produced from pelagic organisms, algae and bacteria. Graded thin laminae of silt are interpreted as formed from highly diluted turbidity currents, illustrated as the Td division in figure 4.3.2.

The moderate quartz dissolution and cementation of the sandstone may be due to the clay coatings of the mineral grains. It is known from much younger marine sandstone formations that clay coating reduce the amount of quartz cementation during deep burial (Storvoll & Bjørlykke, 2004). The Brøttum Formation in the Lillehammer area is supposed to have been subjected to temperatures of about 300°C with formation of albite and chlorite (Morad, 1988).

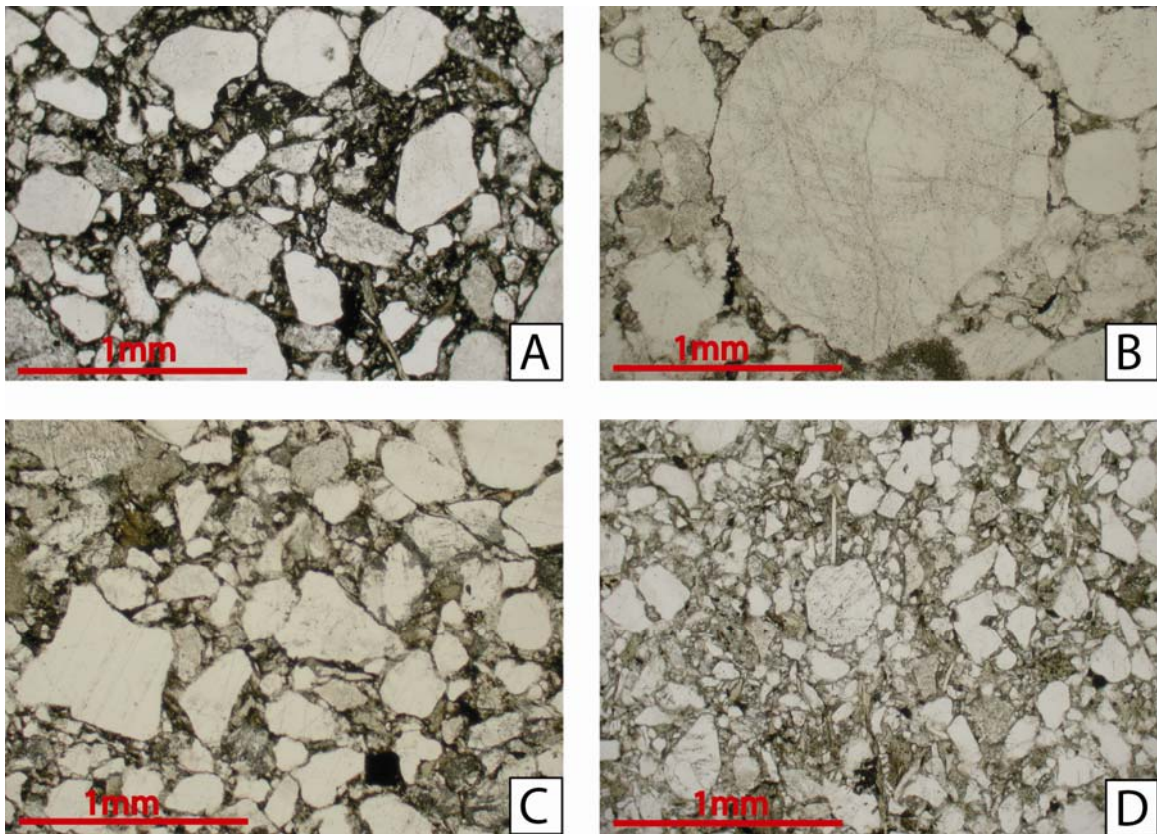


Figure 5.2.1 A representative assembly of sandstone lithologies from the Brøttum Formation. (A) Coarse sandstone at 328 meter, Messenlivegen. (B) Gravel (mps=5mm) at 31,5 meter, Fredrik Collets veg. (C) Medium grained sandstone at 17 meter, Fredrik Collets veg. (D) Fine/very-fine sandstone at 389,5 meter, Messenlivegen.

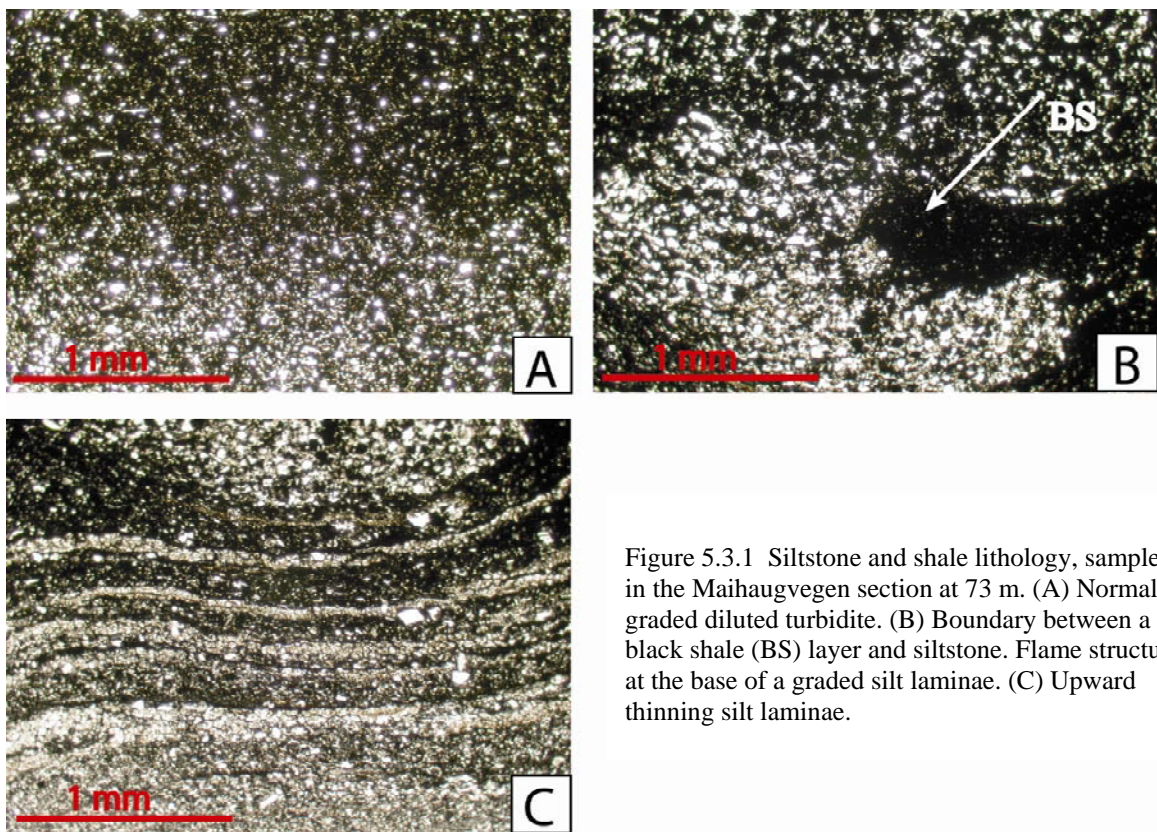


Figure 5.3.1 Siltstone and shale lithology, sampled in the Maihaugvegen section at 73 m. (A) Normal graded diluted turbidite. (B) Boundary between a black shale (BS) layer and siltstone. Flame structure at the base of a graded silt laminae. (C) Upward thinning silt laminae.

6 Facies

6.1 Introduction- Facies

The sedimentary facies analysis is based on approximately 1000 m of logged strata from 5 localities, comprising 7 sections. The logged sections are presented in Appendix 4 and respective locations are illustrated in figure 2.2.1. Three major classes of facies are identified, facies A: Black Shale, facies B: Siltstone, and facies C: Sandstone. Class B and C are further subdivided into six lithofacies based on descriptive sedimentological criteria, illustrated in table 6.1.

A sedimentary facies is defined as a lithological unit that differs macroscopically from adjacent lithologies. Ideally it should be a distinctive rock that formed under certain conditions of sedimentation, reflecting a particular process, set of conditions, or depositional environment (Reading & Levell, 1996). The sedimentary facies are defined on the basis of bed thickness and geometry, grain-size, colour, texture, fossils and sedimentary structures. Units with similar characteristics are classified as one facies, and these are considered as the basic building blocks in a sedimentary succession (Gressly, 1838; Walker, 1979).

Table 6.1 Facies recorded from the Brøttum Formation, Lillehammer. HDT=High density (concentration) turbidity current, LDT= Low density (concentration) turbidity current.

Code		Facies	Interpretation
A	A1	<i>Black Shale</i>	<i>Hemipelagic deposition</i>
B	B1	<i>Structureless siltstone</i>	<i>Dilute suspension from gravity current</i>
	B2	<i>Laminated Siltstone</i>	<i>Thin LDT</i>
C	C1	<i>Normal graded sandstone</i>	<i>LDT to HDT</i>
	C2	<i>Inverse graded sandstone</i>	<i>Thin LDT with increasing grain sizes</i>
	C3	<i>Non graded sandstone</i>	<i>Rapid deposition from LDT to HDT</i>
	C4	<i>Muddy sandstone</i>	<i>Mud rich HDT or debris flow</i>

6.2 Facies recorded in the Brøttum Formation

Facies distribution in the Brøttum Formation is illustrated in figure 6.2.1 and 6.2.2, table of facies distribution in localities are also included in appendix 2. The five localities comprise the seven sections in Maihaugvegen, Dampsagvegen, Messenlivegen, Fredrik Colletts veg, Åsmarkvegen 1, Åsmarkvegen 2 and Åsmarkvegen 3.

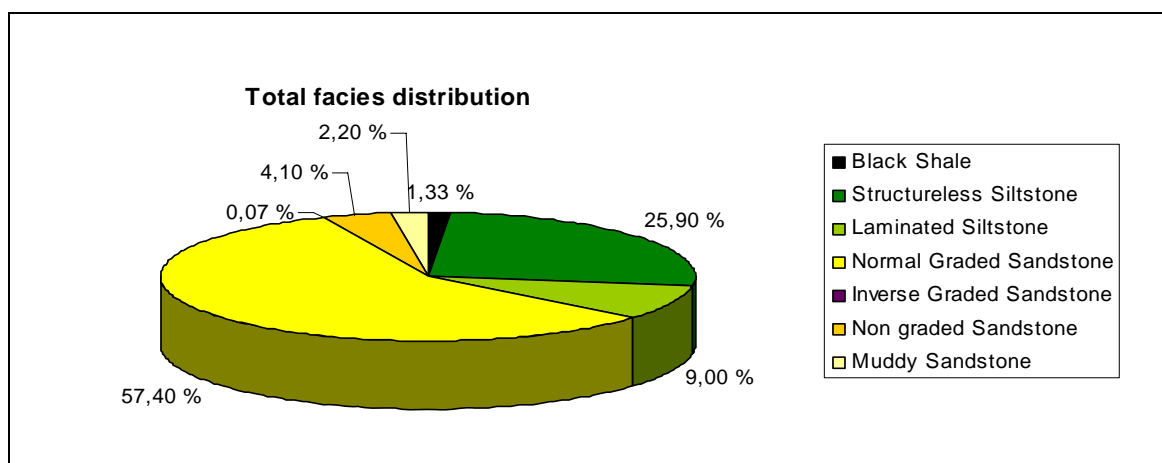


Figure 6.2.1 Total facies distribution in all logged sections.

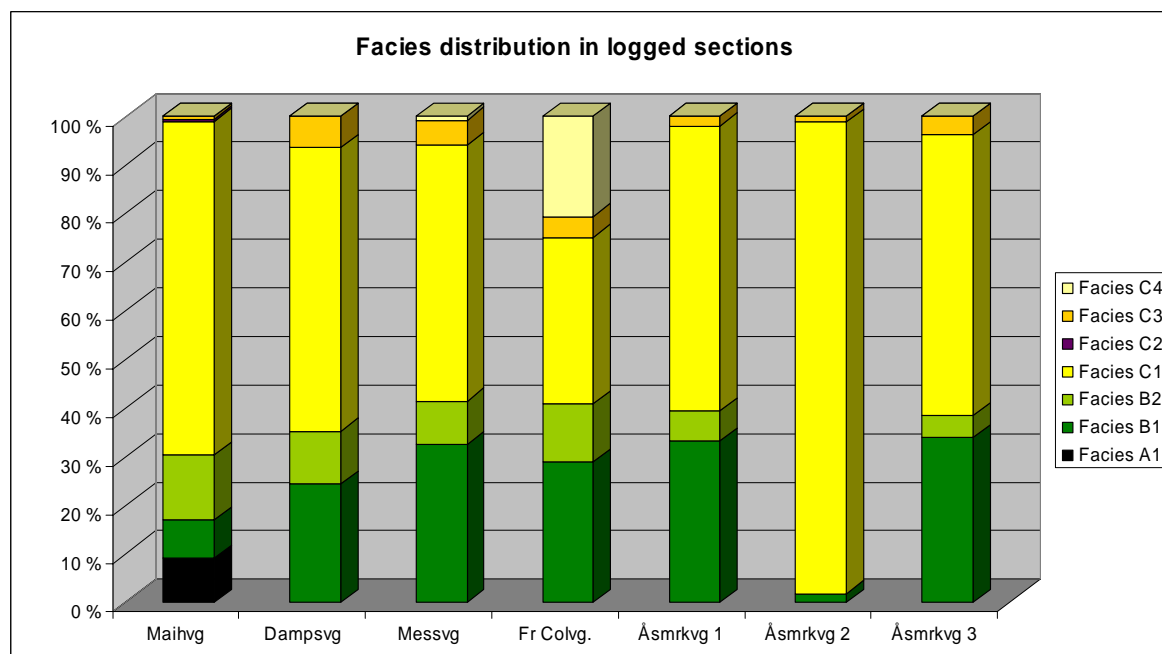


Figure 6.2.2 Facies distribution in different logged sections. Facies A1 = Black shale, Facies B1= Structureless silt, Facies B2 = Laminated silt, Facies C1 = Normal graded sandstone, Facies C2 = Inverse graded sandstone, Facies C3 = Non graded sandstone and Facies C4 = Muddy sandstone. Abbreviations are: Maih. vg. = Maihaugvegen, Damps.vg. = Dampsagvegen, Mess.vg. = Messenlivegen, Fr. Col.vg. = Fredrik Collettsveg, Åsmrk. vg. = Åsmarkvegen.

6.3 Facies A1: Black shale

Description

Black shale facies is recorded in the localities Maihaugvegen and Messenlivegen and makes up just a little percent of the total lithology. These very dark shale units range in thickness from 5,5 meter in association with thick layers of silt and to a couple of cm draping thin normal graded sand-siltstone beds. The facies is characterized by its very fine grain size completely dominated by clay fraction and differs from grey shale by its black stroke as a result of high organic carbon content (>1%). The upper boundary towards the overlaying normal graded and reverse graded sandstone is sharp, while the lower boundary is either sharp or transitional from silt and sand. The upper boundary may be exposed to erosion, though without any clear erosional relief. In the Maihaugvegen location the facies occurs as thick depositional units bounded by thin, normal graded sandstone beds and laminated silt. The outcrop of black shale is in this locality characterized by a concoidal fractured surface, testifying to the homogeneous and massive texture and composition of the shale unit. Within the thickest layers there is a variation in organic carbon content resulting in some areas with a distinct black colour. Pyrite is frequently occurring in both the black shale and adjacent laminae and beds of siltstone.

Interpretation

The black shale facies represents hemipelagic sediments comprising both biogenic and terrigenous components. Biogenic material is produced *in situ* in the overlying water column. Fine-grained terrigenous material is brought out in the deep sea by freshwater plumes from rivers, and wind-blown dust and suspended sediment. In the absence of bottom currents or sediment gravity flows these particles settle vertically under the influence of gravity. Black shales are interpreted to be a result of deposition during low current activity resulting in a pure hemipelagic deposit. Additionally, the finest portions of turbidity currents are in some cases stripped off at density discontinuities within the water column and create very dilute suspension currents. The finest material will settle very slowly as a hemipelagic suspension together with other hemipelagic material brought out in the deep water. The thin beds of black shale recorded in the Messenlivegen are interpreted to be part of the much diluted tail of turbidity currents together with other hemipelagic fallout. The main arguments for interpreting facies A1 as a dominantly hemipelagic deposition are the lack of turbidite

sandstone or siltstone layers and indistinct bedding surfaces, criteria for identifying hemipelagic shale according to Krenmayr (1996).

The pyrite probably formed very early in the bottom sediments when sulphur bacteria produced H₂S by reducing sulphate ions in the sea water with concomitant precipitation of iron sulphide. The formation of FeS₂ implies an anoxic water situation, caused by the consumption of oxygen during breakdown of organic matter settling through the water column. Considerable amounts of pyrite in the black shale facies indicate a very low sedimentation rate over a longer time period.

The black shale facies corresponds to the T_e facies described by Bouma (1962) representing the uppermost interval in the Bouma Sequence. The hemipelagic interval has later been further subdivided by Piper (1978) and Stow & Shanmugam (1980). The equivalent divisions of these classification schemes are E₂-E₃ (Piper 1978) and T₆-T₇ (Stow & Shanmugam 1980). See chapter 6.4.1 for illustration.

6.4 Facies B: Siltstone

Siltstone facies makes up 34,9 % of the total recorded lithology in the Brøttum Formation in the Lillehammer road sections. The facies includes thin to thick packages of silt-dominated beds, both structureless and laminated. Laminae with small pyrite crystals and thin fine-grained sandstone lenses are common in association with both facies B1 and B2.

6.4.1 Facies B1: Structureless siltstone

Description

Facies B1, structureless siltstone, is common in all localities. The beds typically range in thickness from 2 meters to 2 cm, but may be up to 24 meters, as recorded in the Messenlivegen section.

The facies occur in depositional units between units of normal graded sandstone and in association with thick layers of laminated siltstone, facies B2. The upper boundary of the

structureless siltstone units is normally lithologically sharp in contact with overlying sandstone. The siltstone units are occasionally eroded below overlying sandstone beds. This may result in that siltstone beds pinch out when capped under an erosive sandstone body. The lower boundary is texturally sharp or transitional from normal graded sandstone, or the silt has filled up the accommodation space above an uneven surface.

Fine-grained sandstone sheets and lenticular beds represented by facies C1 and C3, together with pyrite laminae are observed in structureless siltstone at various frequencies. Thin and disrupted sandstone lenses of medium sized grains (figure 6.4.1 A) associated with facies B are recorded in the Messenlivegen and Fredrik Colletts veg. One thick package of siltstone representing facies B1 may comprise variation within the fraction fine silt to coarse silt, thus forming bed sets of structureless silt. The grain size sorting in single beds are characterised as good. The structureless siltstone has a light grey to dark grey colour. Lateral variations are hard to recognize due to limited outcrops. This is valid for all facies interpreted in the Lillehammer area.

Interpretation

The thick structureless siltstone beds are interpreted to be deposited by suspended fallout from diluted low density turbidity current or a residual product of a waning high density turbidity current which lost its capacity to carry sediments (Lowe, 1982; Hiscott, 1994). Extreme flow dilution of a turbidity current as a result of reversing buoyancy and flow lofting of the upper part of the flow (Sparks *et al.*, 1993) may lead to very slow deposition of the finest fraction resulting in thick packages of structureless mudstones (Stow & Wetzel, 1990).

Siltstone that appears to be structureless may have been deposited too quickly to have developed lamination. Another topic in structureless siltstone is whether the facies may be faintly laminated, but as a result of poor quality of outcrops the siltstone beds appear structureless.

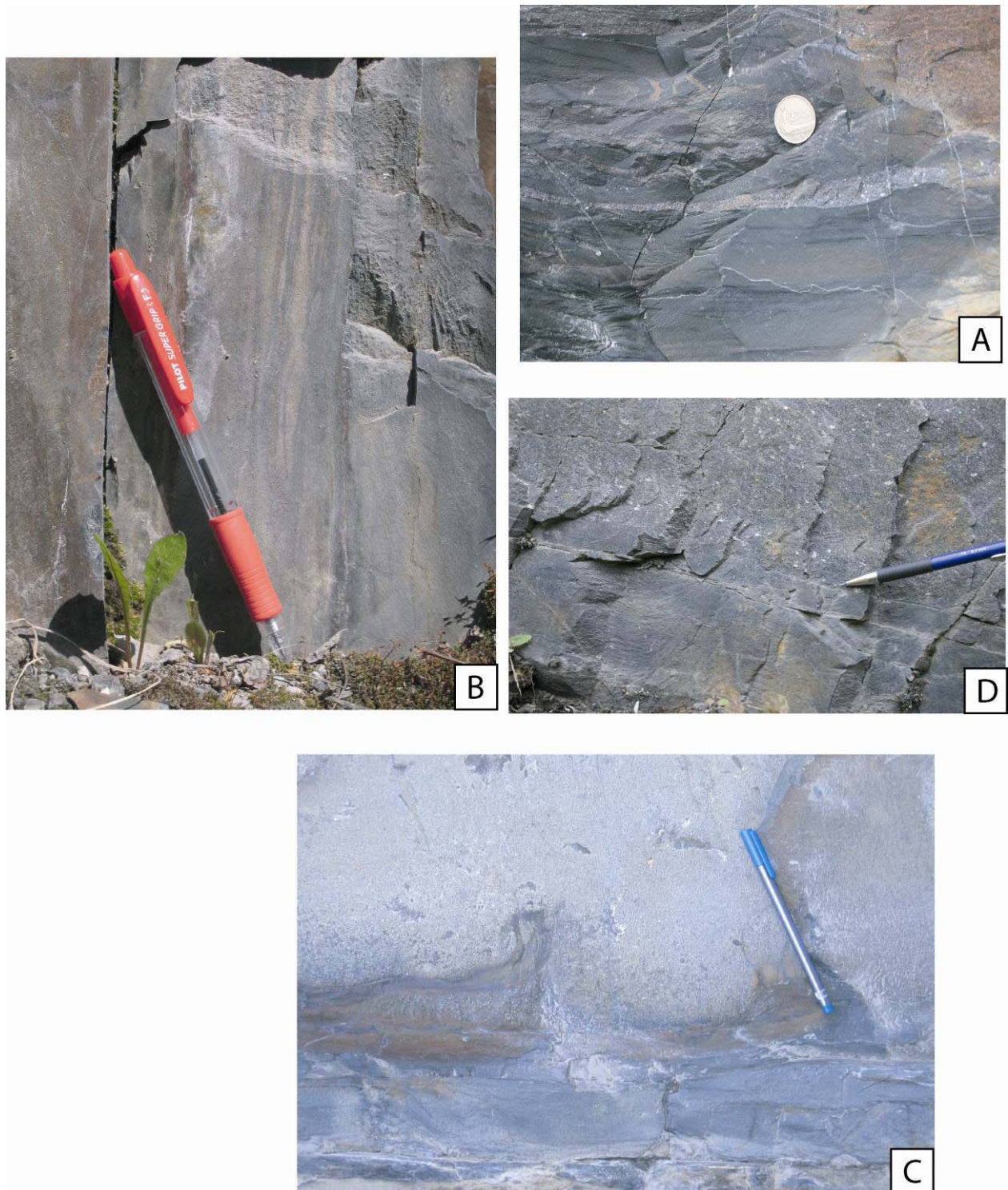


Figure 6.4.1 Sedimentary structures observed in the Brøttum Formation: A) Thin sandstone lenses, Messenlivegen, B) Laminated sandstone, Maiahaugvegen, C) flame structures, Maihaugvegen and D) amalgamated surfaces, Åsmarkvegen 2.

Thin lenses of coarse-grained siltstone and fine-grained sandstone in association with structureless siltstone are also interpreted to be deposits of a distal diluted sheet-like turbidite or depositional lobe. The lenses may also have been formed from the reworking and redeposition from bottom currents. Presence of pyrite in some of the siltstone beds indicates that anoxic bottom water may have existed, at least during some time periods.

Muddy turbidites have been subdivided into three subdivisions numbered E1 to E3 (Piper, 1978) and further into nine subdivisions, from T0 to T8 by Stow & Shanmugam (1980). The corresponding divisions of Bouma (1962), Piper (1978) and Stow & Shanmugam (1980) are illustrated in figure 6.4.2. According to these classification schemes facies B1 will be equivalent to subdivision T₄-T₅ (Stow & Shanmugam, 1980) and E₁ (Piper, 1978) and the Td interval of an ideal Bouma Sequence (Bouma, 1962).

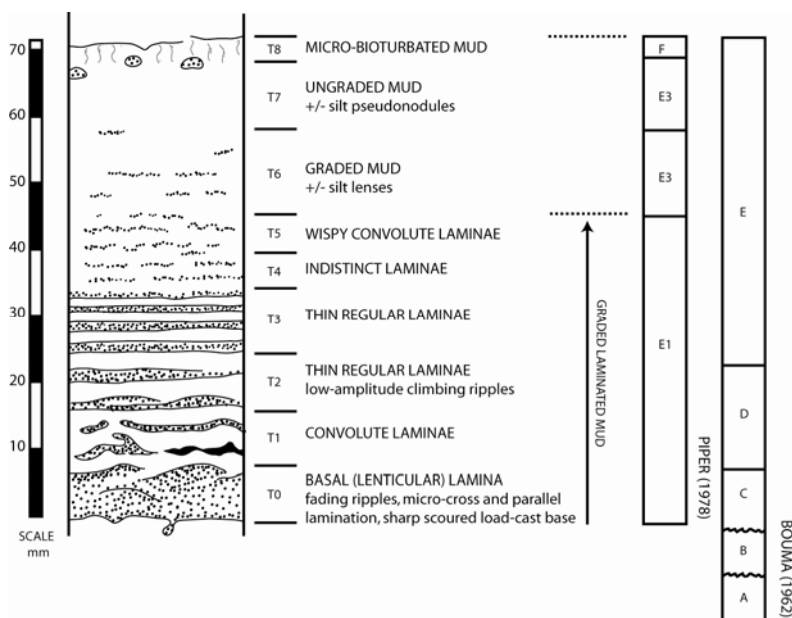


Figure 6.4.2. Standard sequence of structure in an 'ideal' fine-grained turbidite unit. Nine structural divisions from T0 to T8 are compared with the divisions of Bouma (1962) and Piper (1978). Modified from Stow and Shanmugam (1980).

6.4.2 Facies B2: Laminated siltstone

Description

Facies B2 has much of the same characteristics as facies B1, structureless siltstone, with individual beds or intervals ranging from 5 m to 20 cm. The laminated siltstones are sporadically interbedded with thin beds of coarse siltstone, normal- and ungraded sandstone.

The beds may have a sheet-like or lenticular form, commonly ranging in lateral extent from 10 cm up to 20cm. The siltstone beds show a fine parallel to wavy lamination. Clay and fine silt are dominating the grain fraction of the facies. Lamination is represented as a variation in colour (figure 6.4.1 B) due to input of slightly coarser silt or fine sand laminae.

The upper boundary is generally sharp and irregular due to erosion. This results in pinch-out of siltstone beds when thin beds are capped under an erosive sandstone body in the same way as for facies B1. The lower boundary is sharp or transitional from normal graded sandstone and structureless sandstone, or filling up an accommodation space on top of an uneven surface. Pyrite laminae are also represented, as in the structureless siltstone facies.

Interpretation

The laminated siltstone facies is interpreted to be thin deposits of a waning low density turbidity current or part of a dilute and dispersed high-density turbidity current (Lowe, 1982; Hiscott, 1994).

In a turbulent flow, coarse- and fine-grained particles settle separately during deposition depending on their fall velocity resulting in plane parallel laminated siltstone. Where wavy lamination occurs in smaller or larger scale, the sediment may be exposed to bottom current and traction processes before or during deposition (Hesse & Chough, 1981; Lowe, 1982; Shanmugam, 1997)

Thin sheet sandstone beds in association with laminated siltstone indicates slow deposition related to diluted tails of turbidity currents. Laminated siltstone facies may be difficult to recognize in weathered or strongly tectonized outcrops, and beds interpreted as facies B1 may originally have been part of the laminated siltstone facies.

Thin bedded turbidites as described for facies B2 and scarcity of convolution suggests slow deposition from suspension. As illustrated in figure 6.4.2, facies B2 corresponds to the Bouma's T_d division, Piper's E₁ division and Stow & Shanmugam's T₂-T₃ division.

6.5 Facies C: Sandstone

The sandstone facies is subdivided into four lithofacies: Normal graded sandstone (C1), inverse graded sandstone (C2), non graded sandstone (C3), and muddy sandstone (C4). The normal graded sandstone is dominating throughout the sections. The sandstone facies appears in isolated beds, or packages of varying thickness both upward fining and upward coarsening. Grain size is generally altering from medium to very fine; however, gravel and pebble are recorded in some beds near base.

6.5.1 Facies C1: Normal graded sandstone

Description

Facies C1 is the most frequent sandstone facies and comprises 57, 40 % of all logged facies in the sections. Variation in grain size and thickness is considerable. Beds may range from 10 cm to 7,2 m in thickness. Generally, the thinner beds vary from medium to very fine sand and the thicker beds from coarse to fine sand, all grading upwards into the silt fraction. The normal grading may represent the entire bed, but are in most cases restricted to the uppermost part of the deposition, leaving the lower part more structureless and non graded in character. The term 'thin-bedded' is commonly used for beds thinner than 20-30 cm, and thick-bedded for beds over one metre.

Some sandstone units exceeding 1m in thickness may consist of two or more amalgamated individual depositional beds with amalgamation surfaces that have been too subtle to identify; therefore, composite bed sets may have been interpreted and logged as one bed. The amalgamation surfaces are generally identified as surfaces with abrupt textural changes between adjacent sandstone lithologies (figure 6.4.1 D). Thin discontinuous shale lamina and shale clasts along a particular stratigraphical level in a sandstone unit has been applied as a criterion in addition to abrupt textural change to confirm the presence of an amalgamated surface where it otherwise has been difficult to identify two separate sandstone beds in contact. Outcrops partly covered with vegetation such as trees, brushes and lichen on the rock surface itself, may also have resulted in the interpretation of one bed instead of several; this is considered a problem in the Dampsagvegen section.

The normal graded beds comprise beds in which the grading represents the entire bed thickness to beds where only the last few centimetres are graded, ending in very fine silt. The normal grading is the result of grading of the quartz and feldspar framework grain population with the fines distributed throughout and increasing in volume in the uppermost part. Maximum grain size near base may measure more than one centimetre, although 5mm is common where the grading starts in coarse sand. Many beds are non graded in the lower part and most of the remaining part of the bed, whereas the uppermost few centimetres present a normal grading.

Beds tend to have sharp and flat bases, with little or no indication of erosion on a scale exceeding a few tens of centimetres. Sporadically erosional sole marks as grooves, which are cut into the underlying mud by current scouring, are recorded in the Maihaugvegen and Åsmarkvegen sections. These sole marks may indicate a palaeocurrent direction, described in chapter 8. A common feature is post-depositional load cast and flame structures at the lower boundary with wavy or flame-shaped tongues of mud that have projected upward into the overlying sandstone (figure 6.4.1 C). The thick beds, mainly in the Messenlivegen and Åsmarkvegen sections, clearly indicate a highly erosive flow with 1-2 m relief of the base.

The upper boundary may be slightly erosive but are normally represented as a gradational transition from the normal graded sandstone bed to an overlying silt layer. Sand dykes intruding the upper mudstone layer are recorded from the Åsmarkvegen locality (figure 6.4.5 A). Except from the presence of shale clasts these sandstone beds are fairly structureless, but some beds of facies C1 include plane-parallel stratified sandstone interval (figure 6.4.5 B) near top. In a few beds current ripple lamination occurs in the uppermost part of the very fine silt.

In the Maihaugvegen section at 11,5 meter, a 0,5 meter thick bed is recorded with an inversely to normal graded character. The bed is inverse graded from medium grained sandstone to very coarse sandstone, and then again normal graded into fine sandstone.

Most beds include a siltstone cap but may lack the whole or part of it when eroded and filled with a new sandstone deposit.

The sandstone beds of facies C1 have a sheet like or lenticular shape in outcrops where the upper boundary is flat or highly undulating without any indication of erosion.

Convolute laminae occur in the Maihaugvegen section in connection with a package comprising very thin normal graded sandstone beds, making up a total of approximately 2 meter. The lamination and folding are confined to the single bed of 15 cm, where the strata above and below show no indication of deformation.

In addition to the normal graded sandstones recorded in the logged sections there are recognized a thick package of amalgamated sandstone beds on top of the Messenlivegen section and the Åsmarkvegen 3 section (figure 2.2.1). These beds can be followed laterally over the hills in the Vårsætergrenda and further east of the Lillehammer town. The amalgamated bed sets may range up to 5 meter in thickness and are made up of coarse to medium grained sandstone, whereas sandstone lithology towards the upper boundaries are represented by more fine grained material.

Interpretation

Normal graded beds of the type present in facies C1 reflect unhindered settling from clastic material suspended in turbidity currents. As the flow decelerates in time and space, the upward components of turbulence become too weak to support the coarser grains, which gradually settle towards the base of the flow, see figure 6.4.5 C (e.g. Dott, 1963; Lowe, 1982).

Scarcity of stratification and the typical grading near the top of the beds are attributed to rapid fall out of sediment as the turbulent flow lost its momentum that suppressed sorting of grains and formation of traction current structures. Rapid deposition may also have lead to unstable initial grain packing, liquefaction and sand dyke intrusions.

Kneller and Branney (1995) explained the depositional mechanism of ungraded, structureless sandstones in the lower part of the beds as deposits from high-density turbidity currents with non-Newtonian rheology and the upper graded part as formed from currents having an Newtonian rheology. Gani (2004) named deposits of high-density turbidity currents *densites* that are represented by beds with a normal grading restricted to the upper part of the bed. The structureless well sorted sand in the lower part of the bed may also be a result of a flow with little finer grains and well sorted sand fraction.

Beds showing an inverse grading in the lower part and normal grading in the upper part have been discussed by several authors. Sanders (1965) suggested a two layer bed with a lower 'inertia-flow' layer overlaid by a normal graded layer in the upper part. The inertia-layer is explained as a result of medium sand and pebbles separating in a shaker mechanism (Bagnold, 1968), as explained in chapter 6.5.2. The inverse grading could also be a result of frictional freezing of a transient traction carpet beneath a high-concentration turbidity current (Lowe, 1982) representing the S₂ stage of Lowe sequences.

Short-lived surge-type flows and steady flows encountering an abrupt change in slope gradient typically deposit sand beds of the facies C1 type (Stow, *et al.* 1996; Mulder and Alexander, 2001) (Figure 4.3). Kneller (1995) introduced the concept of waxing, steady, and waning turbidity currents, which may also produce reverse grading. A surge type hyperpycnal flow is analogue to a waxing-then-waning flood (Mulder, *et al.* 2003) and therefore capable to produce deposits with reverse-then-normal grading. These flows are low-concentrated and medium turbidity currents.

The occurrence of shale clasts in the beds suggest an erosive turbidity current while absence of ripped-up clasts indicate turbidity currents flowing too slowly to achieve any erosion of the bed. The few beds comprising laminated sandstone may represent upper flow regime conditions, while silt ripples represent a current that have decelerated to the lower flow regime with traction mechanisms (e.g. Middleton & Hampton, 1976).

Flame structures and associated load structures are probably caused mainly by loading of water-saturated mud layer which are less dense than the overlying sands and therefore squeezed into the sandstone layer. The flame shaped tongues may show the same overturned orientation, suggesting that loading may have been accompanied by some horizontal drag or movement between the mud and sand bed. Convolute laminae as those described above are generally interpreted as a result of plastic deformation of partly liquefied sediment after deposition. The triggering mechanism for liquefaction may be slumping.

Normal graded and structureless beds as described here correspond to the Ta interval of the Bouma Sequence (figure 4.4), or the S₃ interval described by Lowe (1982) The plane parallel laminated sandstone corresponds to the Tb interval and silt ripples to the Tc interval of the Bouma Sequence.



Figure 6.5.1 Sedimentary structures observed in the Brøttum Formation: A) Sand dyke intruding mud deposits, Åsmarkvegen, B) plane-parallel stratified sandstone, Åsmarkvegen 2 and D) normal graded sandstone

Beds formed as dunes showing a distinct undulating boundary may represent deposits from currents in which the ratio of bedload to suspended load varies with time. As the strength of a tractional current decreases, deposition from suspension increases resulting in large dune formed beds (Pickering *et al.*, 1989).

6.5.2 Facies C2: Inverse graded sandstone

Description

Facies C2 is only observed in the Maihaugvegen section and comprises 0,07 % of the total facies recorded. The bed is inverse graded from very fine to fine sand and is plane parallel laminated. The colour is grey to light grey. Both upper and lower boundary is sharp and flat towards the other beds. The inverse graded bed is associated with thick beds of structureless siltstone (facies B1) and thin normal graded sandstone beds of facies C1.

Interpretation

Bagnold (1968) suggested that inverse grading was a result of dispersive pressure mechanism that acted to size-sort grains. The larger grains were pushed to the top of the flow and the smaller ones to the base. Middleton (1970) suggested another hypothesis where reverse grading was the product of a kinetic sieve mechanism whereby small grains fall downwards between large grains during flow, displaying the larger grains upward.

The inverse graded sandstone bed representing facies C2 may be the deposits of several succeeding thin low density turbidity currents. The inverse grading of the bed may thus be 'apparent', as a result of a general increase in grain size of the sand fraction of a series of thin turbidites.

6.5.3 Facies C3: Non graded sandstone

Description

Non graded sandstone beds are recorded in all logged sections and comprise 4,10 % of the total facies. The beds range from 5cm to 3m in thickness. Most beds are very fine to medium grained. Thin facies C3 beds (generally <20cm) are associated with thin beds of normal

graded sandstone and facies B. Silt and clay content in these beds are higher than for the thicker beds. Thicker beds (generally >50cm) ordinarily show a coarser grain size than the thinner beds and are associated with thicker beds of facies C1. The deposits are moderately to well sorted and have a light grey colour.

Both the upper and lower boundaries are typically sharp and flat. However, the basal contact may be slightly too deeply erosive. Thick beds have normally been eroded to a certain extent by the next sand-rich flow, thus resulting in an amalgamated surface between two succeeding sandstone layers. This surface is not always easy to recognise in outcrops. All beds within this facies are structureless but may contain shale clasts near top or base, as recorded in the Messenlivegen section. The non graded sandstone beds have a sheet-like geometry.

Interpretation

Presence of rip-up clasts near bed base, sheet like geometry and sharp flat bases indicate a turbidity current origin of the facies C3 sandstone beds, according to criteria for these type of beds (Hiscott, *et al.* 1997).

Non graded sandstone of facies C3 may have several causes. Where beds are clearly amalgamated towards an overlying sandstone bed, it has been exposed for a highly erosive flow. The bed can thus originally have been a normal graded bed of facies C1 with the topmost part removed and with the lowermost part having a structureless property. In the case where the beds are <15 cm thick the supposedly lack of normal grading may be a result of poor outcrop where it is difficult to recognize the grading at the very top of the bed.

Non graded structureless beds are generally interpreted to be deposits of high-concentration turbidity currents (Lowe, 1982). Short-lived surge type high-concentration turbidity currents may undergo collapse fall-out as the flow loses its momentum and becomes unstable. The sediment may pass briefly through a basal zone of hindered settling where modified grain flow, fluidized flow and liquefied flow support are operating mechanisms. A high concentration turbidity current may also go through continuous aggradations beneath the flow where sediments pass through an active basal layer of hindered settling (traction carpet), or continuous traction beneath a sustained steady flow (Stow and Johansson, 2000)

6.5.4 Facies C4: Muddy sandstone

Description

Muddy sandstone is recorded in the Messenlivegen section and the Fredrik Colletts veg section. It comprises 2,2 % of the total recorded facies. The facies is characteristic for its poor sorting; the clay content is higher than for the other sandstone facies, resulting in a darker grey matrix colour. The average grain size is fine sand near base, commonly grading up to fine silt. In some cases the beds seem to represent muddy sandstone grading into sandy silt. Internal sedimentary structures are absent in all beds.

The muddy sandstone facies occurs in beds varying in thickness from 10 cm to 2.5 m. The thinnest beds occur most frequently and lack normal grading. Beds tend to have sheet like geometry with sharp and flat boundaries. However, some beds have a more lenticular outline with undulating boundaries.

Interpretation

The normal graded muddy sandstone is interpreted to have been deposited by mud-rich high density turbidity currents or debris flows (Pickering *et al.*, 1989). In case of a turbidity current, rapid mass deposition due to a high intergranular friction may have prevented a complete normal grading of the sediments.

The high clay content may have resulted in a cohesive flow with matrix strength that froze when the force related to the shear resistance of the flow became equal to the force due to gravity. Such *en masse* deposition may explain the large variation in grain size and particle shape. The present data do not allow drawing any definite conclusion as regards which of these main types of gravity flow currents may have been responsible for the facies C4 muddy sandstone.

6.6 Shale clasts in facies C1 and C3 sandstone beds - Discussion

Shale clasts are fine grained (silt-clay grade), coherent sedimentary particles or clasts that occur within a sandstone bed. Johansson and Stow (1995) made a classification scheme based

on descriptive analysis resulting in twelve different clast types. Shale clasts occur in both normal graded sandstone beds and in structureless and normal graded beds.

In the logged sections at Lillehammer, shale clasts appear in the sandstone beds in three primary positions; near base, centred in the bed or near top. This classification does not consider clast shape or size, but generally the larger clasts are more spherically than the smaller one. Smaller dish shaped clasts are the most common one. Table 6.6.1 illustrates the frequencies of shale clasts in the different positions throughout the logged sections.

Table 6.6.1 Frequency of shale clasts in sandstone beds. Each recorded event may consist of one or several shale clasts in groups

Shale clasts recorded in sandstone beds			
<i>Logged sections</i>	<i>Near top</i>	<i>Centred</i>	<i>Near base</i>
Åsmarkvegen 1	2	1	1
Åsmarkvegen 3	0	2	3
Messenlivegen	1	4	5
Maihaugvegen	0	1	2
Fredrik Colletts veg	1	1	4
Dampsagvegen	0	1	0

Each recorded occurrence either contains several clasts closely related to each other or as isolated clasts. Shale clasts near base of sandstone beds are interpreted as raft-type clasts or flame-type clasts. Raft type clasts indicate high energy erosion. Flame-type clasts indicate low energy erosion (Johansson and Stow, 1995).

Shale clasts that occur in the centre of normal graded beds may be indication of two amalgamated sandstone beds. The first bed is eroded by a second turbidite flow, leaving bits and peaces of a capped silty drape layer between. This is confirmed by shale clasts lying along one definite stratigraphical horizon. According to Johansson and Stow (1995) this is indicative of a low energy erosion flow.

Clasts that appear near top of a sandstone bed may also be a post-depositional feature caused by liquefaction of sand intruding an overlying silt layer. These are called top-bed rip-down clasts. Isolated floating clasts are explained by Johansson and Stow (1995) to be emplaced by

deposition from an HDT by continuous aggradation or deposition from a sandy debris flow by plug freezing after a short or long transport. Mutti (1992) explained floating shale clasts in top of turbidite sandstone beds as the result of rather long transport of clast fragments, derived either by bottom rip-up or by collapse from muddy margins of a channelized current, allowing the clasts to move upwards in the flow due to their hydraulic properties of high buoyancy.

The common presence of clay clasts in the Brøttum turbidite sandstone beds in the Lillehammer area demonstrate that the depositional environment changed from events of quiet sedimentation to events of high-energy turbidity current activity.

7 Facies associations

7.1 Introduction - Facies associations

A facies association is defined as a group of facies thought to be genetically or environmentally related to each other (Collinson, 1969). Treating each facies in isolation when interpreting the environment may be ambiguous while facies association provides additional information. Facies associations are the architectural elements of a sedimentary succession, representing different depositional environments or subenvironments (Reading & Levell, 1996).

Definition and identification of facies and their genetic associations in the Brøttum Formation in the Lillehammer area have resulted in five main types of facies associations; however, each facies association may contain sub-facies associations, as defined in table 7.1. The main facies associations defined and interpreted in terms of depositional subenvironment and architectural element are FA 1: Basin plain, FA 2: Depositional lobe, FA 3: Basin floor channel, FA 4: Major channel and FA 5: Channel-levee. The interpreted facies associations are illustrated in appendix 3, table of facies association distribution and in sedimentary logs enclosed in appendix 4.

Table 7.1. Facies associations in the Brøttum Formation in the Lillehammer area, including facies, architectural elements and general characteristics.

Code		Facies Association/Architectural element	Facies content	Characteristics
FA 1	FA 1.1	Basin plain – thin bedded turbidites	B1, B2, C1, C2	Thin sheet sandstone Slide deposit Pyrite laminae
	FA 1.2	Basin plain – hemipelagic shale	A1, B1	Black shale with pyrite laminae Structureless siltstone
FA 2	FA 2.1	Lobe	B1, B2, C1, C2, C3, C4	Upward coarsening and thickening to aggradational sandstone packages
	FA 2.2	Lobe-channel	B1, B2, C1, C3, C4	Upward fining and thinning sandstone packages
FA 3	FA 3.1	Basin floor channel infill	B1, B2, C1, C3	Upward fining and thinning sandstone packages
FA 4	FA 4.1	Major channel	B1, C1, C3	Upward fining and thinning sandstone packages
FA 5	FA 5.1	Channel-levee	B1, B2, C1, C3	Slide and slump deposit Fine grained turbidite sandstone

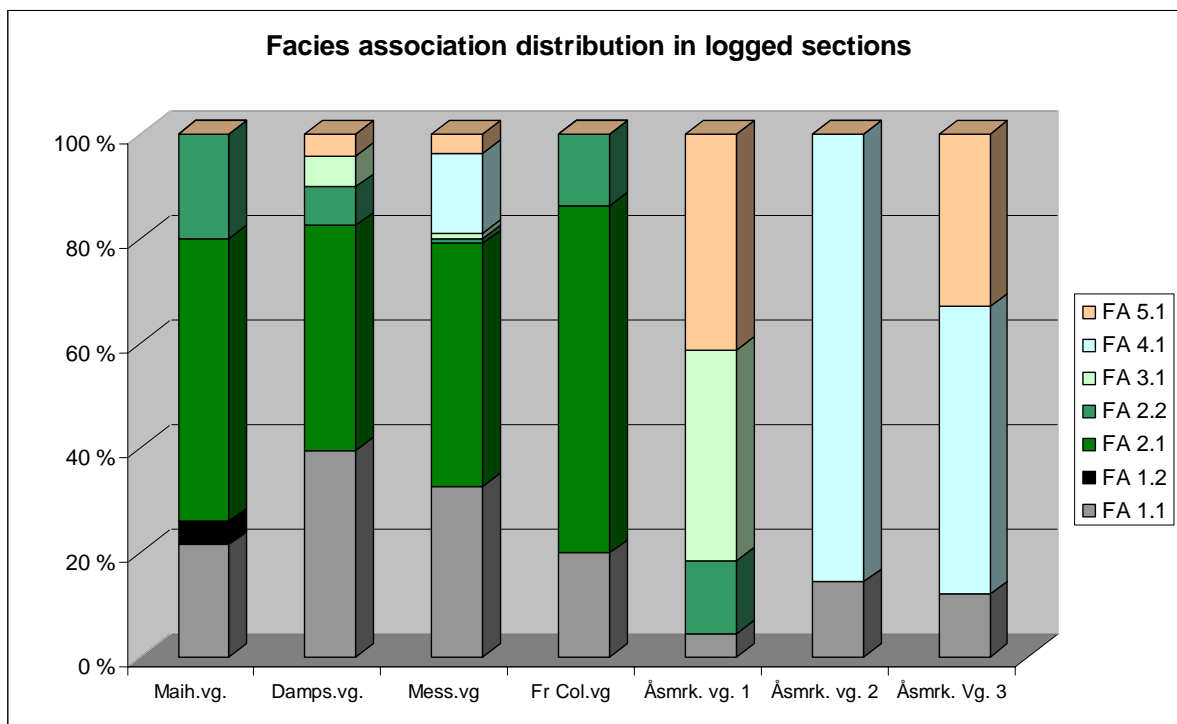


Figure 7.1 Facies associations in the seven logged road sections. Note that FA 5.1 and 4.1 are only recorded in locality Åsmarkvegen 2 and Åsmarkvegen 3, whereas FA 1.2 is only recorded in the Maihaugvegen section. Abbreviations are: Maih. vg. = Maihaugvegen, Damps.vg. = Dampsagvegen, Mess.vg. = Messenlivegen, Fr. Col.vg. = Fredrik Colletsveg, Åsmrk. vg. = Åsmarkvegen.

Figure 7.1 above demonstrates facies association distribution in the different logged sections. The facies associations seem to be more specific of the particular locality or stratigraphic level in the Lillehammer turbidite succession, compared with the facies

distribution (figure 4.2.2). Facies Association 4.1 and 5.1 are only recorded in the Åsmarkvegen 2 and Åsmarkvegen 3 locations. The intra lobe basin plain facies association (FA 1.1) is the only association recorded in all sections.

7.2 Facies Association 1: Basin plain

Hemipelagic clay-rich deposits and very thin-bedded turbidites are characteristic facies of the basin plain facies association. In a submarine fan depositional environment comprising channels and depositional lobes there will be deposited fine grained sediments from suspension both between active channels and lobes and in the very distal parts of the fan. The basin plain facies association includes two sub-facies associations, FA 1.1 and FA 1.2. They are related to the two different settings.

7.2.1 Facies association 1.1: Basin plain – thin bedded turbidites

Description

Facies association 1.1 comprises very thin beds and laminae composed of fine grained facies including black shale (A1), structureless silt (B1), laminated silt (B2), normal graded sandstone (C1) and non graded sandstone (C3). There is no distinct trend in which order the facies included in FA 1.1 occur, but structureless silt of facies B1 and laminated silt of facies B2 dominate the succession.

FA 1.1 is recorded in all localities and covers 26% of the total recorded facies. There are 20 units of interpreted intra lobe basin plain facies associations, ranging from 1,1 meter to 27,3 meter in thickness, with no typical thickness trend of the units. They are recorded in association with all other facies associations. The Messenlivegen and the Dampsagvegen are the logged sections with highest percent of FA 1.1. These sections also include the thickest units of this facies association.

More than 50% of the units of FA 1.1 are succeeded by FA 2.1 units, prograding or aggrading lobe. This facies association is also the most frequent association underlying

FA 1.1 in the total recorded lithology. Facies association FA 1.1 typically alternates with FA 2.1; however, in the uppermost part of the Messenlivegen section and the Åsmarkvegen locality the FA 1.1 is more frequently associated with FA 3.1 (Basin floor channel) and FA 4.1 (Major channel).

The facies association is dominated by thick beds of laminated and structureless siltstone including parts of more organic rich hemipelagic deposits. Sheet like sandstone beds of facies C1 (normal graded sandstone) and C3 (non graded sandstone) are normally interbedded in the mudstone. They may show thicknesses over 1 meter but are more commonly less than 0,5 meter. Generally, the facies C1 and C3 are included in FA 1.1 where the facies association is developed with very fine to fine sand as dominating grain size. The thickest sheet sandstone beds are represented by very fine sandstone, whereas the thinnest beds may be up to lower medium in grain size. The overall bed surface geometry appears to have been even and parallel, but the thinnest sandstone sheets may reveal a more lens-shaped geometry. Sandstone beds of FA 1.1 occur isolated, or in clusters with more narrowly spaced to each other, as in the lower Messenlivegen section. There is no obvious trend in facies distribution within the facies association FA 1.1.

Facies A1, the hemipelagic black shale, is only recorded in the Messenlivegen section in a 26,5 meter thick unit consisting of mainly normal graded sandstone and siltstone beds. The various FA 1.1 units are at the base bounded by gradational to texturally sharp, conformable contact to underlying facies associations. The upper boundary can be erosive where FA 1.1 is overlaid by beds of the facies associations FA 3.1 or FA 4.1.

Thin packages of folded sandstone beds occur both in the Messenlivegen and the Fredrik Colletts veg sections within the facies association. These deformed sandstone bodies consist of very fine to fine sand layers that seem to be ripped off their original depositional site and folded. The deformed sandstone beds described here are isolated from other sandstones, they are folded either once or twice, revealing a 1-2 meter thick package in the fine grained sediments.

Interpretation

The fine grained sediments, dominantly represented by facies B1 and B2, sporadically by sheet sandstone of facies C1 and C3, are thought to reflect a distal environment basinward of active depositional lobes, the basin floor where the more sand-concentrated turbidity currents only once in a while reached out. The thin bedded sandstone intervals within the FA 1.1 are thus considered equivalent to the coarser and more thick-bedded sandstone beds of the depositional lobes of facies association FA 2.1. When a turbidity current moves downslope, the current becomes diluted by entraining water and deposits progressively finer grained material from suspension. The diluted turbidity currents accumulate as peripheral fringes around the sand rich lobes (Mutti, 1977).

The amount of sheet sandstone beds within the FA 1.1 is controlled by the distance to the channel-lobe complex. In areas, during time intervals where hemipelagic sedimentation predominated, the channel and lobes have moved gradually, or switched abruptly, towards other depositional sites at the basin floor, thus resulting in strongly reduced amount of sand sedimentation relative to the amount of fine hemipelagic fraction.

In stratigraphic intervals where FA 1.1 units are interbedded with FA 3, FA 4 and FA 5 the basin plain facies association is interpreted to have formed as a distal part of a channel-levee deposit between active lobes, or the very top of a channel-infill deposit. The units associated with FA 2.1 tend to be thicker and are probably related to a more distal part of channels and depositional lobes.

The folded sandstone bodies in the Messenlivegen and the Fredrik Colletts veg (figure 7.3.2) sections are interpreted to have been derived by sediment collapse along the slopes of a channel-levee deposit. Through sliding, rotation and folding these detached sediment packages of coherent sand may have moved far from its original setting. Hydroplaning causing reduced friction at the base might have been a mechanism for their displacement (cf. Mohrig et al. 1999, see also chapter 4).

7.2.2 Facies association 1.2: Basin plain – hemipelagic shale

Description

Facies association 1.2 represents the most fine-grained assemblage of sedimentary facies that is recorded in the study area. The facies included in FA 1.2 are black shale (A1) and structureless siltstone (B1). The structureless siltstone is represented as a few thin (<10cm) layers randomly distributed in the shale. Pyrite laminae occur, as described in chapter 5.3 for the black shale facies. The facies association is recorded in the Maihaugvegen section only. In the Maihaugvegen section a 5,7 meter thick unit directly overlies the FA 1.1, as described in chapter 7.2.1. The facies association FA 1.2 comprises 1% of the total lithology that has been logged in the seven road sections in Lillehammer. The boundary between these two facies associations in the Maihaugvegen section is texturally gradual. However, the hemipelagic shale FA 1.2 does not comprise sandstone sheets of facies C1 or C3, as the FA 1.1 does.

Succeeding the FA 1.2 unit in the Maihaugvegen, the FA 2.1 introduces a prograding lobe that starts with the inverse graded sandstone layer (facies C 2). The boundary between the two facies associations is conformable with the FA 2.1 facies association commencing a new depositional environment being characterized by laminated siltstone and thin sandstone beds.

Interpretation

The very fine grained deposits without any sandstone sheets suggest an even more distal environment than that described for FA 1.1. The hemipelagic sedimentation reflects long periods of time during which the fan system was abandoned. Periods of long hemipelagic sedimentation within deep-marine turbidite fan systems can generally either be related to major lateral avulsion of the main feeder channels or to rise in relative sea level, may be of a fourth-order eustatic cyclicity, as suggested by Eschard (*et al.* 2004).

7.3 Facies association 2: Depositional lobe

The depositional lobe facies association comprises two sub-facies associations. The lobe (FA 2.1) is an upward coarsening unit, whereas the lobe-channel succession (FA 2.2) is an upward fining unit. The lobe facies association (FA 2.1) either consists of channelized sandstone bodies and therefore succeeded by FA 2.2 or the lobe facies association consists of unchannelized sandstone beds. The depositional lobe facies associations make up a total of 44% of the recorded lithology.

7.3.1 Facies association 2.1: Lobe

Description

The individual facies that are included in the lobe facies association are B1 (structureless sandstone), B2 (laminated sandstone), C1 (normal graded sandstone), C2 (inverse graded sandstone), C3 (non graded sandstone) and C4 (muddy sandstone). The facies association FA 2.1 is the most frequent recorded facies association in the logged sections, comprising 38% of the total lithology divided on 15 units. Even though the facies association is dominating throughout the logged sections, it is completely lacking in the Åsmarkvegen locality in all three sections logged along this road.

The FA 2.1 is either upward coarsening and thickening, or upward coarsening and then aggrading. The base typically starts with a conformable lower boundary with siltstones of facies B1 and B2, succeeded by an upward increasing amount of sandstone sheets, ending in medium to coarse sandstone beds, as exemplified in figure 7.3.2. The top of the lobe unit may show some degree of upward fining. Sandstone sheet beds representing this facies association may include shale clasts near base of beds.

The units of the FA 2.1 vary in thicknesses between 4,5 meters and 46 meters, with an average of 23 meters. The thickest units are always upwards thickening and coarsening to aggrading and occasionally slightly upward fining in the top, whereas the thinner units are only upward coarsening and thickening.

In the Messenlivegen section there are two occurrences of FA 2.1 units with a lower sand/mud ratio than for the other logged units. The units reveal a prograding to aggrading package trend of facies B beds, structureless siltstone, with sheet sandstone beds in thicknesses up to a couple of meters. These units are closely associated with FA 1.1.

FA 1.1 is the most common underlying and overlying facies association units; however FA 2.1, FA 2.2 and FA 1.2 may succeed the FA 2.1 lobes.

Interpretation

The upward coarsening to thickening and aggrading stacked sheet sandstone beds with minor siltstone beds are interpreted to represent lobe elements formed by basinward progradation and aggradation of the turbidite depositional fan system.

The term *lobe* is used by many authors in different senses. Lobes were originally defined by Mutti and Ghibaudo (1972) as non-channelized bodies, 3-19 meters in thickness, composed of thick bedded sandstone alternating with thinner-bedded and finer-grained deposits. The term *lobe* in the sense of Stow *et al.* (1996) refers to a lobe-shaped, low-relief depositional mound, usually generated at the distal ends of channels, and produced by the stacking of individual turbidite beds.

Where the lobe has a more thinning upward trend near the top, it might have been terminated by a small channel segment, as described for FA 2.2, or the lobe may have started to move laterally, for example due to avulsion, and therefore revealing a retrograding lobe pattern at the site of the logged section.

The units recorded in the Messenlivegen section of fringed sheet sandstone beds represent a more distal environment of the lobe. The fringed sheet sandstone beds are located in the transition towards the basin plain facies association.

Individual sandstone lobes of basin floor fan systems may extend from a few kilometres to tens of kilometres and even more for modern fans (Stow *et al.* 1996) and represent the maximum down-current extent of the sand transported to the basin in an outer-fan environment. *Depositional lobes* with dominantly conformable lower boundaries are

supposed to fill depressions in the basin floor, compensating for uneven basin floor topography (Mutti 1985). Lobes of facies association 2.1 may well have formed in this way.

7.3.2 Facies association 2.2: Lobe-channel

Description

The facies association is recorded in 8 units, all of them comprising upward fining and thinning trends. The units range from 3,3 meters to 10,5 meters in thickness, and with an average thickness of 7,2 meters.

The facies included are structureless silt (B1), laminated silt (B2), normal graded sandstone (C1), non graded sandstone (C3) and muddy sandstone (C4). The lower part of the unit may start with a more than 2 meter thick gravely sandstone (facies C3) fining up into thin layers of silt. Facies association 2.2 is closely associated with FA 2.1 that is recorded directly below in all occurrences, except for one locality in the Dampsagvegen. Here, the facies association seems to follow a more levee or basin plain deposit associated with the lobe.

The lower boundary of facies association 2.2 sandstone beds may be slightly erosional with scour structures. The upper boundary of FA 2.2 units is transitional to the overlying facies associations FA 1.1, or the boundary is texturally sharp to the next unit of FA 2.2.

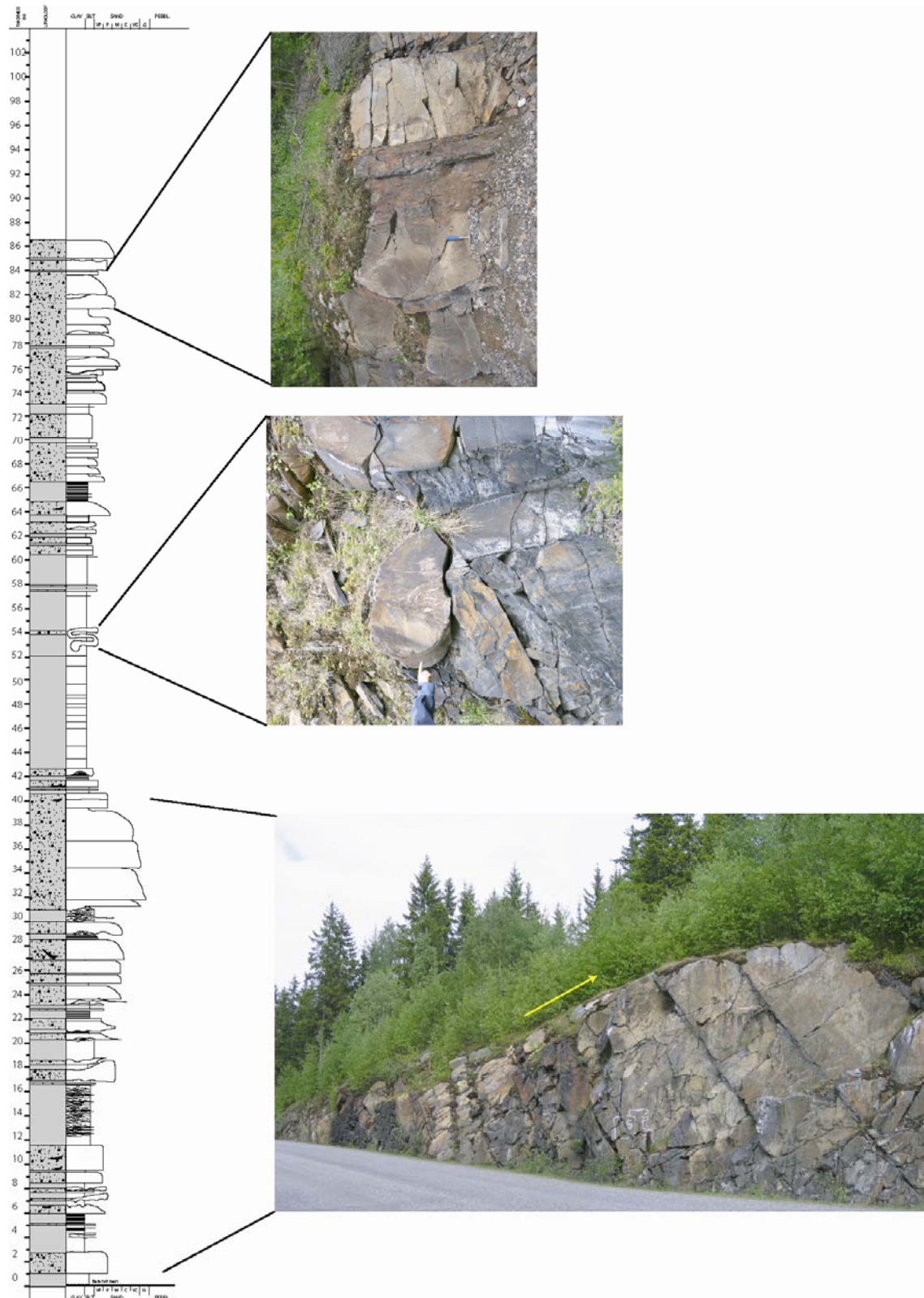


Figure 7.3.2. The Fredrik Colletts veg log section. Upward coarsening and thickening lobe at base. Yellow arrow for point towards the youngest bed. Middle: Folded sandstone body related to channel-levees and top: Stacked normal graded sandstones in lobe association.

Interpretation

The facies association 2.2 is thought to be genetically closely related to FA 2.1 and are interpreted to be the channel-fill succession of *channelized lobes*. Fining- and thinning upward trends of turbidite sandstone successions are commonly applied as indicators of channel-fills (Mutti & Ricci Lucchi, 1978; Walker, 1978). The close association to the lobe suggests that the lobes were attached to the channels without an intermediate bypass zone. When such a lobe system progrades basinwards, the turbidity currents will start to drop their sediments at a later stage, thus filling up the channel. The transition from lobe-channel to the associated lobe of non-channelized sandstone beds is commonly associated with a break of slope (Wynn *et al.*, 2002), where the channel is widening and the currents loose their capacity to carry sediments.

7.4 Facies association 3.1: Basin floor channel infill*Description*

Individual facies included in the FA 3.1 units comprise structureless siltstone (B1), laminated siltstone (B2), normal graded sandstone (C1) and non graded sandstone (C3). The facies association is recorded in the Åsmarkvegen 1, Dampsagvegen and the Messenlivegen section.

The 4 logged units are exposing upward fining and thinning packages of beds and bed sets, from gravel sized (up to 10 meter) amalgamated sandstone beds in the lower part to thin fine grained sandstone or siltstone beds in the top. The sand/mud ratio varies in the different channel succession. The thinnest units tend to have a higher sand percent than the thicker units. The average thickness is 9 meters, which is higher than for the lobe-channels. Sandstone beds located at the lower boundary of the facies association are erosional with approximately one meters of relief towards the FA1.1 or FA 5.1 facies association beds below. These facies associations are also succeeding the channel units.

The basin floor channel infill represents 4 % of the total logged lithologies in the Lillehammer area.

Interpretation

The facies association 3.1 is related to basin plain facies association (FA 1) and levee facies association, and *not* to lobes like the channel succession described in chapter 7.3.2. The basin floor channel infill can be distinguished from the lobe-channel of facies association 2.1 by thicker sandstone beds, generally higher erosion at the bed and connection to dissimilar facies associations.

The FA 3.1 is interpreted to reflect the infill of a channel entrenched or incised on the basin floor. The individual channels are thought to be part of a distal distributary channel complex where sediments are brought out onto the sea floor in a mid-fan or outer fan area. The channels may represent proximal parts of lobe-channels or/and distal parts of the major channels described below.

7.5 Facies association 4.1: Major Channel*Description*

The major channel facies association, representing the FA 4.1, comprises facies B1 (structureless siltstone), B2 (laminated siltstone), C1 (normal graded sandstone) and C3 (non graded sandstone). Among these, sandstone facies are dominating.

The units are only recorded in the Åsmarkvegen 2, Åsmarkvegen 3 and the Messenlivegen section in a total of 12 units. Facies C1 may show lamination as observed in the Åsmarkvegen 2 section (figure 6.5.1). These units cover 17 % of the logged strata and are characteristic of upward fining and thinning units from 3,5 meter to a maximum of 25 meter in thickness. The association are closely associated with FA 5.1 and FA 1.1. Compared to the basin channel infill facies association, these units is typical more sand prone with little interbeds of silt. In the Åsmarkvegen 2 section there is no siltstone beds represented at all in 5 of the 6 units. The base of the lowermost sandstone is commonly erosive with granule grain size, fining up to medium sandstone. The total packages are upward fining and are normally topped by fine sand. Amalgamated sandstone beds of FA 4.1 are illustrated in figure 6.4.1. It has not been possible to recognize any transition lateral from channels into levee or overbank deposits due to limited outcrops.

The major channel successions in the Åsmarkvegen and Messenlivegen sections are succeeded by a thick unit of amalgamated channel-sandstone beds, recorded in the Vårsætergrenda and the hill district east of Lillehammer town. This package of thick-bedded major channel sandstone bodies are in the order of 100 meter thick, at least. This major channel complex is well exposed in the Lillehammer Stamp mill on the boarder to Hedmark County. Figure 7.5.1 illustrates the sandstone package here with stacked channels, each 3-5 meters thick representing a meandering major channel complex. Such channels have been described to have widths varying from 300 m to > 1,5 km for channels cropping out in the basin floor of the Tanqua Karoo turbidite systems (Johnson, 2001) and in seismic interpretation of migrating channels of the deep-water depositional systems in Block 34 of the Lower Congo Basin offshore Angola (Pedersen, 2003).

Sandstone beds within some of these FA 4.1 facies association units locally display lateral accretion surfaces (figure 7.5.1.), indicating a meandering course (Mutti et al., 1985, p 562).

Interpretation

The sand rich facies association FA 4.1 is interpreted to reflect major channels located in mid-fan positions of a submarine fan. Well developed channels in this position evolve where the main conduit of a point-sourced fan complex reaches out on the unrestricted basin floor in association with levees and basin plain deposits (Bouma, 2000). These channels are more often associated with levees than smaller channels of FA 2.2 and FA 3.1.

The submarine channels representing FA 4.1 might have been main conduits for sediment transfer far out in the deep-marine basin. The major channels probably developed in down-current direction into FA 3.1 successions. Finally, when the large channels systems were no longer capable of containing the head of the gravity current, gradual overflowing took place, and sheet-sand deposition commenced.

The upward fining motif of the FA 4.1 packages is thought to reflect declining energy of the turbidity currents, whereas stacked thick units towards the top suggest

aggradation during a period of balance between rate of sediment supply and accommodation within the channel complex. The channel successions interpreted as FA 4.1 and FA 3.1 facies associations are both interpreted to be mixed types, both erosional and depositional, (cf. Mutti & Normark, 1987)

The major channel succession recorded in the hills east of the Lillehammer town, consisting of vertically stacked channel-fills are interpreted to represent the uppermost and most proximal part of the studied submarine fan complex in the Lillehammer area. Individual channel-fill complexes rarely exceed thicknesses of about hundred meters and widths of one to two kilometres in ancient submarine fan systems (Mutti & Normark, 1987). However, in the Lillehammer area channel-fill complexes of the major channel facies association FA 4.1 form together a sandstone body that must have covered many square kilometres in lateral extent of a huge midfan segment.



Figure 7.5.1 Channel complex at the Lillehammer Stamp Mill, arrow points at bed units showing lateral accretion surfaces. Person for scale.

7.6 Facies association 5.1: Channel-levee

Description

The channel levee facies 5.1 includes facies B1 (structureless siltstone), B2 (laminated siltstone), C1 (normal graded sandstone) and C3 (non graded sandstone) and covers 8 % of the facies associations.

The facies is recorded in 4 of 8 logged sections. Here the levee facies strata are associated with FA 2.1, lobe; FA 3.1, basin channel infill; FA 4.1, major channel and FA 1.1 basin plain. FA 3.1 and FA 4.1 are the most common associated units. The 8 units interpreted to represent FA 5.1 show no distinct facies sorting and thickness trends within the units. The most common facies are sandstone beds represented by fine to lower medium grain sizes randomly interbedded with siltstone beds. Individual beds in the units are 0,1-1 meter thick. Beds may be sheet like; however, lens shaped beds are often represented. Synsedimentary deformation is common, demonstrated by folded sandstone and siltstone beds. Some of the deformed sandstone beds have complex overturned folds and have been disrupted along fold limbs with the beds stretched into lenses that pinch out laterally.

Figure 7.6.1 illustrates a 13 meter long section from the Åsmarkvegen 1 with very fine and thin sandstone beds which are detached from underlying strata and folded due to slumping and sliding. Figure 7.6.2 illustrate parts of a FA 5.1 unit as a syn-sedimentary duplex structure where the sediments have been exposed to sliding and suddenly stopped. The FA 5.1 units are 9 meter thick in average. The thickest units recorded are underlying the major channel facies association. When the units are underlying a major channel or basin floor channel infill it might reveal an erosional boundary.

Interpretation

Channel-levees are formed as a result of overbank deposition when turbidity currents partly overflow the channel banks. Such overbank fine grained sand, silt and clay are deposited from relatively diluted turbulent suspensions spilling over channel margins, continuing down-slope of the levee ridges into adjacent basin plain, thus building up the levee ridges themselves and adjacent fine grained material in interchannel areas. This

gravity flow will partly change from a turbulent flow to a traction current. These traction currents can often carries a high volume of sediment (Bouma, 2000).

Unconsolidated and unstable sediments on the channel flank are sensitive to slumping and sliding due to a relative high slope gradient towards the basin plain (figure 7.3.2). The cohesive clay sediments can move due to the concept of hydroplaning (chapter 4.4). The scale of movement varies from cm to km. Where sliding and slumping sediments are observed in FA 5.1 there is probably no more than some tens meters of displacement. Because slumping involves plastic deformation a slump will freeze once applied shear falls below some critical value. This is exemplified from figure 7.6.1 described above.

In many large fan systems, the upper/middle fan is typically dominated by one single feeder channel flanked by mud-dominated levees (Richards *et al.* 1998), as described for FA 4.1 (major channel) and FA 3.1 (basin floor channel infill).

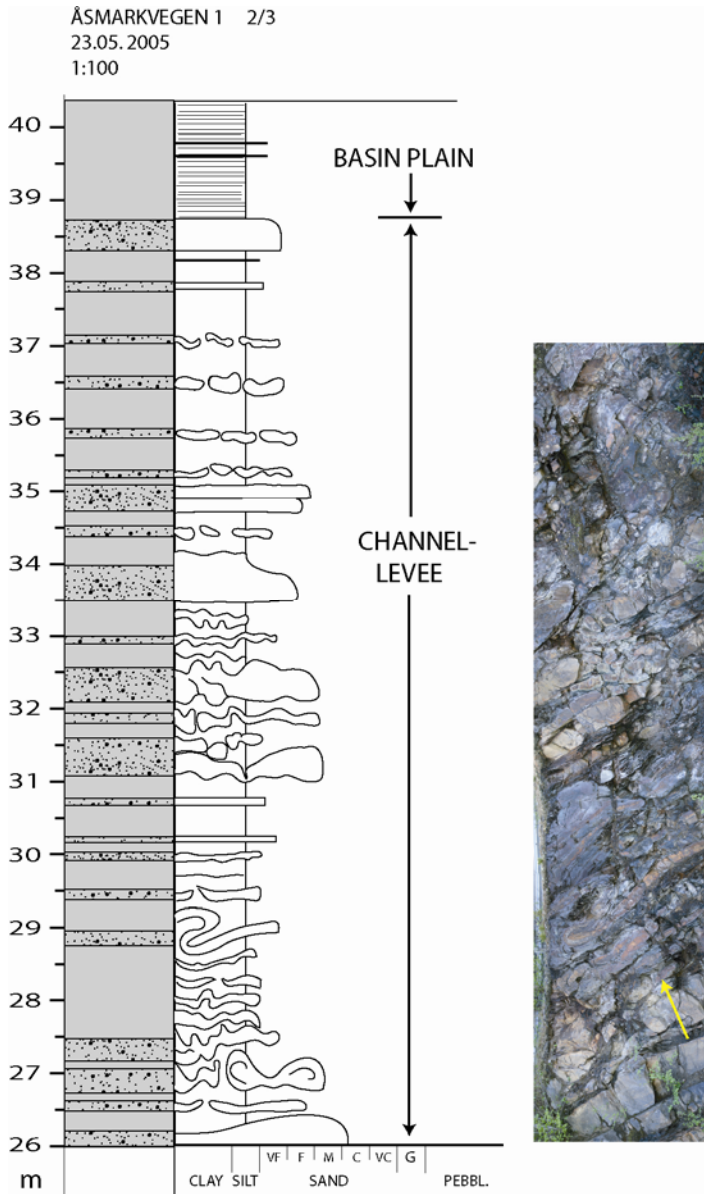


Figure 7.6.1 Channel-levee facies association, very fine and thin sandstone beds which are detached from underlying strata and folded due to slumping and sliding, Åsmarkvegen 1. Arrow points towards the youngest bed.

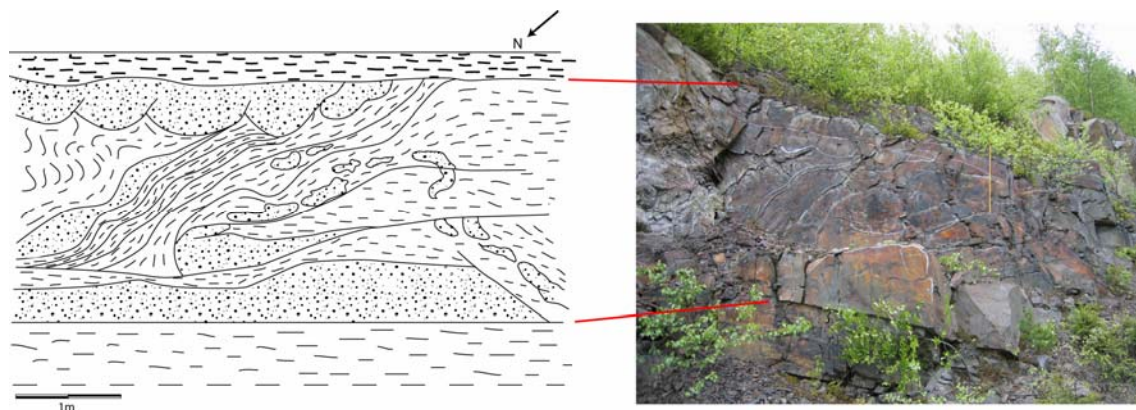


Figure 7.6.1 Syn-sedimentary duplex structure related to a channel-levee, the sediments have been exposed to sliding and suddenly stopped, Åsmarkvegen 3.

8 Depositional environment

8.1 Introduction

Facies association, described and interpreted in chapter 6, is in the present chapter further integrated in an interpretation of the overall depositional environment of the Brøttum Formation in the Lillehammer area as a prograding submarine fan complex (LSFC).

Johannes Walter's Law of Facies (1894) is important when interpreting facies occurring in vertical contact with each other: *Where there is a conformable vertical succession of facies, with no major breaks, the facies are the product of environments that were once laterally adjacent.*

8.2 Classification systems

Submarine fans are eminent features on the sea floor comprising canyons, channel-levee systems and distal depositional lobes (e.g. Mutti & Ricci Lucchi, 1972; Normark, 1970; Normark & Piper, 1972; Mutti, 1992) that have developed seaward of a major sediment point source. Several different classification systems describing both ancient and modern deep-water lobes and channels have been suggested (e.g. Normark, 1970; Walker, 1978; Mutti, 1985 and Reading & Richards, 1994).

The early models were mainly based on studies of the ancient rock record. These models included deep-water systems fed only by a single feeder channel that developed downslope into distributary channels and lobes in upper, middle and lower fan segments (Normark, 1970; Walker, 1978). In studies of ancient fans the subdivision in an inner, middle and outer fan is commonly used rather than upper, middle and lower fan as for modern fans. However, these terms have been widely used both for ancient and modern fans by different authors; in some

ancient fans middle and outer fan will according to Mutti & Ricci Lucchi (1972) fall within the middle fan as defined by Normark (1970), illustrated in figure 8.2.1.

Mutti (1985) suggested a fan model where the volumes of gravity flows within the system were a function of sea level changes. The new model opened up for three different deep-water depositional systems. During sea-level lowstand there would develop channels with detached lobes, while sea-level at shelf edge developed channels with attach lobes and finally, where sea-level stand was above shelf edge, channel-levee complexes without lobes developed.

Shanmugam & Moiola (1988) separated deep-sea systems into four types based on tectonic setting. The groups of fan development of this classification are called immature passive margin fans (North-Sea type), mature passive margin fans (Atlantic type), active-margin fans (Pacific type) and mixed-type settings. However, this classification system has some inherent problems. For instance, both the active-margin type and the passive-margin type are typically sand-rich.

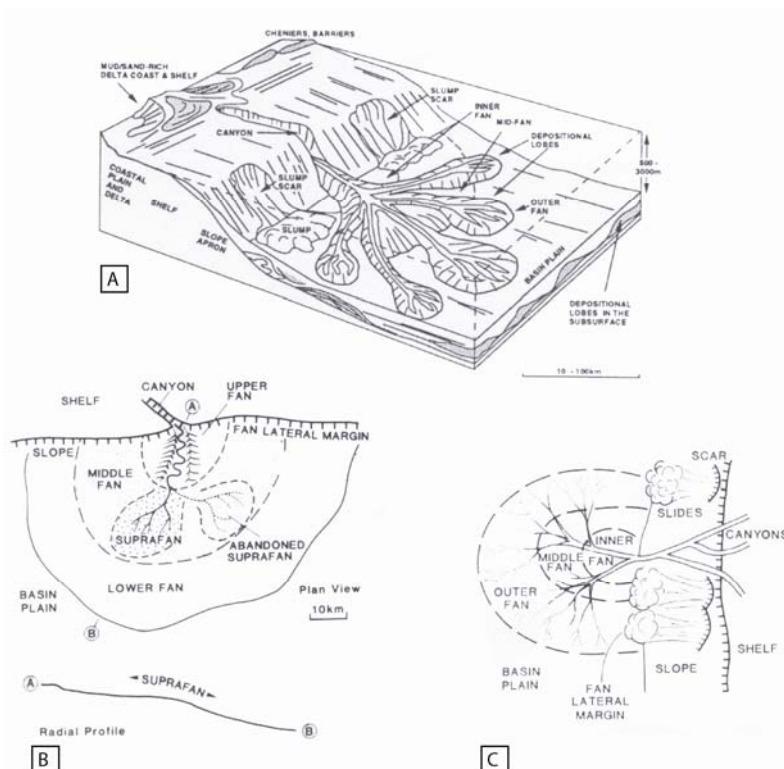


Figure: 8.2.1. Different depositional models of submarine fans. A: Reading & Richards (1994), a sand/mud-rich submarine fan. B: Submarine fan model of Normark (1970, 1978) and C: Model of Mutti & Ricci Lucchi (1972) based on observation in ancient systems.

Problems with classification systems led to two different approaches in the 1990s. One was based on a hierarchical sense as in the same way as was being done for fluvial and aeolian sequences (Mutti & Normark, 1987; Ghosh & Lowe, 1996), the other method developed further an environmental classification of deep-sea systems (Reading, 1991; Reading & Richards, 1994).

The first approach established a number of elements, each bounded by a distinctive surface and containing a particular facies. Mutti & Normark (1987) named the largest scale the first order, following the hierarchical principle of sequence stratigraphers, whereas Ghosh & Lowe (1996) followed the facies modellers starting with the smallest unit as first order. Reading & Richards (1994) introduced a classification system based on the volume and grain-size of available sediments and the nature of supplying systems. Three different supplying systems include point-sourced submarine fans (figure 8.2.1), multiple-sourced submarine ramps and linear-source slope aprons that might be mud-rich, mud/sand-rich, sand rich or gravel-rich, thus resulting in twelve different systems.

The latest approach to a classification scheme was suggested by Piper & Normark (2001). They included evaluation of sandy and muddy elements rather than classifying entire systems as either sandy or muddy. In addition to source-sediment volumes and grain size, turbidity processes and basin morphology are important.

It is difficult to compare modern fans with ancient systems. Modern fans are generally delta fed and mud rich, but have a low probability of being preserved in the ancient record, and the study of modern systems are focused on the morphology and surface geology. The ancient submarine fans are instead described detailed with facies and stacking pattern of facies associations in field. In addition, both modern and ancient submarine fans are revealing a high degree of variability in scale, mean grain size and facies distribution (Pickering *et al.*, 1989).

8.3 Model of the Lillehammer Submarine Fan Complex

The Brøttum Formation recorded at Lillehammer represents a deep marine turbidite fan complex comprising major channels, channel-levees, lobes and distal basin plain. The facies associations described and interpreted in chapter 6 correspond to architectural elements and building blocks of submarine fans (Normark, 1970; Normark & Piper, 1972; Mutti, 1992).

The general vertical trend of the Brøttum Formation succession recorded in the Lillehammer area is progradational from an outer fan environment at the base to a mid fan environment in the upper part. The distal outer fan of the system consists mainly of basin plain mudstone, prograding lobe successions that occasionally are channelized and basin floor channels. The interpretation of an outer fan environment in the lower part of the logged succession is supported by observation of thick layers of black shale at Vingnes west of Lake Mjøsa and north in the Maihaugvegen road. These locations can both be traced to lie stratigraphically below the lowest part of the logged section. The more proximal part of the fan complex, interpreted to be the mid fan environment, consists of facies associations representing prograding lobes with associated channels, major channels, channel-levees and transitional basin plain associated with intra lobe environments.

The Lillehammer Submarine Fan Complex represents a deep-marine clastic system close to a mixed mud/sand-rich system supplied from a point source, as defined by Reading & Richards (1994). The percentage of shale and silt based on facies are 36. The sand in the system is mainly to be found in lobes; however 27 % of the facies association records are comprised of channel sandstones.

The sections obtained in the Maihaugvegen, Dampsagvegen and the Messenlivegen can be correlated, their positions are shown in figure 2.2.1 and strike/dip of these beds in the area is illustrated in figure 2.2.2. The average strike and dip is both 83° and are used for calculating the distance between the sections. The distance between the top of the Maihaugvegen and the base of the Dampsagvegen section is approximately 285 meter

and the top of the Dampsagvegen section and the base of the Messenlivegen section are overlapping if the average strike and dip of 83° is to be true.

From these three logged sections are at least two fans recognised, probably three.

The first fan is registered in the bottom of the Maihaugvegen section, in the first 79 meters. The top is draped by hemipelagic mud that may indicate that the system was abandoned for a time. The new upward coarsening lobe successions succeeding the hemipelagic mud is reflecting the activation of a new fan system. The second fan is represented in the upper part of the Maihaugvegen section, the Dampsagvegen and the lowest part of the Messenlivegen section. Thick deposits of facies association 1.1 (basin plain- thin bedded turbidites) in the Messenlivegen section from 229-253 meter completely dominated by clay and silt fraction may indicate a major lateral shift of the fan. The major channel successions on the upper part of the Messenlivegen section right above the basin plain facies association may be part of a new fan (number three) where channels were meandering and moving into the area. These three logged sections are alone illustrating the prograding system from an outer fan to a mid fan environment. The top of the logged section in the Messenlivegen shows a lower dip than the lower part of the section. The thick sandstone packages observed above the Messenlivegen section are nearly horizontal with a low gradient relief as registered in the Haugen area (figure 2.2.2). The beds logged in the south eastern area represent the top of a large synclinal while the more northwestern part of the area represent the flank of the synclinal.

The logged section in Fredrik Colletts veg and the logged sections in the Åsmarkvegen locality are more than 830 meter from the Fredrik Colletts veg section and are difficult to correlate. However, the beds logged in this area are probably representing the same fan system as the uppermost fan in the Messenlivegen section. The facies associations in these localities are dominated by lobes evolving into channel-levees and major channels in the upper part of the Åsmarkvegen section. The top of the Åsmarkvegen 3 section is ending up in a very thick package of stacked channel sandstone bodies, representing the same environment as in the top of the Messenlivegen locality. The logged sections in Fredrik Colletts veg and the Åsmarkvegen locality are thus

representing the same fan as for the upper part of the Messenlivegen section with a lateral shift.

A conceptual model of the Lillehammer Submarine Fan Complex is presented in fig. 8.3.1. The vertical logg is a simplified development of the submarine fan comprising basin plain, upward coarsening lobes and upward fining channel infill. The top of this system is not registered, neither is the base. However, the uppermost thick sandstone packages observed above the Messenlivgen and the Åsmarkvegen 3 sections are included and may represent the outer part of the inner fan environment. The base of the conceptual model is also including thick black shale succession as registered below the Maihaugvegen section. Thickness of each fan interpreted in this system is hard to estimate due to little information on either base or top of most of them. The second fan starting in the middle of the Maihaugvegen section and may include the Dampsagvegen section and the first part of the Messenlivegen section are approximately 400 meters, comprising 10 lobes, and are not succeeded by stacked channel sandstones. The lower most part of the Messenlivegen section is interpreted to be part of a lobe-channel (FA 2.2), but may be part of the basin floor channel infill (FA 3.1) as interpreted in the uppermost part of the Dampsagvegen section.

The fan that is thought to start in the Messenlivegen section (at 229 meter) is at least 170 meter, when including estimated 100 meter of stacked channel sandstones in the Vårsetergrenda and Røyslimoen area south-east of the Messenlivegen locality results in a 300 meter thick system.

The model in figure 8.3.1 illustrate the prograding system where the lowermost part is represented by figure A, basin plain and figure B, stacked lobes, the outer fan setting.

The upper part of the logg represent a mid fan setting with braided major channels.

The depositional model of Mutti & Ricchi Lucchi (1972) in figure 8.2.1 illustrate the same inner, middle and outer fan parts of a prograding submarine fan as described for the Lillehammer Submarine Fan Complex.

Position of logged sections in model

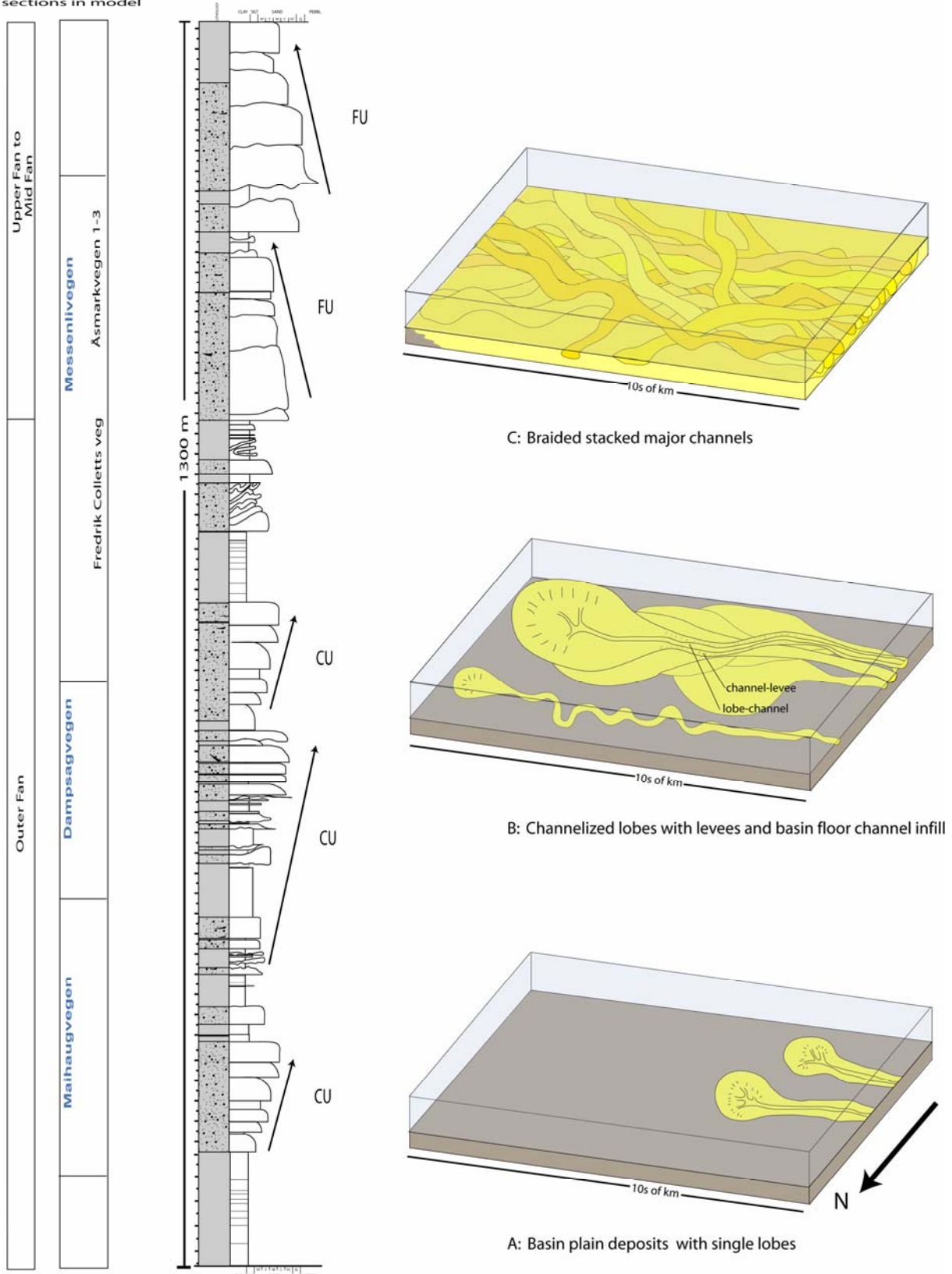


Figure 8.3.1. An idealized fan progradation within the Lillehammer Submarine Fan Complex. The outer fan comprising basing plain and lobes while the mid fan is dominated by major channels. FU= Fining upwards, CU = Coarsening upwards.

The size of the fans representing a mixed mud/sand-rich system like this is thought to be moderate, but varies according to volumes of sediments and accommodation space. Reading and Richards (1994) estimate these systems to be in the order of 500-3000 meter thick and 10-100 km long.

The total thickness of the system is approximately 1300 meter when including a couple of hundred meters of shale below the logged section and approximately 100 meters of stacked channel sandstones succeeding the section. The Lillehammer area is approximately 25 km east of the most western part of the Hedmark Basin deposits, which means the succession logged in the Lillehammer is at least 25 km from the basin margin. The lateral extent of the fan complex in down slope direction is therefore suggested to be in the order of at least 50 km.

There are very few data indicating paleocurrent direction in the logged sections. Four measurements from grooves interpreted in the Maihaugvegen and the Åsmarkvegen localities are plotted in figure 8.3.2.

These data demonstrate an average paleocurrent trend of $88,5^\circ$ or $268,5^\circ$. All data measured are distributed within a sector of 64° . The little deviation of azimuths recorded could imply they are representative data of the paleoflow. Paleocurrent structures measured earlier indicate that the sediment was supplied mainly axially from the south and laterally from the west (e.g. Nystuen, 1987). As a conclusion of this are the sediments in the Lillehammer area interpreted to be deposited from west towards east in the deep marine fan environment of the Hedmark Basin.

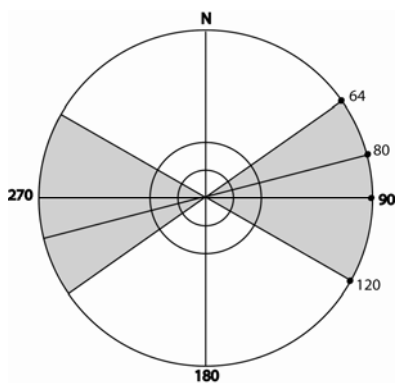


Figure 8.3.2 Paleocurrent trends in the Brøttum Formation, the Lillehammer area.

Controlling factors

Basin configuration and local tectonic features on the sea floor contribute to variability in fan shapes. Fan shaped deposits as discussed here are more likely to develop in large open basins than in small restricted basins (Bouma *et al.*, 1985).

Position of the Brøttum Formation in the Hedmark Basin is illustrated in figure 7.3.3. This is a large rift basin and tectonic activity is thought to be the most important controlling factor of the development of the Lillehammer Submarine Fan Complex.

The major factors controlling the development of a submarine fans and other deep marine sedimentation is tectonic activity, sea-level changes, climatic variations, or a combination of these factors (Stow *et al.*, 1996). However, sediment supply may be the most important single factor that controls the depositional type. Sediment supply is regulated by tectonic activity and morphology of the source area, frequency and magnitude of flows and climate.

Local factors as depth of water, shape and size of the basin, synsedimentary tectonic and differential compaction are local factors that may affect the deep water deposition and shape of fan.

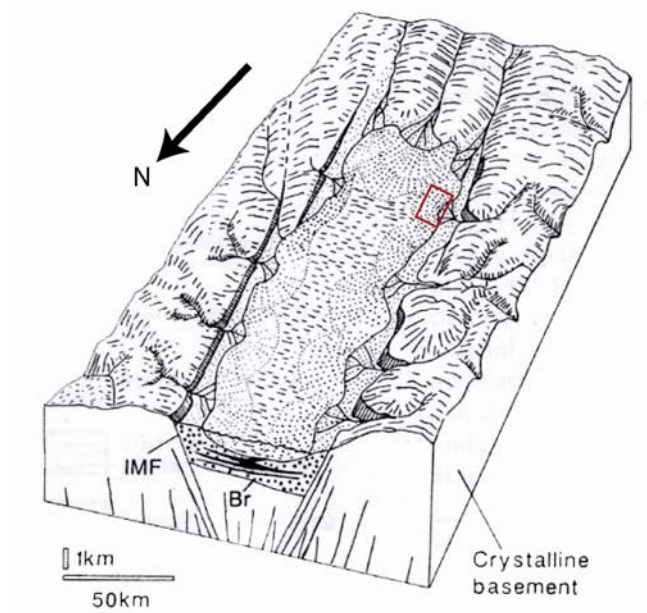


Figure 8.3.3. The Brøttum Formation in the Lillehammer area located in the Hedmark Basin, illustrated with a red square. Modified from Nystuen (1987).

Submarine fans are fed either from canyons associated with a sediment-rich shelf, a moderately sized mixed-load delta or a coastline (Stow *et al.* 1996). The Hedmark Basin is a large rift basin, and the fan complex is therefore not constrained by the basin topography. The system described here is probably fed directly from a river. The narrow margin of the basin gives little time for the sediments to be reworked by tides and waves. This may explain the high clay content in sandstones as described in chapter 5.

The lack of very coarse clastic submarine sediments like conglomerates in the sedimentary record may indicate that the point source supplying the system was too far away from the Lillehammer site during the depositional time. By this reason, the coarsest debris, as boulder and gravel, were dropped in an inner fan that is not recorded in the Lillehammer area. However, the stratigraphically upward transition from a basin plain environment to an environment completely dominated by aggrading major channels, as in The Lillehammer stamp mill locality, suggests an overall prograding system. The upward fining channel deposits are indicating minor sea level rises controlled by sea level fluctuations. Fan shape is controlled by sediment type. An increase in sand content leads to a decrease in levee stability and increased channel switching as recorded in the top of the Messenlivegen and Åsmarkvegen 3 section.

8.4 Comparison with the Cretaceous Vøring Basin on the Mid Norway shelf

The Vøring Basin, located on the outermost Mid Norway shelf includes basin-floor fans deposited during the Campanian-Maastrichtian in Late Cretaceous. The deep Late Cretaceous Vøring Basin has a complex history including crustal extension as well as phases of compression and faulting of the western marginal ridge of the basin, the Gjallar Ridge (Brekke 2000). A presentation of the structural and sedimentological evolution of the Vøring Basin submarine fan systems is compiled by Fjellanger *et al.* (2005). The following discussion is based on this publication. Submarine fans in the Vøring Basin reveal both similarities and dissimilarities with the Lillehammer Submarine Fan Complex.

Interpretation of sedimentary processes and depositional environment of the Vøring Basin is based on sedimentological core description for all exploration wells drilled in the area. Six main sedimentary facies groups have been identified in the Vøring Basin cores (figure 8.4.1).

The facies recognized in the Vøring Basin (VB) are comparable with the facies interpreted for the Lillehammer Submarine Fan Complex (LSFC). The abbreviations VB and LSFC are applied below for simplicity in the further discussion.

Facies T1 (VB), graded sandstone, includes the Bouma divisions as described for facies C1 (LSFC), normal graded sandstone. Inverse graded sandstone representing facies C1 (VB) is not observed in the Lillehammer area. Stratified sandstone, facies T2 (VB) is observed and described under facies C1 (LSFC), normal graded sandstone. Facies S1, overturned deposits (VB) occurs in FA 5.1 (channel-levee). Facies C2, top only graded sandstone (VB) corresponds to facies C3 (LSFC), non graded sandstone. Facies H1, heterolithic sandstone (VB) may occur in FA 1.1, basin plain thin-bedded turbidites, or FA 5.1, channel-levee, interpreted in the Lillehammer Submarine Fan Complex. Figure 8.4.1 illustrate where the different facies dominate in the depositional model.

The dominant depositional process in the Vøring Basin is interpreted to be concentrated density flows, in the sense of Mulder & Alexander (2001), see also figure 4.3.

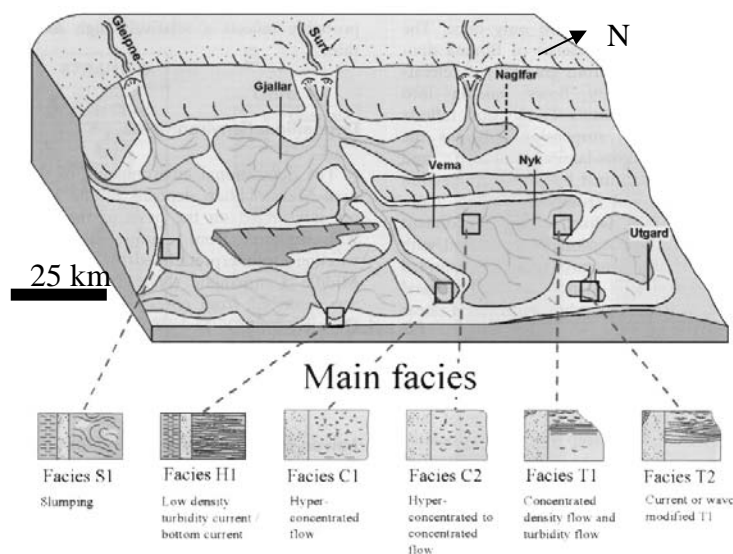


Figure 8.4.1 A schematic illustration of the depositional environments of the Upper Cretaceous fan systems in the Vøring basin. Typical locations of the main facies are shown below. From Fjellanger *et al.*

(2005). North direction and approximately scale is found from structure map (fig. 14) in Fjellanger *et al.* (2005). Modified from Fjellanger *et al.* (2005).

The cores from the wells drilled at the Nyk High, Vema Dome, and Utgard High represent depositional systems from the Lower-Middle Campanian time, while the core drilled at the Gjallar Ridge is representing a Maastrichtian system.

The Nyk High is represented by stacked, massive, normally graded sandstones deposited by hyper-concentrated and concentrated density flows passing into turbidity currents. The thickness of the succession suggests an aggradational sheet system. The sediments are interpreted to represent mid-fan position at the termination of the main fan channels, thus corresponding to the uppermost part of the logged sections in the Messenlivegen and the Åsmarkvegen 3 locality.

The same deposits that dominate in the Nyk High succession are recorded in the core drilled at the Vema Dome. However, a higher degree of sandstone amalgamation and more abundant shale clasts dominate in this area. The depositional succession on the Vema Dome is thought to represent the same basinal position as for the Nyk well, a mid fan position.

Deposits in the Utgard High shows alternating graded and heterolithic sandstones with a thick unit of massive sandstone at the top. The Utgard High is therefore interpreted to represent a more distal part of the fan than interpreted for the Nyk and Vema Highs, see figure 8.4.1 of position in fan. The depositional succession at the Utgard High may represent the same environment as interpreted for the Maihaugvegen sections in the Lillehammer Submarine Fan Complex.

A uniform character of the sandstone beds in the Nyk-Vema area indicates that the supply of sand was governed by one or a few relatively stable point-sourced feeder system. However, the well sorted, fine-grained nature of most sandstone units indicates that the sediments may have been derived from a relatively shallow outer shelf environment on which the sand has become sorted by shallow-marine current activities. Canyons have dissected the shelf-slope break leading the sorted sediments out in a wide deep basin; the depositional development was probably controlled by fault intersections

or relay ramps. This palaeobasinal setting is quite different from the Hedmark Basin where sediments probably were supplied more and less directly from rivers across a very narrow shelf, or may be no shelf at all, into a steep submarine slope, resulting in poorly sorted sandstone (see chapter 5). If the hinterland bedrock had a uniform grain composition there could be a possibility of a direct fluvio-deltaic source also to the Vøring Basin according to Fjellanger *et al.* (2005).

The Upper Campanian-Lower Maastrichtian submarine depositional clastic successions cored in the Gjallar Ridge in well 6704/12-1 are dominated by normal graded sandstones (figure 8.4.2). Depositional processes are interpreted to be density flows with a transition to turbidity current flows. The successions at the Gjallar Ridge are suggested to represent mid to outer fan position of the turbidite system. The same type of environment is also interpreted for most of the logged sections in the Lillehammer area. The most common facies is normal graded sandstones in both cases. The interpretation is supported by a uniform nature of sandstones and scarcity of coarse-grained and amalgamated sandstones associated with inner fans. The Campanian-Maastrichtian succession of well 6704/12-1 reveals an overall similarity in thickness (about 1300 meters) and stacking pattern of mudstone and sandstone units as compared with the Lillehammer Submarine Fan Complex (see figures 8.3.1 and 8.4.2)

Distances from shelf edge (Vøring Basin) and basin margin (Hedmark Basin) appear to have been in the same order, about 25-30 kilometers, and a corresponding dimension of about 50 kilometers for the fans in both basins. In this respect and in terms of facies, facies associations, thickness and overall architecture the submarine fan complexes in the Vøring and Hedmark basins appear rather similar, despite different types of basin.

The major difference between the turbidites of the Upper Cretaceous successions in the Vøring Basin and the Neoproterozoic turbidites in the Hedmark Basin is related to the degree of sorting and volume of clay matrix content. The higher content of clay matrix and much less sorted sandstones in the LSFC compared to the Vøring Basin turbidites is thought to be related to differences in the structural framework of the two basins, alternatively to major differences in lithology of bedrock source rocks of the two basins.

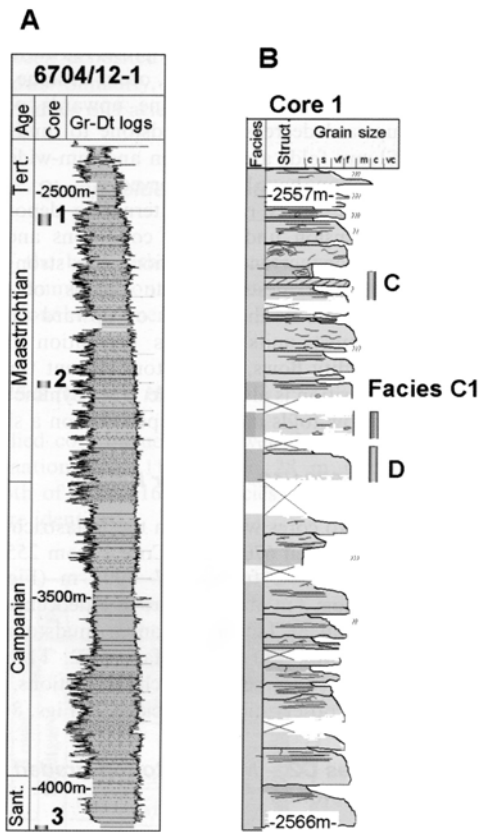


Figure 8.4.2 shows Gr-Dt log and core sample from well 6704/12-1 on Gjallar Ridge. Log from 3500m to 2500 m shows similar pattern as for the LSFC. The succession may contain two fans where the first is introduced with a thick package of shale as for the Maihaugvegen section described above.

9 Seismic modelling

9.1 Introduction

A synthetic seismic model is generated for one of the logged sections for the aim to discuss seismic resolution of a turbidite system under respectively shallow and deep burial on a general scope of view. The stratigraphy and vertical arrangement recorded in the Brøttum Formation are thus applied for generating synthetic seismic data corresponding to this type of deep-marine turbidite succession. The petrophysical data applied for the succession is by this reason taken from overall data bases for siliciclastic deposits at different depths of burial.

The lithological units from the logged section in the Messenlivegen locality is upscaled, and this procedure has resulted in intervals of shale and sand as illustrated in figure 9.2.1. The eleven beds (numbered from 1 to 11) have a thickness variation between 11 and 79 meters within the 400 meter thick modelled section. The 1D synthetic seismograms generated are a product of a source pulse convolved with the reflectivity model representing the Messenlivegen section.

9.2 Petrophysical data

To create a synthetic seismogram, a geometrical model with petrophysical properties of densities, p- and s- velocities are required for each respective layer in the model.

Compaction of sediments due to stress of overburden reduce the porosity of the sediments and increase the sediment density of the rock. As the physical properties of the rock changes with depth, p- and s-velocities will change when propagating through a sedimentary column.

Processes contributing to compaction and porosity loss are: 1) Mechanical compaction which comprises rearrangement, bending, ductile deformation and breakage of grains. 2) Chemical compaction which involves dissolution at contacts between grains or along stylolites and a corresponding precipitation of minerals (cement) in the pore space. In addition, dissolution of thermodynamically unstable grains that are load bearing is contributing to the chemical compaction process (Bjørlykke, 2003).

The intensity of compaction or porosity loss varies considerably with the lithology at the same effective stress as a result of different mineral composition and primary sorting of grains (Bjørlykke, 2003).

Mechanical compaction is mainly dominant in the upper 2-3 km in a sedimentary basin, while chemical compaction control compaction intensity below 2,5 km of sediments where temperatures have reached 80-100°C. The magnitude of the mechanical compaction depends on the effective stress in the basin and the mechanical strength of the sediment grain framework (Bjørlykke & Høeg, 1997). Shales without significant cementation are highly compressible down to 2 km and have a low shear strength which is indicative by the low seismic velocities below 2 km/s (Bjørlykke & Høeg, 1997).

When fine grained particles like clay and fine silt get deposited, the resulting mud sediment is loosely packed, uncemented and with a very high interstitial water content. This results in a very high porosity (80%) and low velocities. However, within the first 1000 meter of burial this type of sediment loose more than half of the porosity due to mechanical compaction, which gives a denser packing (Gilles, 1997).

Moderately to poorly sorted sand deposits with lithic fragments show a higher degree of compaction at low to moderate stresses than well-sorted sands (Pittman & Larese, 1991). In the absence of carbonate cements, well sorted sandstones keep their physical properties down to 2,5-3 km.

Where chemical compaction starts as a function of mineralogy and temperature, the quartz cementation in sandstones prevents further mechanical compaction (Bjørlykke, 2003). In shales, dissolution of smectite and precipitation of illite are the most important reaction.

As a result of larger surface area, fine grained sandstones will compact faster than coarser grained sandstones under the same temperature condition during chemical compaction. This is in contrast to mechanical compaction where well-sorted coarse grained sandstones are more compressible.

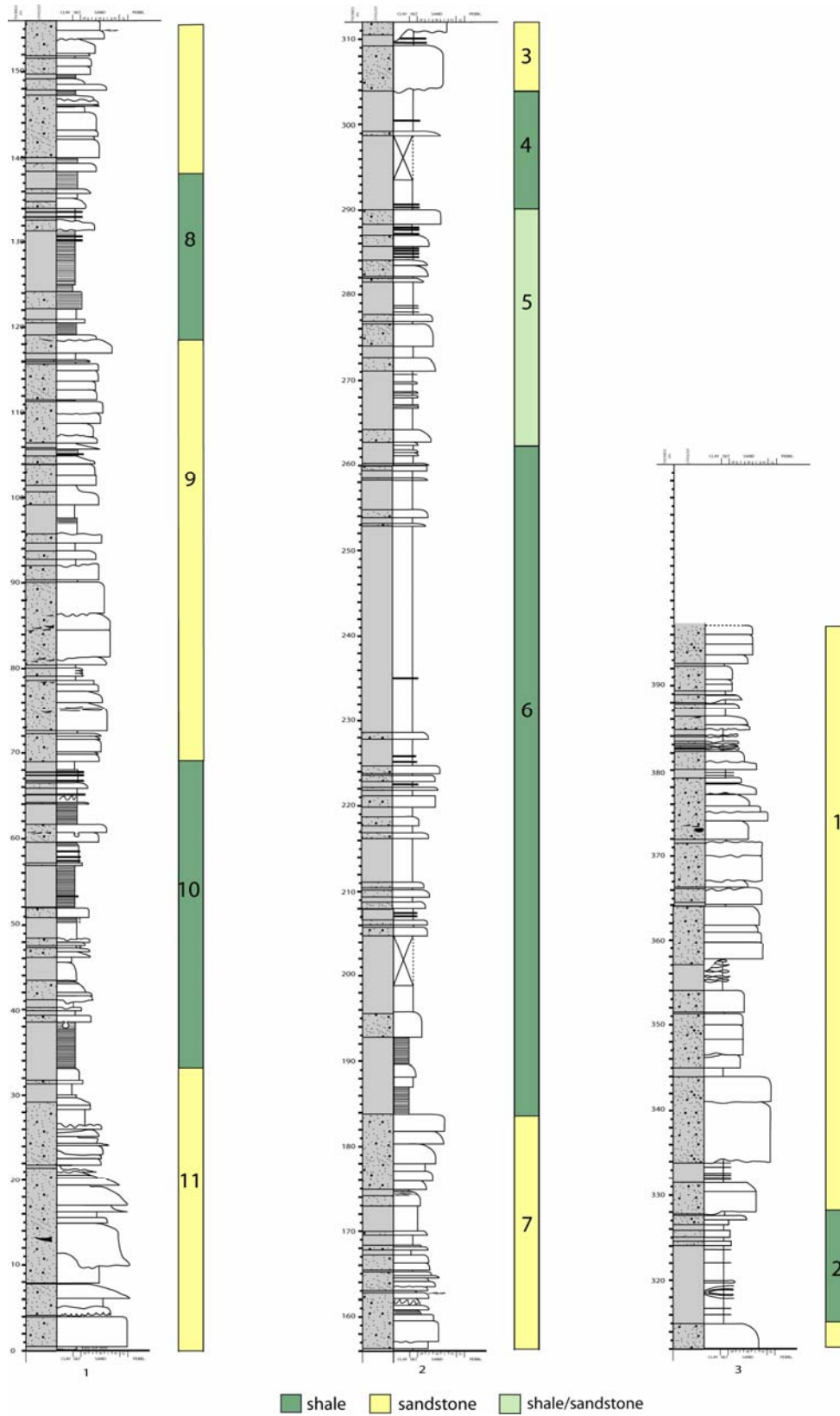


Figure 9.2.1 Upscaled modell of the Messenlivegen section. Layers are numbered from the top and down.

There are several published porosity-depth relations for both shale and sandstones.

The porosity-depth trends used in this modelling are shown in table 9.2.1 below and are based on average values of several porosity-depth trends published (Gilles, 1997 p 224-225). The porosity of sandstone is calibrated towards 15 % estimated clay content.

Porosity values used for shale is 80 % near seafloor, 12 % at 1500 m and 7 % at 4000 m.

Sandstone porosities at 1500 meter is 25%, at 2000 m 15 % and at 4000 m 10 %. Densities are calculated from these porosities and a linear formula is assigned to each layer or block in the two different models.

The bulk densities for shale and sandstone calculated for the two different cases are found from the bulk density formula:

$$\rho_b = \rho_f \phi + \rho_m (1 - \phi)$$

ρ_b = bulk density

ρ_f = density of fluid (brine water)

ρ_m = density of solid phase (lithology)

ϕ = porosity

$$\rho_{shale} = 2,67 \text{ g/cm}^3 \text{ and } \rho_{sandstone} = 2,65 \text{ g/cm}^3$$

Table 9.2.1 Porosity trends within the modelled section for case 1, 1500 meter of overload and case 2, 3500 meter of overload. Sandstone- and shale-layers in the Messenlivegen section represented by numbers 1-11, with the respective density values for each layer.

Layers case 1	Thickness	Density	Layers case 2	Thickness	Density
Water	1000m	1,000 g/cm ³	Water	1000m	1,000 g/cm ³
Shale overburden (mechanical compacted)	1500 m	1,361-2,340 g/cm ³	Shale overburden (mechanical compacted)	2500 m	1,361-2,470 g/cm ³
1 Sandstone	69 m	2,250-2,257 g/cm ³	Shale overburden (chemical compacted)	1000 m	2,470-2,560 g/cm ³
2 Shale	13 m	2,351-2,353 g/cm ³	1 Sandstone	69 m	2,460-2,464 g/cm ³
3 Sandstone	11 m	2,258-2,259 g/cm ³	2 Shale	13 m	2,56 g/cm ³
4 Shale	14 m	2,355-2,357 g/cm ³	3 Sandstone	11 m	2,465-2,466 g/cm ³
5 Shale/sandstone	27 m	2,300 g/cm ³	4 Shale	14 m	2,560 g/cm ³
6 Shale	79 m	2,361-2,374 g/cm ³	5 Shale/sandstone	27 m	2,500 g/cm ³
7 Sandstone	45 m	2,271-2,276 g/cm ³	6 Shale	79 m	2,560 g/cm ³
8 Shale	20 m	2,381-2,384 g/cm ³	7 Sandstone	45 m	2,473-2,475 g/cm ³
9 Sandstone	50 m	2,278-2,283 g/cm ³	8 Shale	20 m	2,560 g/cm ³
10 Shale	36 m	2,393-2,398 g/cm ³	9 Sandstone	50 m	2,477-2,480 g/cm ³
11 Sandstone	33 m	2,286-2,290 g/cm ³	10 Shale	36 m	2,560 g/cm ³
Shale (not part of model)	-	2,404 g/cm ³	11 Sandstone	33 m	2,482-2,484 g/cm ³
			Shale (not part of model)	-	2,560 g/cm ³

Experimental studies have shown that there are relatively clear relations between seismic velocities, porosity, and clay content (Vernik & Nur, 1992). A small amount of cement (like quartz cementation) at the grain contacts increases the stiffness of the sediment and thereby the seismic velocity. Other factors that may also affect velocities in sedimentary rocks are pore fluid, grain size, sorting, grain to grain contacts per grain, pore pressure, anisotropy, contact stiffness, and contact size (Storvoll & Bjørlykke, 2004).

The velocity-depth trends used for the different lithologies in the model are based on log data from the Norwegian Shelf (Storvoll *et al.* 2005). The velocity is increasing with depth as a result of reduced porosity in sediments and increased cementation. The velocity-depth trends are thus different in the upper 2,5 km where the cementation of quartz yet have not significantly increased the bulk density. Below this zone the chemical compaction are supposed to be significant and therefore results in increasing velocities. The velocities applied in the model are dissimilar for the two cases due to different overburden, the second case with 3500 meter of sediments are influenced by chemical compaction while the first case is not.

The velocity data discussed in Storvoll *et al.* (2005) are both sonic velocities and seismic velocities and are not directly comparable. However, the seismic velocity-depth curve is assumed to be close to a velocity –depth gradient estimated from sonic logs representing the same sedimentary package (Storvoll *et al.*, 2005).

Velocities representing sandstones under mechanical compaction (case 1) is taken from values representing sandstones from all wells studied in the northern North Sea (Storvoll *et al.* 2005, figure 6). The p-velocities from 1500- 2000 meter of burial corresponds to velocities of approximately 2400-2600 m/s. The shale units under same conditions have a lower p-velocity-depth trend (see figure 9.2.2), with a range from 2100-2556 m/s. These values are calculated from shaly units of Oligocene to Early Cretaceous age in the North Sea, which is similar to the normally compacted shale trend line published by Japsen (2000).

The velocity around 2,5 km of burial is a bit lower than the estimated trend line published by Storvoll *et al.*(2005, figure 5) for the same lithology, but are calibrated towards the velocity-depth trend used for chemical compaction of shale. The velocity-depth trend used for shales below 2,5 km (Storvoll *et al.*,2005 figure 9) are thus varying from 2500 m/s to 3050 m/s on the deepest buried layer (3500m).

The p-velocity for sandstones are higher than for shale units at the same depth, due to a higher framework volume, ranging from 3100-3450 m/s for the deepest buried model (Storvoll *et al.*, 2005 figure 8, Jurassic sandstones). Sandstones have generally higher velocities than shales due to cementation. The densities, though, are higher in shales, which may be a result of a denser packing of grains (Jakobsen, 2003).

The density and p-velocity depth trends for case 1 and case 2 are illustrated in figure 9.2.2-9.2.5 in the geophysical models generated. These data are used when performing the dynamic ray tracing and generating the synthetic seismograms described below. In addition to the overload, 1000 meter of water is added to the sedimentary column. S-velocities are calculated directly from p/s velocity ratios, for this study the ratio 1,7321 is used.

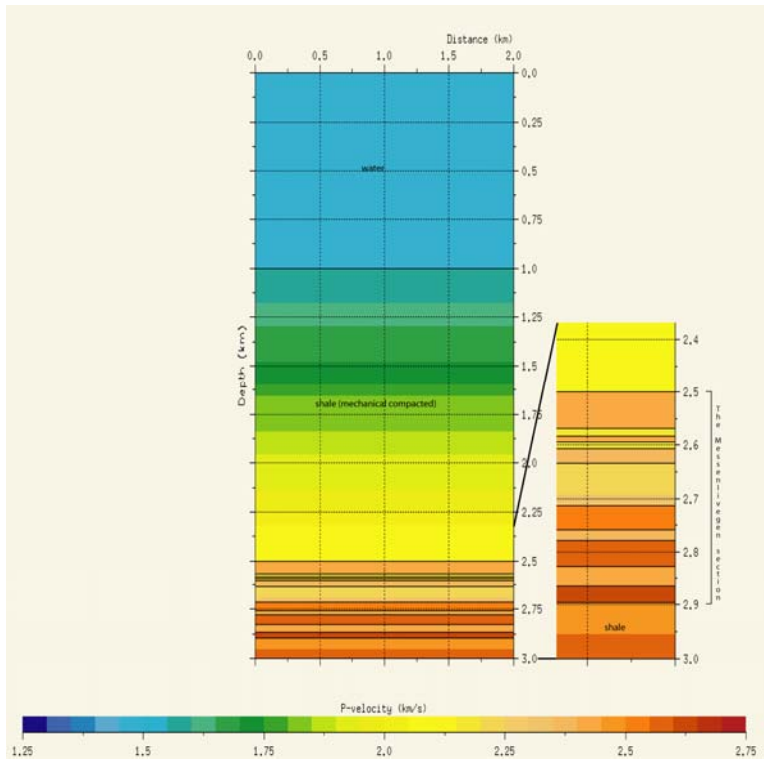


Figure 9.2.2 P-velocities for case 1, the modeled section is buried under 1500 meter of sediments.

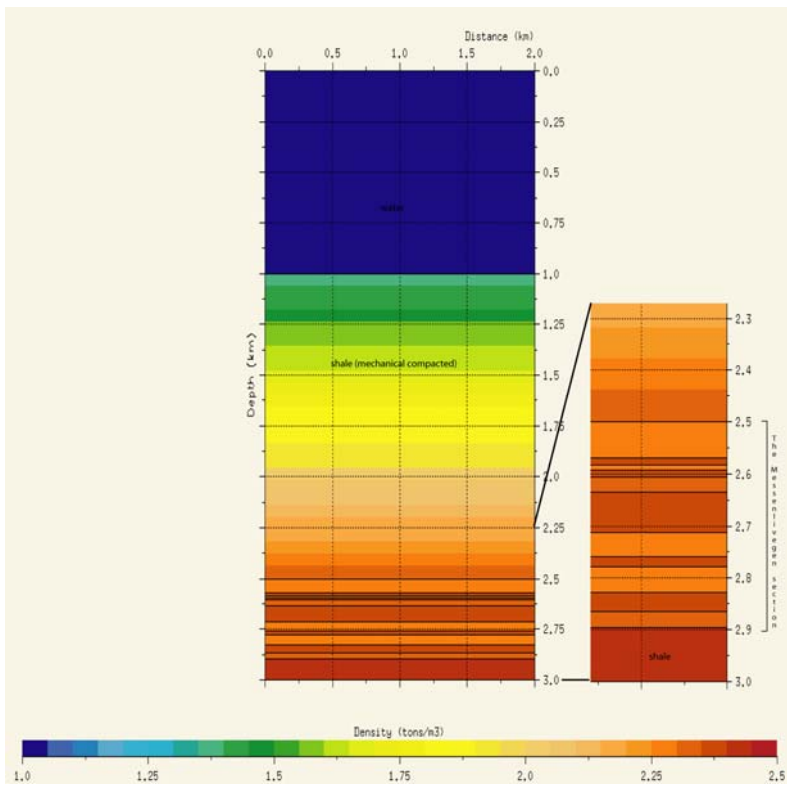


Figure 9.2.3 Densities for case 1, the modelled section is buried under 1500 meter of sediments.

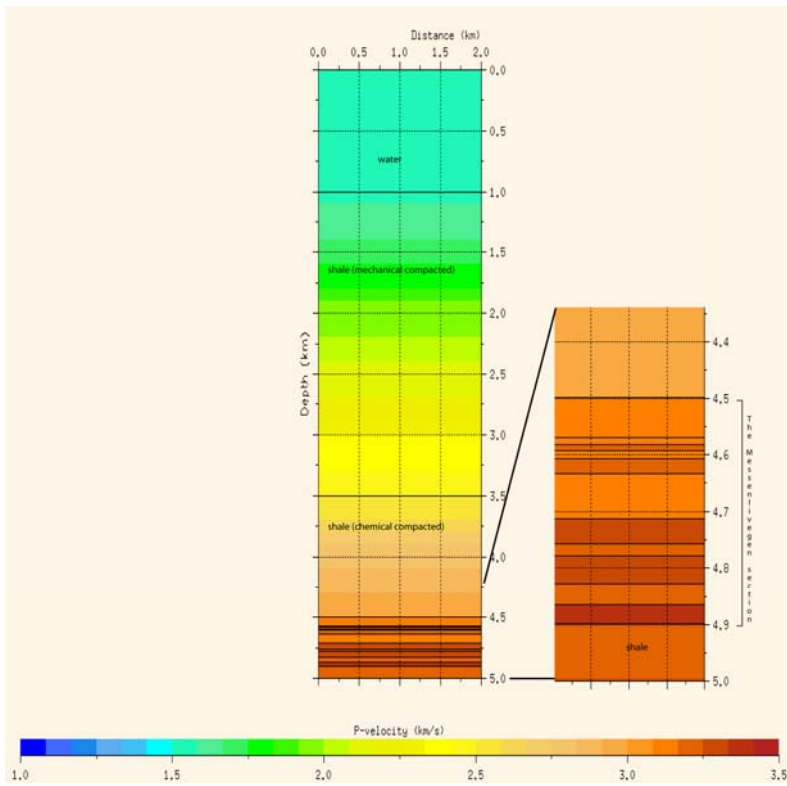


Figure 9.2.4 P-velocities for case 2 where the modelled section is buried under 3500 meter of sediments.

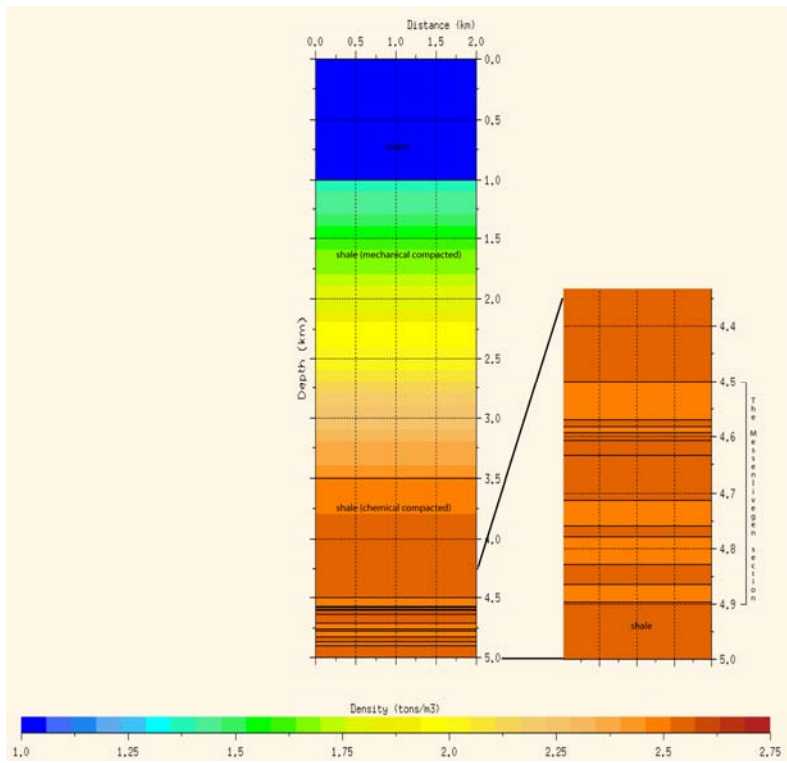


Figure 9.2.5 Densities for case 2 where the modelled section is buried under 3500 meter of sediments.

9.3 Methods

Seismic modelling involves generating traveltimes and amplitudes of seismic waves propagating through a specified sub-surface reflectivity model, which is associated with a specified velocity-depth model (Yilmaz, 1987).

The Norsar 2d Ray Modelling program is used to create 1D synthetic seismograms of the Messenlivegen section.

The geometrical models comprise flat horizontal layers as illustrated in figure 9.2.2-9.2.5. The horizons are defining blocks with respective petrophysical parameters as described in section 9.2. A survey is defined before the ray tracing is executed. Ray tracing uses the information of densities, p- and s- velocities to calculate the impulse of the reflectivity series which are needed for calculating synthetic seismograms. Normal Incidence Paths (NIP) is applied where each shot has only one associated receiver situated at the same position (SR points), hence zero offset.

The type of ray tracing used in this study is dynamic ray tracing. Dynamic ray attributes calculated are location of ray paths, traveltime along paths and dynamic properties of the seismic wave field such as geometrical spreading factors, wavefront curvature, and amplitude coefficients along the ray paths. In order to account for intrinsic attenuation in an approximative way, a wavelet with different center frequency for the shallow and deeper model is employed.

The convolution of a source signal $s(t)$ with the impulse response of the reflectivity model $r(t)$ yields the synthetic seismogram:

$$x(t) = s(t) * r(t)$$

In this study the Berlage wavelet has been used as a source signal, figure 9.3.1. The Berlage is a causal wavelet and differs from the symmetrical, zero phase Rayleigh and Ricker pulses which have their main peak pointed at the various reflectors. The choice of a Berlage

wavelet ensures sufficient flexibility for modelling a wide range of seismic waveforms observed in both field and processed data (Aldridge, 1990).

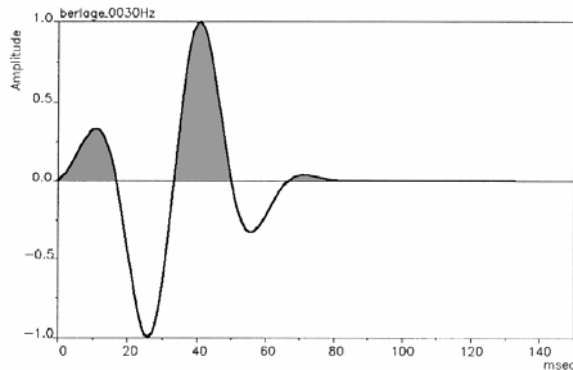


Figure 9.3.1 The Berlage wavelet

For the deepest buried model, a Berlage 20 Hz is applied, the result is further compared with a case with a hypothetical 100 Hz pulse as source signal to evaluate the differences. For the shallow model a Berlage 40 Hz pulse is selected.

Due to geometrical spreading and transmission losses of the source signal an exponential scale factor in time t ($e^{0.7t}$) is used to enhance the signal on the plot (figure 9.4.1).

9.4 Synthetic seismograms

All forward seismic models were generated using vertical-incidence ray tracing and a Berlage wavelet. A trough (white) represents a negative impedance boundary, and a peak (black) represents a positive impedance boundary.

The interfaces can only be fully resolved within the seismic model generated using a 100 Hz wavelet for the case two situation. However, this is not realistic and is only used to assist the interpretation of the 20 Hz wavelet case.

The seismic response can be approximated as a convolution between the reflectivity series and the source pulse.

The following equation describes the p-wave reflection coefficient (normal incident plane-wave) expressed by the differences in acoustic impedance (Z) across the surface:

$$R = (Z_2 - Z_1) / (Z_1 + Z_2)$$

Where Z_1 and Z_2 are the acoustic impedances of two vertically adjacent rock bodies respectively. Acoustic impedance (Z) is defined as the product of rock density (ρ) and seismic p-velocity (v_p). From this it can be inferred that reflection strength are increasing with increasing acoustic impedance contrast.

Description

Figures 9.4.1 and 9.4.2 illustrate the synthetic seismogram for shallow and deep burial. A hypothetical situation with a source pulse of 100 Hz is added for comparison in figure 9.4.1.

Within the 400 meter thick target zone there are 12 interfaces that theoretically could be seismically resolved in the synthetic seismograms. The first interface corresponds to the top of the first layer.

The variation in seismic resolution when using different seismic pulse frequencies is easy to observe, when considering the deep buried model (figure 9.4.1 B). However, the 100Hz case is not a realistic one, and is here included merely as an ideal reference.

Red arrows in figures 9.4.2 A and B indicate the expected time position of the various interfaces following from the spikogram.

When the acoustic impedance is increasing across a surface, the event will show a positive initial peak as for the first reflector in the shallow burial model. To make the interpretation easier, the arrows indicating the interfaces are referred to the first negative through of the pulse (cf. figure 9.3.1). This through is associated with a large amplitude and is therefore easier to detect.

Figure 9.4.2 A illustrates the synthetic seismogram under 1500 meter of overburden. The source pulse has a center frequency of 40 Hz. Vertical resolution depends upon the wavelength of the pulse. The minimum vertical resolution of a layer thickness is $\frac{1}{4} * \lambda$. This means that layers with thicknesses below $\frac{1}{4}$ of the wavelength is not perfectly resolvable due to destructive interference.

An average seismic velocity in the modelled interval for 1500 meter of burial is 2,3 km/s.

The average wavelength λ depends on the velocity and the frequency: $\lambda = v/f$

The wavelength are thus 57,5 meters and the seismic resolution is approximately 14 meters according to the $\lambda/4$ criterion.

A shorter pulse will improve the seismic resolution as shown in figure 9.4.2 A with the 100 Hz case. However, in a realistic situation attenuation with depth will result in lower frequencies and larger wavelengths.

From figure 9.4.2 A we see that interfaces 2-6 are more or less well resolved. The seismic response interferes due to thin layers of respectively 13, 11 and 14 meters. However, the position of the arrow indicating where the assumed reflection of each interface is expected, has a correct position regarding troughs or peaks. The true amplitudes are decreasing with depth, while in figure 9.4.2 A there is an increasing trend for the first interfaces representing layers 2, 3 and 4. This implies a constructive interference between the responses (tuning effects). The amplitudes are visually larger than for interface number 1 which is not the case when looking at the true amplitude magnitudes (spikogram at the bottom of figure 9.4.2 A and B).

Interfaces 7-12 have a seismic expression which corresponds to the true amplitudes. Positive amplitudes has an arrow pointing at a trough and negative amplitudes points at a peak. The small lobes associated with the Berlage wavelet has interfered, though the interfaces are resolved.

The 79 meter thick layer dividing the two fans thought to be present in the Messenlivegen can be identified from the seismic. However, the model discussed here is upscaled and assigned only two different lithologies. In a real situation the source pulse will penetrate all beds resulting in reflection seismic including more noise (intrabed multiples).

Figure 9.4.2 B shows the synthetic seismogram for the model under 3500 meter of overload. A 20 Hz wavelet is used as a source pulse. The average velocity in this interval is 3,20 km/s which results in a wavelength λ of 159 meters and a vertical seismic resolution of

approximately 40 meter. Layers below this thickness will therefore be difficult to resolve by the seismic.

The first reflection coefficient now gives a negative response and the first arrow should therefore point at a positive peak as can be seen from figure 9.4.2B. The negative sign of the reflectivity as opposed to the shallow burial case, is a result of differences in velocities and porosities used for the deep and shallow burial. Shales have a higher velocity and lower density at greater depths than sandstones. While under shallow burial sandstones are having the highest velocities and the lowest densities.

The amplitudes from the spikogram show that interface number 5 has a distinct low magnitude. This interface response is therefore not contributing much to the synthetic seismic. Number 5 interface has a low amplitude due to a lithology representing a mixed shale and sandstone properties. The acoustic impedance across this surface is therefore smaller.

The seismic responses of interfaces 2, 3, 4, 5 and 6 are expected to be larger when comparing with the true amplitudes in the spikogram. These layers are below the seismic resolution of 40 m and have therefore interfered with each other. This interference is destructive and results in weak reflections. Interface number 4 is positive and should therefore point at a through, this is not the case.

Interfaces 6 and 7 are both represented with a negative impedance. These interfaces are approximately 80 meters apart and therefore above the vertical resolution but with reversed polarity. Regardless interferences on both sides, this thick layer is still difficult to detect. However, one can sense a shift in seismic expression and therefore a possible shift in depositional pattern.

The amplitude magnitudes for interfaces 10 and 11 are fairly much the same as for number 2 and 3 according to the spikogram. This can not be seen from the synthetic seismogram. Interfaces 2 and 3 are distorted due to destructive interference caused by thin layers below the vertical seismic resolution. At the same time the last interfaces have probably caused a

constructive interference resulting in false strong reflectors. All reflectors from 8 to 12 are represented by peaks or troughs as expected from the spikogram.

The 20 Hz pulse used in this case is longer and therefore extends to a deeper time than in the seismogram generated for shallow burial. The main differences between the shallow and deep model are the number of interpretable events in the seismogram and their relative positions. The deep model has only 8 apparent events while the shallow model has 17.

Table 9.4.1 summarizes how well the different interfaces in the two models are resolved.

Table 9.4.1 Degree of resolution of each interface corresponding to the top of each layer.

Shallow burial		Deep burial	
<i>Layer</i>	<i>Resolved</i>	<i>Layer</i>	<i>Resolved</i>
1- 69m	Excellent	1- 69m	Good
2-13m	Less good	2-13m	Not good
3-11m	Less good	3-11m	Not good
4-14m	Less good	4-14m	Not good
5-27m	Less good	5-27m	Not resolved
6-79m	Less good	6-79m	Good
7-45m	Good	7-45m	Not good
8-20m	Good	8-20m	Less good
9-50m	Good	9-50m	Less good
10-36m	Good	10-36m	Less good
11-33m	Good	11-33m	Less good
12-----	Good	12-----	Good

Discussion

Both the reflection coefficients and the corresponding seismic resolutions are highly dependent on the petrophysical data used in the model. Densities of compact shale and sandstone have very similar values and porosities and velocities picked for each case are therefore the most sensitive values in the model. Small changes in porosities or velocities could give other results than illustrated here if the acoustic impedances changed accordingly and enough to change amplitude strengths and signs significantly. The values used in this study are selected from published porosity curves (Giles, 1997) and velocity-depth trends of same lithology in the North Sea (Storvoll *et al.*, 2005). Choosing values from trend lines are probably not the best match of values for this turbidite system, and for a more detailed study one should spend more time on evaluating porosity and velocity depth trends of turbidity deposits. This is beyond the scope of this study, which is why simple trend lines are used.

However, when creating synthetic seismogram there is often limited information available and in that sense this study can serve as a realistic example of a seismic modelling of a turbidite system.

Note that further seismic processing of the synthetic data are outside the scope of this thesis. Increased resolution could have been obtained if deconvolution techniques were applied.

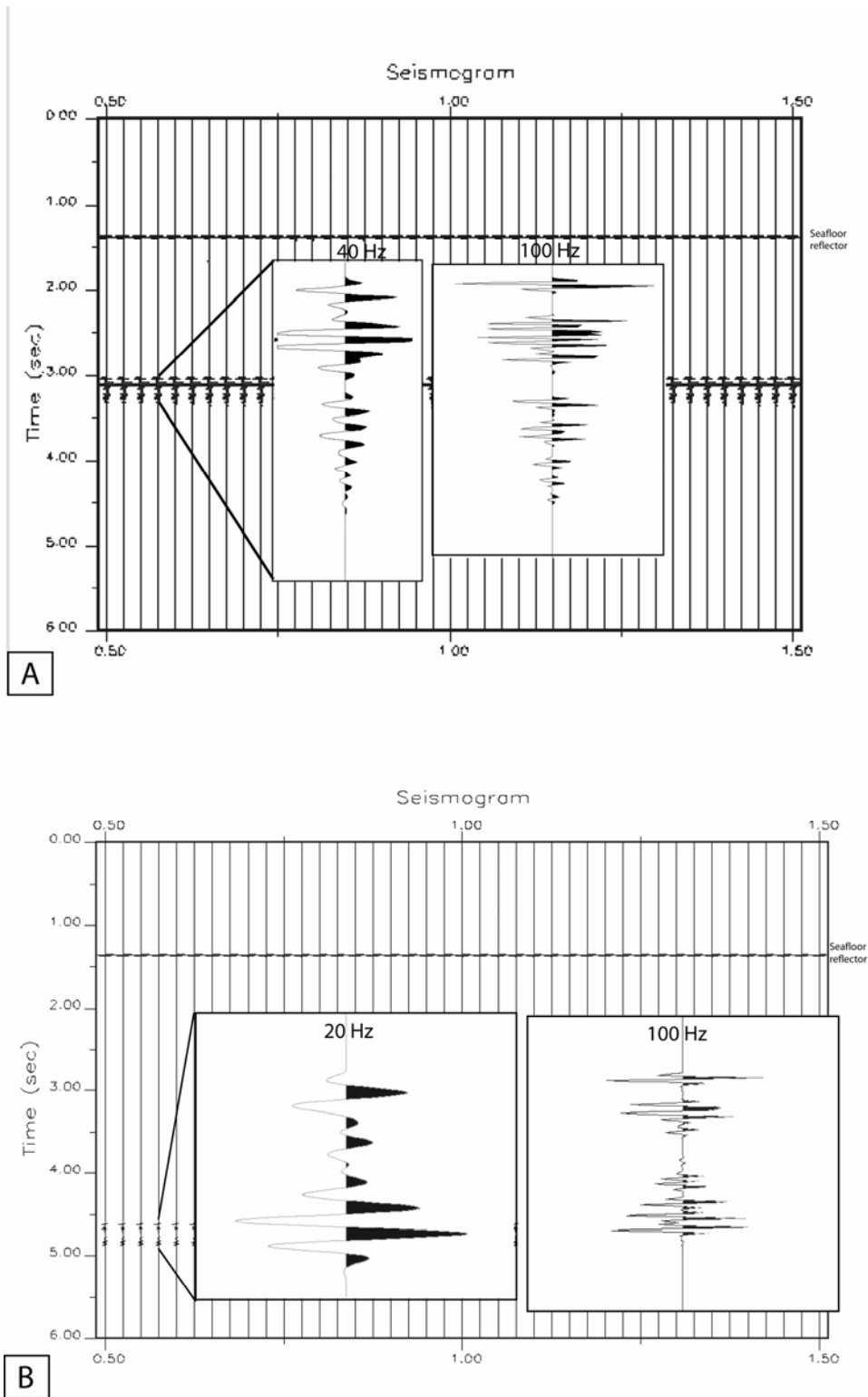


Figure 9.4.1 Synthetic seismograms. A) Seismogram illustrating model under 1500 meter of burial with a 40 Hz Berlage pulse. B) Seismogram illustrating model under 3500 meter of burial with a 20 Hz Berlage pulse. Seismograms with a 100 Hz pulse are included for comparison..

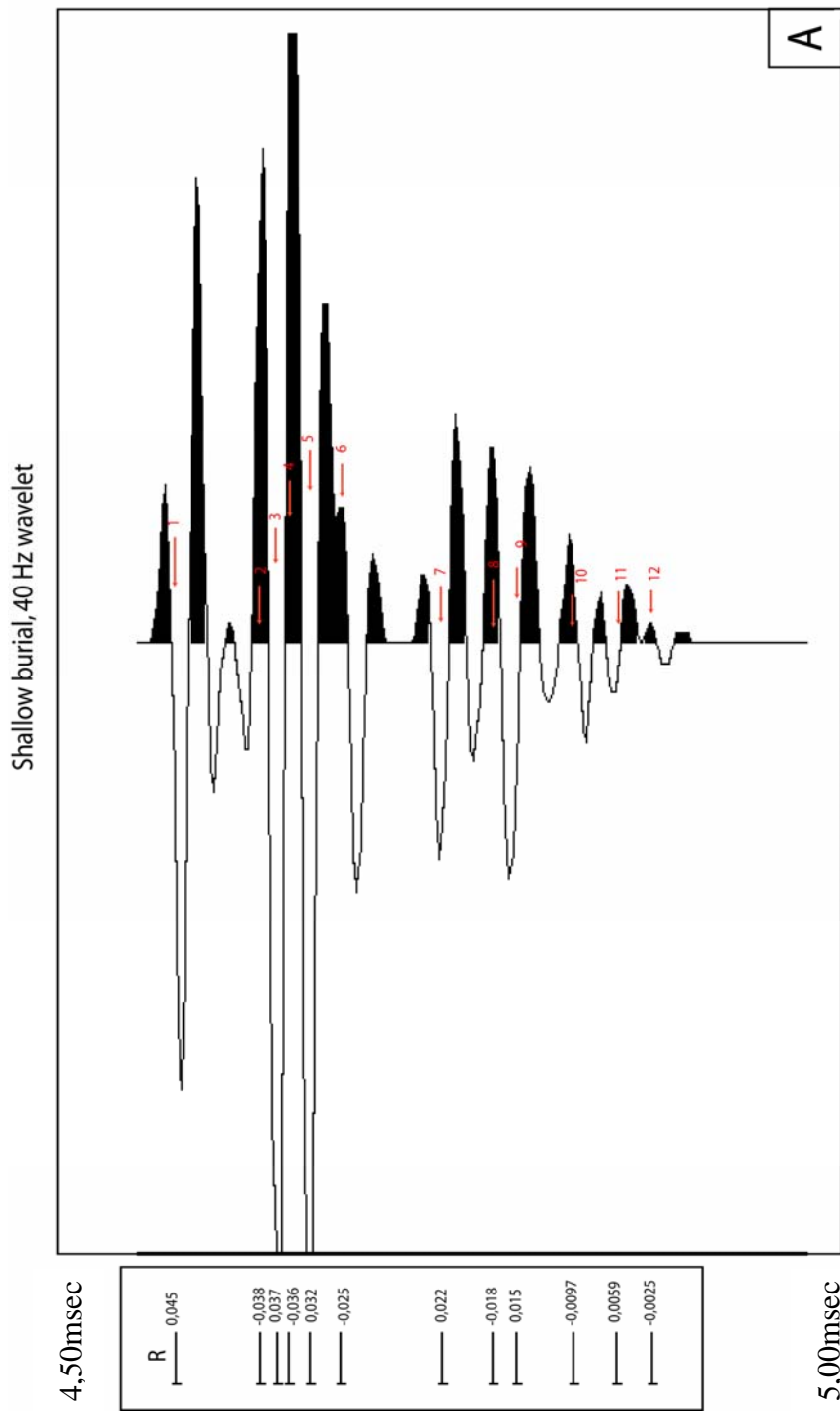


Figure 9.4.2 A. Synthetic seismogram for model under shallow burial. Spikogram with reflection coefficient at the bottom. Arrows are illustrating the true time positions of the interfaces (referred to first main peak of wavelet).

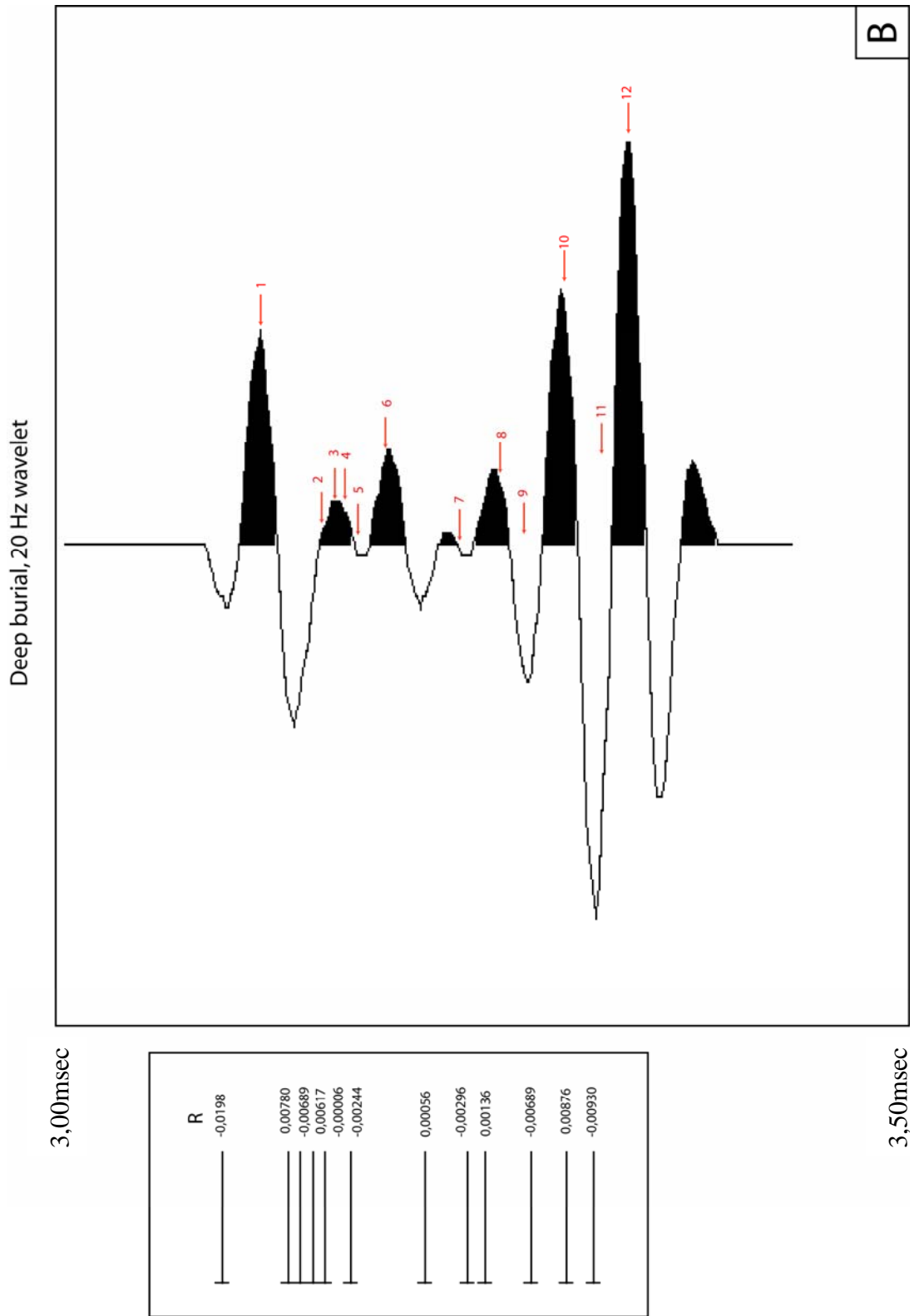


Figure 9.4.2 B. Synthetic seismogram for model under deep burial. Spikogram with reflection coefficient at the bottom. Arrows are illustrating the true time positions of the interfaces (referred to the first main peak of the wavelet employed).

10 Discussion

An interesting, superior aspect with the present study has been to compare overall reservoir properties that can be anticipated of the Brøttum Formation at similar depths of burial as actual Mesozoic and Cenozoic turbidite reservoirs. For discussions regarding depositional architecture and environment, I refer to chapter 8.

The sandstone facies represented in the Lillehammer Submarine Fan Complex (LSFC) has a clay matrix content reaching 30 percent. The high clay content indicates that the Brøttum turbidite sandstones also had a low porosity values at similar burial depths as for the Cretaceous turbidites of the Vøring Basin, which were compared with the LSFC in chapter 8. In contrast to the sandstones of the LSFC, the Cretaceous submarine fans of the Vøring Basin contain well sorted sandstones with low clay content, which gives excellent reservoir qualities (Fjellanger *et al.*, 2005).

Provenance and basin configuration are here though to be the major factors in control of sandstone properties in both basins. In the Vøring Basin, the sediments had to pass through a wide shelf and were exposed to tidal currents and waves which reworked the material before the sediments were dropped in the basin (Fjellanger *et al.*, 2005). This was not the situation in the Hedmark rift basin; the sediments were most likely transferred directly to the basin over a very narrow basin margin shelf, resulting in poorly sorted sediments. Due to unconfined basin floor geometry in both basins, sediments have accreted similar architectural elements like lobes, lobe-channels, levees and major channels in an inner, middle and outer fan setting, despite different clay content in sandstones. The same vertical stacking pattern of these basic architectural elements is recognized for several other submarine fans described in the literature (chapter 8). By this reason, following the principles of Walther's Law, it is reasonable that the lateral organization of facies also is fairly well of corresponding pattern.

The Lillehammer Submarine Fan Complex has most likely never been any good reservoir, although the black shale units in the deep-marine system must have been petroleum source rocks that have yielded hydrocarbons during the stage of burial and heating. (The dark colour of the clay matrix may be due to some remnants of dead carbonaceous matter formed from cracked oil residues, but this has not been tested in the present project.) However, the depositional geometry of the deep-marine clastic system preserved in the Lillehammer area is comparable with other fan systems. The Lillehammer Submarine Fan Complex is therefore considered appropriate as a field analogue for other and much younger deep marine fan systems.

The synthetic seismograms of the Messenlivegen section show that different depths of the model results in quite different events on the seismic. Interfaces that are highly resolvable at 1500 meters of burial may change the character entirely and will be hardly recognized at depths below 3500 meters of burial.

The synthetic model below 1500 meter of overload reveals two sections separated with a period with small amplitudes or no reflections between interface 6 and 7. This low reflective period is associated with the thick shale layer dividing two fans described in chapter 8.

In the model where the overload is 3500 meter, has visible events on the synthetic seismogram decreased to half of the numbers seen in shallow model. It is possible to detect a change in the seismic character from interface 2-7, but without the depositional model it is not possible to tell why the change has happened. The first interfaces (2-5) have a destructive interference, while the thick homogeneous shale layer between interface 6 and 7 gives no reflection. Constructive interferences in the lowest part of the section are in addition creating false strong reflectors in the lower part of the model. Increased resolution could have been obtained if deconvolution techniques were applied. The use of analogue models would increase the understanding of a seismic section as represented here in a synthetic model. Thin sandstone layers interbedded with shale resulting in interference is difficult to detect from a thicker homogeneous layer.

11 Conclusions

The Brøttum Formation in the Lillehammer area was deposited as a turbidite system in the Neoproterozoic time, the Lillehammer Submarine Fan Complex. The fan complex was deposited in a wide rift basin, the Hedmark Basin, at the western margin of continent Baltica.

Seven facies have been identified and organized into seven facies associations, representing architectural elements of the submarine fan complex. The fan complex includes basin plain-thin bedded turbidites, basin plain-hemipelagic shale, lobe, lobe-channel, basin floor channel infill, major channel and channel-levee.

Individual fans of the Lillehammer Submarine Fan Complex are thought to represent an outer and middle to inner fan environment. This is supported by scarcity of very coarse clastic material associated with the innermost fan environment, and presence of hemipelagic shale in the lower part of the logged sections.

Architectural stacking pattern of facies associations demonstrates two or three prograding fans with a thick unit of aggrading channel sandstones on top. The fan complex is inferred to have had a basinward extent of at least 50 km, measured from the alleged basin margin position in the west and downslope to the east.

Depositional pattern and distribution of architectural elements are controlled mainly by tectonics, basin configuration and variation in sediment supply. Climate and relief in hinterland area, and basin margin morphology were the main factors for controlling sediment influx.

Synthetic seismograms of the Messenlivegen section illustrate those different burial depths of the model results in quite different events on the seismic. Interfaces that are highly

resolvable below 1500 meter of burial may change the character entirely and will be hardly recognized below 3500 meter of burial. The amplitudes change polarity in the deeper model compared to the shallow model as a result of different velocity and density trends. Only half of the seismic events are shown in the deepest model compared to the shallow model. Reflections associated with most interfaces are recognizable, but difficult to distinguish from each other. The shallow model reveals good seismic resolution of two fans separated by a thick layer of homogenous shale. The same model under a thicker overload does not have the same obvious trends, but is recognizable when you know what to expect.

References

- Aldridge, D.F.** 1990: Short note. The Berlage wavelet. *Geophysics* 55, No 11, 1508-1511.
- Armstrong, L. A., Ten Have, A., and Johnson, H.D.** 1987: The geology of the Gannet field, central North Sea, UK sector. In J. Brooks and K. Glennie (Eds.): *Petroleum geology of NW Europe*. London: Graham & Trotman, 533-548.
- Bagnold, R.A.** 1962: Auto-suspension of transported sediment: turbidity currents. *Proceedings of the Royal Society of London, Series A* 265, 315-319.
- Bagnold, R.A.** 1968: Deposition in the process of hydraulic transport. *Sedimentology* 10, 45-56.
- Bjørlykke, K.** 1974: Glacial striation on clast from the Moelv Tillite of the late Precambrian of southern Norway. *American Journal of Science* 274, 443-448.
- Bjørlykke, K., Englund, J.O. and Kirkhusmo, L.** 1967: Latest Precambrian and Eocambrian stratigraphy of Norway. *Norges Geologiske Undersøkelse* 251, 5-17.
- Bjørlykke, K., Elvsborg, A. and Høy, T.** 1976: Late Precambrian sedimentation in the central Sparagmite basin of South Norway. *Norges Geologiske Undersøkelse* 56, 233-290.
- Bjørlykke, K. and Høeg, K.** 1997: Effects of burial diagenesis on stresses, compaction and fluid flow in sedimentary basins. *Marine and Petroleum Geology*, 14, 267-276.
- Bjørlykke, K.** 2003: Compaction (consolidation) of sediments. In Middleton G.V. (Ed) *Encyclopedia of Sediments and Sedimentary Rocks*. Kluwer Academic Publishers, 161-168
- Bockelie, J.F. and Nystuen, J.P.** 1985: The southeastern part of the Scandinavian Caledonides. In D.G. Gee and B.A. Stuart (Eds.): *The Caledonide Orogen – Scandinavia and Related Areas*, 69-88.
- Bouma, A.H.** 1962: *Sedimentology of some Flysch Deposits: A Graphic Approach to Facies Interpretation*. Elsevier, Amsterdam, 168.
- Bouma, A.H., Normark, J.M. and Barnes, N.E.** 1985: *Submarine fans and related turbidite systems*: New York, Springer-Verlag, 351pp
- Bouma, A.H.** 2000: Fine-grained, mud-rich turbidite systems: Model and comparison with coarse-grained, sand-rich systems. In Bouma, A.H. and Stone, C.G. (Eds.): *Fine-Grained Turbidite Systems*. AAPG Memoir, 72 Society of Economic Paleontologists and Mineralogists, Special Publication 68, 9-19.
- Brekke, H.** 2000. The tectonic evolution of the Norwegian Sea Continental Margin with emphasis on the Vøring and Møre Basins. In: A. Nøttvedt *et al.* (eds): *Dynamics of the Norwegian Margin*. Geological Society, London, Special Publications, 167, 327-378.
- Carmen, G.J. and Young, R.** 1981: Reservoir geology of the Forties oilfield. In: *Petroleum geology of the continental shelf of NW Europe*. London: Heyden, 371-379.
- Carter, R.M.** 1975: A discussion and classification of subaqueous mass-transport with particular reference to grain-flow, slurry-flow and fluxoturbidites. *Earth Science Reviews* 11, 145-177.
- Collinson, J.D.** 1969: The sedimentology of the Grindslow Shales and the Kinderscout Grit: a deltaic complex in the Namurian of northern England. *Journal of Sedimentary Petrology* 39, 194-221.
- Coussot, P. and Meunier, M.** 1996: Recognition, classification and mechanical description of debris flows. *Earth-Science Reviews* 40, Issues 3-4, 209-227.

- Dasgupta, P.** 2003: Sediment gravity flow—the conceptual problem. *Earth Science Reviews* 62, 265-281.
- Dewey, J.F.** 1969: Evolution of the Appalachian/Caledonian orogen. *Nature* 222, 124-129.
- Dott, R.H.Jr.** 1963: Dynamics of subaqueous gravity depositional processes. *AAPG Bulletin* 47, 104-128.
- Englund, J.-O.** 1972: Sedimentological and structural investigations of the Hedmark Group in the Tretten- Øyer- Fåberg district, Gudbrandsdalen. *Norges Geologiske Undersøkelse* 276, 1-59.
- Englund, J.-O.** 1966: Sparagmittgruppens bergarter ved Fåvang, Gudbrandsdalen. En sedimentologisk og tektonisk undersøkelse. *Norges Geologiske Undersøkelse* 238, 55-102.
- Escard, R., Albouy, E., Gaumet, F. and Ayub, A.** 2004: Comparing the depositional architecture of basin floor fans and slope fans in the Pab Sandstone, Maastrichtian, Pakistan. In Lomas, S.A. & Joseph, P. (Eds.): *Confined Turbidite Systems*. Geological Society Special Publication 222, 159-185.
- Esmark, J.** 1829: *Reise fra Christiania til Trondhjem*. Christiania, Oslo. 81.
- Fjellanger, E., Surlyk, F., Wamstecker, L.C. and Midtun, T.** 2005 Upper Cretaceous basin-floor fans in the Vøring Basin, Mid Norway shelf. In: B. Wandas *et al.* *Onshore-offshore Relationships on the North Atlantic Margin*. NPF Special Publication, 12, 135-164.
- Gale, G.H. and Roberts, D.** 1974: Trace element geochemistry of Norwegian Lower Palaeozoic basic volcanics and its tectonic implications. *Earth and Planetary Science Letters* 22, 380-390.
- Gani, M.R.**, 2004: From turbid to Lucid: A straightforward Approach to Sediment Gravity Flows and Their Deposits. *The Sedimentary Record* 2 (3), 4-8.
- Gee, D.G.** 1975: A tectonic model for the central part of the Scandinavian Caledonides. *American Journal of Science* 275-A, 468-515.
- Gee, D.G.** 1978: Nappe displacement in the Scandinavian Caledonides. *Tectonophysics* 47, 393-419.
- Gee, M.J.R., Masson, D.G., Watts, A.B. and Allen, P.A.** 1999: The Saharan debris flow: an insight into the mechanics of long runout submarine debris flows. *Sedimentology* 46, 317-225.
- Ghosh, B. and Lowe, D.R.** 1996: Architectural element analysis of deep-water sedimentary sequences: Cretaceous Venado Sandstone member, Sacramento Valley, California. *Journal of Sedimentary Research*
- Giles, M.R.** 1997: *Diagenesis: A quantitative perspective. Implications for basin modelling and rock property prediction*. Kluwer Academic Publishers. 525.
- Gressly, A.** 1838: *Obersevationes Gèologiques sur le Jura Soleurois*. *Neue Denkschriften der Allgemeinen Schewizerischen Gesellschaft für diegesamnten Naturwissenschaften* 2, 112.
- Hampton, M.A.** 1972: The role of subaqueous debris flow in generating turbidity currents. *Journal of Sedimentary Petrology* 42, 775-793.
- Harms, J.C.** 1974: Brusby Canyon Formation, Texas: a deep-water density current deposit. *Geological Society of America Bulletin* 85, 1763-1784.
- Harms, J.C. and Fahnestock, R.K.** 1965: Stratification, bed forms and flow phenomena (with example from Rio Grande). In Middleton, G.V. (ed.): *Primary Sedimentary Structures and their Hydrodynamic Interpretation*. Society of Economic Paleontologists and Mineralogists, Special Publication 12, 84-115.

- Hartz, E.H.** and **Torsvik, T.H.** 2002: Baltica upside down: a new plate tectonic model for Rodinia and the Iapetus Ocean. *Geology* 30, 255-258.
- Holme, A.C.A.F.** 2002: The Biskopåsen Formation: a conglomeratic turbidite system in the Hedmark rift basin. Cand. Scient. Thesis, Department of Geology, University of Oslo, 175, Appendices.
- Heller, P.L.** and **Dickinson, W.R.**, 1985: Submarine ramp facies model for delta-fed, sand-rich turbidite systems. *AAPG Bulletin* 69, 960-976.
- Hesse, R.** and **Chough, S. K.** 1981: The Northwest Atlantic Mid-Ocean Channel of the Labrador Sea: II. Deposition of parallel laminated levee-muds from viscous sublayer of low density currents. *Sedimentology* 27, 697-711
- Hiscott, R.N.** and **James, N.P.** 1985: Carbonate debris flows, Cow Head Group, western Newfoundland. *Journal of Sedimentary Petrology* 55, 735-745.
- Hiscott, R.N.** 1981: Deep-sea fan deposits in the Macigno Formation (middle-upper Oligocene) of the Gordana Valley, northern Apennines, Italy – Discussion. *Journal of Sedimentary Petrology* 51, 1015-1021.
- Hiscott, R.N.** 1994: Traction-carpet stratification in turbidites: fact or fiction? *Journal of Sedimentary Research* 64-A, 204-208.
- Hiscott, R.N., Pirmez, C.** and **Flood, R.D.** 1997: Amazon submarine fan drilling: a big step forward for deep-sea fan models. *Geoscience Canada* 24, 13-24.
- Holtedahl, O.** 1920: Om Trysil- (Dala-) sandstenens og sparagmittavdelingens alder. *Norges Geologiske Tidsskrift* 6, 17-48.
- Holtedahl, O.** 1921: Engerdalen, Fjeldbygningen inden rektangelkartet Engerdalens område. *Norges Geologiske Undersøkelse* 89, 74.
- Hsu, K.J.** 1989: *Physical principles of sedimentology* New York. Springer-Verlag, 233
- Jakobsen, I.S.** 2003: Sediment composition in the Gullfaks area. A study of the distribution of velocity and density in wells from the Gullfaks, Valemon, Rimfaks and GullV fields. Cand. Scient. Thesis, University of Oslo, 108.
- Japsen, P.** 2000: Investigation of multi-phase erosion using reconstructed shale trends based on sonic data; Sole pit axis, North Sea Neogene uplift and tectonics around the North Atlantic: *Global and Planetary Change*, 24, 189-210.
- Johansson, M.** and **Stow, D.A.V.** 1995: A classification scheme for shale clasts in deep-water sandstones. In A.J. Hartley and D.J. Prosser (Eds.): *Characterization of Deep Marine Clastic Systems*. Geological Society Special Publication 94, 221-241.
- Johansson, M.** and **Stow, D. A. V.** 1998: Deep-water massive sands, California: tectonic setting and sand supply controls. *Geoscience 98 Abstracts Volume*. 12.
- Johnson, A.M.** 1970: *Physical Processes in Geology*. Freeman, Cooper & Co, San Francisco, 577.
- Johnson, S.D, Flint, S.** and **Hinds, D.** 2001: Anatomy, geometry and sequence stratigraphy of basin floor to slope turbidite systems, Tanqua Karoo, South Africa. *Sedimentology* 48, 987-1023.
- Kneller, B.** 1995: Beyond the turbidite paradigm: physical models for deposition of turbidites and their implications for reservoir prediction. In A.J. Hartley, & D.J. Prosser (Eds.): *Characterization of deep-marine clastic systems*. Geological Society Special Publication 94, 31-49.

- Kneller, B. and Buckee, C.** 2000: The structure and fluid mechanics of turbidity currents: a review of some recent studies and their geological implications. *Sedimentology* 47, 62-94.
- Kneller, B.C. and Branney, M.J.** 1995: Sustained high-density turbidity currents and the deposition of thick massive sands. *Sedimentology* 42, 607-616.
- Krenmayr, H.G.** 1996: Hemipelagic and turbiditic mudstone facies associations in the Upper Cretaceous Gosau Group of the Northern Calcareous Alps (Austria). *Sedimentary Geology* 101, 149-172.
- Kuenen, Ph. H.** 1950: Turbidity currents of high density. Proceedings of 18th International Geological Congress (1948) Reports 8. 44-52.
- Kuenen, Ph.H. and Migliorini, C.I.** 1950: Turbidity currents as a cause of graded bedding. *Journal of Geology* 58, 91-127.
- Kumpulainen, R. and Nystuen, J.P.** 1985: Late Proterozoic basin evolution and sedimentation in the westernmost part of Baltoscandia. In D.G. Gee and B.A. Sturt (Eds.): *The Caledonide Orogen-Scandinavian and Related Areas*. Wiley, Chichester, 331-338.
- Kunz, A.,** 2002: Coarse-clastic submarine fan development in a rift basin. Neoproterozoic Ring Formation, South Norway. Cand. Scient. Thesis, Department of Geology, University of Oslo, 195, Appendices.
- Link, M.H. and Nilsen, T.H.** 1980: The Rocks Sandstone, an Eocene sand-rich deep-sea fan deposit, northern Santa Lucia Range, California. *Journal of Sedimentary Petrology* 50, 583-601.
- Lowe, D.R.** 1982: Sediment gravity flows: II- depositional models with special reference to the deposits of high-density turbidity currents. *Journal of Sedimentary Petrology* 52, 279-297.
- Lowe, D.R.** 1979): Sediment gravity flows: their classification, and some problems of application to natural flows and deposits. In L.J. Doyle, & O. H. Pilkey (Eds.), *Geology of Continental Slopes*. Society of Economic Paleontologists and Mineralogists Special Publication Vol. 27, 75-82.
- Middleton, G.V.** 1993: Sediment deposition from turbidity currents. *Annual Review of Earth Planetary Science* 21, 89-114.
- Middleton, G.V. and Hampton, M.A.** 1976: Subaqueous sediment transport and deposition by sediment gravity flows. In D.J. Stanley and D.J.P. Swift (Eds.): *Marine Sediment Transport and Environmental Management*. Wiley, New York, 197-218.
- Middleton, G.V. and Hampton, M.A.** 1973: Sediment gravity flows: mechanics of flow and deposition. In G. V. Middleton, & A. H. Bouma (Eds.): *Turbidites and deep-water sedimentation* Proceedings of Pacific Section Society of Economic Paleontologists and Mineralogists Short Course Notes, 1-38.
- Middleton, G.V.** 1967: Experiments on density and turbidity currents-III: deposition of sediment. *Canadian Journal of Earth Sciences* 4, 475-505.
- Middleton, G.V.** 1970: Experimental studies related to problems of flysh sedimentation. *Geological Association of Canada Special Paper* 7, 253-272.
- Middleton, G.V.** 1993: Sediment deposition from turbidity currents. *Annual Review Earth Planetary Sciences* 21, 89-114.
- Mohrig, D., Elverhøi, A. and Parker, G.** 1999: Experiments on the relative mobility of muddy Subaqueous and subaerial debris flows, and their capacity to remobilize antecedent deposits. *Marine Geology* 154, 117-129.

- Morad, S.** 1988: Albitized microcline grains of post-depositional and probable detrital origin in the Brøttum Formation sandstones (Upper Proterozoic), Sparagmite Region of southern Norway. *Geological Magazine* 125, 229-239.
- Morley, C.K.** 1986: The Caledonian thrust front and palinspastic restoration in the southern Norwegian Caledonides. *Journal of Structural Geology* 8, 753-765.
- Mulder, T. and Alexander, J.** 2001: The physical character of subaqueous sedimentary density flows and their deposits. *Sedimentology* 48, 269-299.
- Mulder, T., Syvitski, J.P.M., Migeon, S., Faugeres, J.C. and Savoye, B.** 2003: Marine hyperpycnal flows: initiation, behaviour and related deposits. A review. *Marine and petroleum Geology* 20, 861-882.
- Mutti, E. and Ricci Lucchi, F.** 1972): Le torbiditi dell'Appennino settentrionale: introduzione all'analisi di facies. *Memorie della Societa Geologica Italiana* 11, 161-199.
- Mutti, E. and Ghibaud, G.** 1972: Un esempio di torbiditi de conoide sottomarina esterna-Le Arenarie di San Salvatore (Formazione de Bobbio, Miocene) nell' Appennino de Piacenza, *Memorie dell' Accademia della Scienze di Torino, Classe de Scienze Fisiche, Matematiche e Naturali, Serie 4* no. 16, 40.
- Mutti, E.** 1977: Distinctive thin-bedded turbidite facies and related depostional environments in the Eocene Hecho Group (South-central Pyrenees, Spain). *Sedimentology* 24, 107-131.
- Mutti, E. and Ricci Lucchi, F.** 1978: Outer fan depositional lobes of the Laga Formation (Upper Miocene and Lower Pliocene), east-central Italy. In Stanley, D.J., Kelling, G. (Eds.):, *Sedimentation in submarine fans, canyons, and trenches.* Hutchinson and Ross, Stroudsburg, PA. 210-223.
- Mutti, E., Remacha, E., Sgavetti, M., Rosell, J., Valloni, R. and Zamorano, M.** 1985: Stratigraphy and facies characteristics of the Eocene Hecho Group turbidite systems, south-central Pyrenees. In M.D. Mila and J. Rosell (Eds.), *Excursion guidebook of the 6th European regional meeting of International Association of Sedimentologist, Lerida*, 521-576.
- Mutti, E.** 1985: Turbidite systems and their relations to depositional sequences. In: Zuffa, G. G. (Ed): *Provenance of Arenites*, 65-93
- Mutti, E. and Normark, W.R.** 1987 Comparing examples of modern and ancient turbidite systems: problems and concepts. In J.K. Leggett and G.G. Zuffa (Eds.): *Marine Clastic Sedimentology: Concepts and Case Studies.* Graham & Trotman, London, 1-38.
- Mutti, E.** (1992): *Turbidite Sandstones.* Agip and Instituto di Geologia, Università di Parma, 275.
- Nardin, T.R., Hein, F.J., Gorsline, D.S. and Edwards, B.D.** 1979: A review of mass movement processes, sediment and acoustic characteristics, and contrasts in slope and base-of-slope systems versus canyon-fed-basin floor systems. In L.J. Doyle, & O.H. Pilkey (Eds.): *Geology of continental slopes.* Economic Paleontologists and Mineralogist Special Publication 27, 61-73.
- Normark, R.W** 1970: Growth patterns of deep-sea fans. *American Association of Petroleum Geologists Bulletin* 54, 2170-2195.
- Normark, W. R., and Piper, D.J.W.** 1972: Sediment and growth pattern of Navy deep-sea fan. San Clemente Basin, California borderland. *Journal of Geology* 80, 198-223.
- Normark, W.R.** 1978: Fan valleys, channels, and depositional lobes on modern submarine fans. Characters for recognition of sandy turbidite environments. *AAPG Bulletin* 62, 912-931.

- Normark, W.R., and Piper, D.J.W.** 1991: Initiation processes and flow evolution of turbidity currents: Implications for the depositional record. In R.H. Osborne (Ed.): From Shoreline to Abyss: Contributions in Marine Geology in Honor of Francis Parker Shepard (Ed.), SEPM Special Publication 46, 207-230.
- Nystuen, J.P.** 1976: Facies and sedimentation of Late Precambrian Moelv Tillite in the eastern part of the Sparagmite Region, southern Norway. *Norges Geologiske Undersøkelse* 329, 1-70.
- Nystuen, J.P.** 1981: The late Precambrian "Sparagmites" of southern Norway: a major Caledonian allochthon- the Osen-Røa Nappe Complex. *American Journal of Science* 281, 69-94.
- Nystuen, J.P.** 1982: Late Proterozoic basin evolution on the Baltoscandian craton: the Hedmark Group, southern Norway. *Norges Geologiske Undersøkelse*, 375, 74.
- Nystuen, J.P.** 1983: Nappe and thrust structures in the Sparagmite Region, southern Norway. *Norges Geologiske Undersøkelse* 380, 67-83.
- Nystuen, J.P.** 1987: Synthesis of the tectonic and sedimentological evolution of the Proterozoic- early Cambrian Hedmark Basin, the Caledonian Thrust Belt, southern Norway. *Norges Geologiske Undersøkelse* 67, 395-418.
- Nystuen, J.P.** 1999: Late Proterozoic to Cambrian of the Hedmark Basin, Sparagmite Region, Southern Norway. In: Pedersen, G.K. and Clemmensen, L.B (Eds.): Field Trip Guidebook, Excursion B4. International Association of Sedimentology, 19th Regional European Meeting of Sedimentology, August 24-26, Copenhagen 1999, 123-144.
- Nystuen, J.P. and Siedlecka, A.** 1988: The "Sparagmites" of Norway: In: J.A. Winchester (Ed.): Later Proterozoic Stratigraphy of the Northern Atlantic Regions. Blackie, Glasgow and London, 237-252.
- Oftedal, C.** 1943: Om sparagmiten og dens skyvning innen kartbladet ved Rendal. *Norges Geologiske Undersøkelse*, 191, 65.
- Pedersen, K.** 2003: An integrated study of coarse clastic depositional systems; Block 34 offshore Angola and the Ainsa Turbidites, Spain. Cand. Scient. Thesis in Petroleum geophysics/geology. Department of Earth Science, University of Bergen. 156.
- Pickering, K.T., Hiscott, R.N. and Hein, F.J.** 1989: Deep-Marine Environments: Clastic Sedimentation and Tectonics. Unwin Hyman, London, 416.
- Pierson, T.C. and Costa, J.E.** 1987: A rheologic classification of subaerial sediment-water flow. In Costa, J.E., Wicczorek, G.E. (Eds.): Debris Flows/Avalanches: Process, Recognition and Mitigation. Geological Society of America Reviews in Engineering Geology VII, 1-12.
- Piper, D.J.W.** 1978: Turbidite muds and silts on deep sea fans and abyssal plains. In D.J. Stanley and G. Kelling (Eds.): Submarine Canyon and Fan Sedimentation. Dowden, Hutchinson and Ross, Stroudsburgh, 163-176.
- Piper, D.J.W., and Normark, W.R.** 2001: Sandy fans- from Amazon to Hueme and beyond. *AAPG Bulletin* 1407-1438.
- Pittman, E.D. and Larese, R.E.** 1991 Compaction of lithic sands: experimental results and applications. *Bulletin AAPG*, 75, 8, 1279-1299.
- Postma, G.** 1986: Classification for sediment gravity flow deposits based on flow conditions during sedimentation. *Geology* 14, 291-294.
- Postma, G., Nemeč, W., and Kleinspehn, K.L.** 1988: Large floating clasts in turbidites: a mechanism for their emplacement. *Sedimentary Geology* 58, 47-61

- Ramberg, I.B. and Englund, J.O.** 1969: The source rock of the Biskopås Conglomerate at Fåvang, and the western margin of the sedimentation basin of the Brøttum Formation at Fåvang-Vinstra, southern Norway. *Norges Geologiske Undersøkelse* 258, 302-324.
- Reading, H.G.** 1991: The classification of deep-sea depositional systems by sediment caliber and feeder systems. *Journal of Geological Society* 148, 427-430.
- Reading, H.G. and Richards, M.** 1994: Turbidite Systems in Deep- Water basin Margins Classified by Grains Size and Feeder Systems. *AAPG Bulletin* 78, 792-822.
- Reading, H.G. and Levell, B.K.** 1996: Controls on the sedimentary rock record. In Reading, H.G. (ed.), *Sedimentary Environments: Processes, Facies and Stratigraphy*, Blackwell, Oxford, 5-36.
- Richards, M., Bowman, M. and Reading, H.** 1998: Submarine-fan systems I: characterization and stratigraphic prediction. *Marine and Petroleum Geology* 15, 689-717.
- Roberts, D. and Gee, D.G.** 1985: An introduction to the structure of the Scandinavian Caledonides. In D.G. Gee and B.A. Sturt (Eds.): *The Caledonide Orogen – Scandinavia and Related Areas*. Wiley, Chichester, 55-68
- Sanders, J.E.** 1965: Primary sedimentary structures formed by turbidity currents and related resedimentation mechanisms. In G.V. Middleton (ed.): *Primary sedimentary structures and their hydrodynamic interpretation* Society of Economic Paleontologists and Mineralogists Special Publication 12, 192-219.
- Schiøtz, O.E.** 1902: Den sydøstlige dal af Sparagmit-Kvarts-Fjeldet, Norge. *Norges Geologiske Undersøkelse* 35, 135.
- Shanmugam, G.** 1997: The Bouma Sequence and the turbidite mind set. *Earth-Science Reviews* 42, 201-229.
- Shanmugam, G.** 1996: High-density turbidity currents: are they sandy debris flows? *Journal of Sedimentary Research* 66, 2-10.
- Shanmugam, G.** 2000: 50 years of the turbidite paradigm (1950s-1990s): deep water processes and facies models: a critical perspective. *Marine and Petroleum Geology* 17, 285-342.
- Shanmugam, G. and Moiola, R.J.** 1988: Submarine fans: Characteristics, models, classification, and reservoir potential. *Earth Science Reviews* 24, 383-428.
- Shanmugam, G. and Moiola, R.J.** 1995: Interpretation of depositional processes in a classic flysch sequence (Pennsylvanian Jackfork Group), Ouachita Mountains, Arkansas and Oklahoma. *American Association of Petroleum Geologists Bulletin* 79, 627-695.
- Skjeseth, S.** 1963: Contributions to the geology of the Mjøsa districts and the classical sparagmite area in southern Norway. *Norges Geologiske Undersøkelse* 220, 126.
- Simpson, J.E.** 1997: *Gravity Currents in the Environment and in the Laboratory*, 2nd edition. Cambridge University Press, Cambridge, 244.
- Sparks, R.S.J., Bonneau, R.T., Huppert, H.E., Lister, J.R., Hallworth, M.A., Mader, H. and Phillips, J.** 1993: Sediment-laden gravity currents with reversing buoyancy. *Earth Planetary Science Letters* 114, 243-257.
- Stalsberg, M.** 2004: Coarse-clastic turbidite sedimentation: the Neoproterozoic Imsdalen Submarine Fan Complex, Hedmark Basin, South Norway. *Cand.Scient. Thesis in Sedimentology and Petroleum Geology*. Department of Geosciences, University of Oslo, 162.

- Stalsberg, M. and Nystuen, J.P.** 2004: Processes of coarse-clastic deep-water turbidite systems: exemplified by facies and architecture of the Imsdalen fan complex, South Norway. Abstract. In O. Martinsen (Ed.): Deep Water Sedimentary Systems of Arctic and North Atlantic Margins, Stavanger 18-20 October 2004. Abstracts and Proceedings of the Geological Society of Norway, 59.
- Storvoll, V. and Bjørlykke, K.** (2004) Sonic velocity and grain contact properties in reservoir sandstones. In: *Sediment compaction and velocity distribution in sedimentary basins; examples from offshore Norway*. Dr. Scient thesis. Uio. 1-19 + appendices.
- Storvoll, V. and Bjørlykke, K.,** in press: Sonic velocity and grain contact properties in reservoir sandstones. *Sediment compaction and velocity distribution in sedimentary basins; examples from offshore Norway*. Petroleum Geoscience.
- Storvoll, V., Bjørlykke, K. and Mondol, N.H.** 2005: Velocity-depth trends in Mesozoic and Cenozoic sediments from the Norwegian shelf. *AAPG Bulletin*, 89, No 3, 359-381.
- Stow, D.A.V., Reading, H.G. and Collinson, J.D.** 1996: Deep Seas. In Reading, H.G. (Ed.), *Sedimentary Environments: Processes, Facies and Stratigraphy*, Blackwell, Oxford, 395-453.
- Stow, D.A.V. and Wetzel, A.** 1990: Hemiturbidite: a new type of deep-water sediment. In J.R. Cochran, D.A.V. Stow et al. (Eds.): *Proc. ODP Sci. Results* 116, 25-34.
- Stow, D.A.V.** 1994: Deep sea processes of sediment transport and deposition. In K. Pye (Ed.): *Sediment Transport and Depositional Processes*. Blackwell, Oxford, 257-291.
- Stow, D.A.V., Reading, H.G. and Collinson, J.D.** 1996: Deep Seas, chapter 10, In. H.G.) Reading (Ed.): *Sedimentary Environments: Processes, Facies and Stratigraphy*, 395-453.
- Stow, D.A.V. and Johansson, M.** 2000: Deep-water massive sands: nature, origin and hydrocarbon implications. *Marine and Petroleum Geology* 17, 145-174.
- Stow, D.A.V. and Shanmugam, G.** 1980: Sequence of structures in fine-grained turbidites: comparison of recent deep-sea and ancient flysch sediments. *Sedimentary Geology* 25, 23-43
- Surlyk, F.** 1987: Slope and deep shelf gully sandstones. Upper Jurassic, East Greenland; American Association of Petroleum Geologists Bulletin 71, 464-475.
- Surlyk, F., and Noe-Nygaard, N.** 1998: Massive intrusive sandstones, Upper Jurassic Hareelv Formation: a new class of deep water sandstone. *Geoscience* 98, Abstracts Volume 7.
- Sæther, T. and Nystuen, J.P.** 1981: Tectonic framework, stratigraphy, sedimentation and volcanism of the Late Precambrian Hedmark Group, Østerdalen, South Norway. *Norges Geologiske Tidsskrift* 61, 193-211.
- Torsvik, T.H., Ryan, P.D., Trench, A. and Harper, D.A.T.** 1991: Cambrian-Ordovician palaeogeography of Baltica. *Geology* 19, 7-10.
- Törnebohm, A.E.** 1896: Grunddragen af det centrala Scandinaviens bergbygnad. *Kungliga Svenska Vetenskapsakademiens handlingar* 28, 210.
- Vallance, J.W. and Scott, K.M.** 1997: The Osceola mudflow from Mount Rainier: sedimentology and hazard implications of a huge clay-rich debris flow. *Geological Society of America Bulletin* 109, 143-163.
- Vernik, L. and Nur, A.** 1992: Petrophysical classification of siliciclastics for lithology and porosity prediction from seismic velocities. *AAPG Bulletin*, 76, 1295-1305.
- Vidal, G.** 1981: Micropalaeontology and biostratigraphy of the Upper Proterozoic and Lower Cambrian sequence in East Finnmark, northern Norway. *Norges Geologiske Undersøkelse* 362, 53.

- Vidal, G. and Nystuen, J.P.** 1990a: Micropalaentology, depositional environment and biostratigraphy of the Upper Proterozoic Hedmark Group, southern Norway. *American Journal of Science* 290-A, 170-211.
- Vidal, G. and Nystuen, J.P.** 1990b: Lower Cambrian acritarchs and Proterozoic-Cambrian boundary in southern Norway. *Norges Geologiske Tidsskrift* 70, 191-222.
- Walker, R.G.** 1965: The origin and significance of the internal sedimentary structures of turbidites. *Proceedings of the Yorkshire Geological Society* 35, 1-32.
- Walker, R.G.** 1978: Deep-water sandstone facies and ancient submarine fans: models for exploration for stratigraphic traps. *American Association of Petroleum Geologists Bulletin* 62, 932-966.
- Walker, R.G.** 1979: *Facies Models*. Geological Association of Canada, Toronto, 211.
- Walther, J.** 1894: *Einleitung in die Geologie als Historische Wissenschaft*, Bd. 3. Lithogenesis der Gegenwart, 535-1055. Fischer Verlag, Jena.
- Wynn, R.B., Kenyon, N.H., Masson, D.G., Stow, D.A.W. and Weaver, P.P.E.** 2002: Characterization And recognition of deep-water channel-lobe transition zones. *American Association of Petroleum Geologists Bulletin* 86, 1441-1462.
- Yilmaz, O. and Doherty, S.M.** 1987: *Seismic data processing*. Society of Exploration Geophysicists, Tulsa 526pp

Appendix

Appendix 1

Thin section nr	Logg	Position	Description
1	Fred. Col. veg	31,5 meter	Coarse-grained grey sst
2	Fred. Col. veg	17 meter	Dark grey, muddy fine-grained poorly sorted sst
3	Mess. veg.	328 meter	Coarse-grained grey sst
4	Mess. veg.	315 meter	Dark grey, muddy fine-grained poorly sorted sst
5	Mess. veg.	51 meter	Grey siltstone/mudstone
6	Mess. veg.	389 meter	Grey medium-coarse grained sst
7	Mess. veg.	364 meter	Very coarse-grained sst
8	Mess. veg.	46 meter	Dark grey-black, pyritic, very fine clay-siltstone
9	Maih. veg.	73 meter	Dark grey-black, pyritic, very fine clay-siltstone
10	Mess. veg.	356 meter	Grey fine-grained sst
11	Fred. Col. veg	18,5 meter	Dark grey medium grained poorly sorted sst










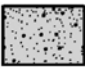

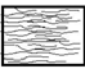
Appendix 2

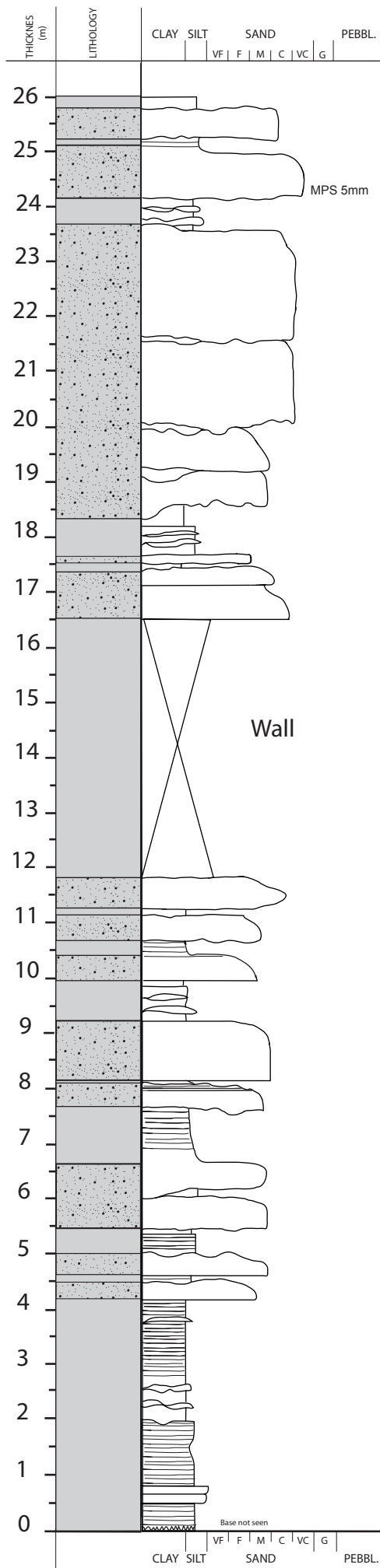
Facies distribution in the Brøttum Formation, Lillehammer.					
Locality	Facies	Number of beds	Total thickness	Thickness of bed	
				<i>max</i>	<i>min</i>
Fredrik Colletts veg 86,4 m	<i>B1 Structureless silt</i>	21	24,90m	5,00m	0,05m
	<i>B2 Laminated silt</i>	7	10,40m	5,00m	0,20m
	<i>C1 Normal graded sandstone</i>	27	29,55m	2,50m	0,20m
	<i>C3 Non graded sandstone</i>	13	3,75m	0,80m	0,05m
	<i>C4 Muddy sandstone</i>	18	17,80m	1,80m	0,20m
Maihaugvegen 127,5 m	<i>A1 Black shale</i>	7	11,50m	5,50m	0,50m
	<i>B1 Structureless silt</i>	35	10,20m	1,50m	0,10m
	<i>B2 Laminated silt</i>	22	17,10m	2,00m	0,20m
	<i>C1 Normal graded sandstone</i>	74	88,00m	4,20m	0,15m
	<i>C2 Inverse graded sandstone</i>	1	0,65m	0,65m	0,65m
	<i>C3 Non graded sandstone</i>	3	0,70m	0,30m	0,10m
Dampsagvegen 124 m	<i>B1 Structureless silt</i>	57	30,15m	2,00m	0,05m
	<i>B2 Laminated silt</i>	30	13,35m	1,25m	0,20m
	<i>C1 Normal graded sandstone</i>	84	72,28m	3,00m	0,10m
	<i>C3 Non graded sandstone</i>	15	7,85m	3,00m	0,05m
Åsmarkvegen 1 61,5 m	<i>B1 Structureless silt</i>	54	20,35m	1,30m	0,05m
	<i>B2 Laminated silt</i>	5	3,90m	1,70m	0,30m
	<i>C1 Normal graded sandstone</i>	51	36,00m	3,40m	0,20m
	<i>C3 Non graded sandstone</i>	19	1,25m	0,40m	0,05m
Åsmarkvegen 2 55,5 m	<i>B1 Structureless silt</i>	5	1,00m	0,40m	0,05m
	<i>C1 Normal graded sandstone</i>	23	53,80m	3,50m	0,10m
	<i>C3 Non graded sandstone</i>	1	0,70m	0,70m	0,70m
Åsmarkvegen 3 97,5 m	<i>B1 Structureless silt</i>	65	33,00m	2,50m	0,05m
	<i>B2 Laminated silt</i>	6	4,40m	1,40m	0,30m
	<i>C1 Normal graded sandstone</i>	77	56,40m	3,00m	0,10m
	<i>C3 Non graded sandstone</i>	9	3,70m	2,20m	0,05m
Messenlivegen 397 m	<i>A1 Black Shale</i>	5	0,10m	0,30m	0,10m
	<i>B1 Structureless silt</i>	100	125,80m	24,00m	0,10m
	<i>B2 Laminated silt</i>	15	34,45m	6,50m	0,60m
	<i>C1 Normal graded sandstone</i>	168	203,65m	7,00m	0,15m
	<i>C3 Non graded sandstone</i>	24	20,00m	2,50m	0,10m
	<i>C4 Muddy sandstone</i>	5	3,10m	2,50m	0,10m

Appendix 3

Facies Association distribution in the Brøttum Formation, Lillehammer									
	Number of beds and thickness								total thickness
<i>Messenlivegen</i>									
FA 2.2	3,3								3,3
FA 1.1	26,5	3,3	12,4	24,3	24,5	14	12,8	2,2	120
FA 2.1	36,2	20	38,6	13,9	20,6	37	4,5		170,8
FA 4.1	11	20,1	25						56,1
FA 3.1	3,7								3,7
FA 5.1	3,6	10							13,6
<i>Maihaugvegen</i>									
FA 1.1	4,2	6,8	16,2						27,2
FA 2.1	46	13,9	8,9						68,8
FA 2.2	10,25	6,9	4,5	3,8					25,45
FA 1.2	5,8								5,8
<i>Fredrik Colletts veg</i>									
FA 2.1	31	26,5							57,5
FA 2.2	11,8								11,8
FA 1.1	17,2								17,2
<i>Dampsagvegen</i>									
FA 5.1	5,25								5,25
FA 1.1	5,1	14,5	2,2	27,3					49,1
FA 2.1	23,35	17	13,1						53,45
FA 2.2	9,2								9,2
FA 3.1	7,3								7,3
<i>Åsmarkvegen 1</i>									
FA 1.1	1,1	1,6							2,7
FA 2.2	8,6								8,6
FA 3.1	15,6	9,2							24,8
FA 5.1	11,8	13,6							25,4
<i>Åsmarkvegen 2</i>									
FA 1.1	9,3								
FA 4.1	7,6	5,4	13,5	10,5	18,6				55,6
<i>Åsmarkvegen 3</i>									
FA 1.1	10,5								10,5
FA 4.1	16,8	10,8	10,5	10,6					48,7
FA 5.1	19,7	5,9	3,5						29,1

Appendix 4

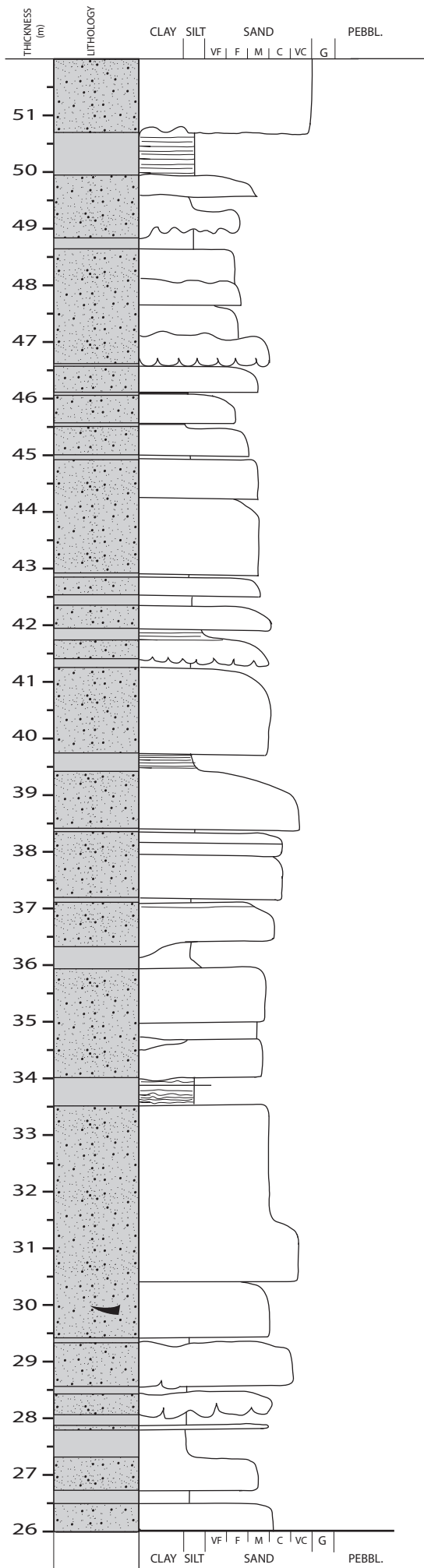
LEGEND	
	Mud clasts
	Pyrite lamina
	Grooves
	Paleocurrent direction
	Ripples
	Flame structures
	Load casts
	Convolute lamina
	Siltstone and black shale
	Sandstone
	Parallel lamination
	Wavy lamination



MAIHAUGVEIEN 1/5
 19.05.2005
 1:100
 32V 0579474
 UTM 6776186

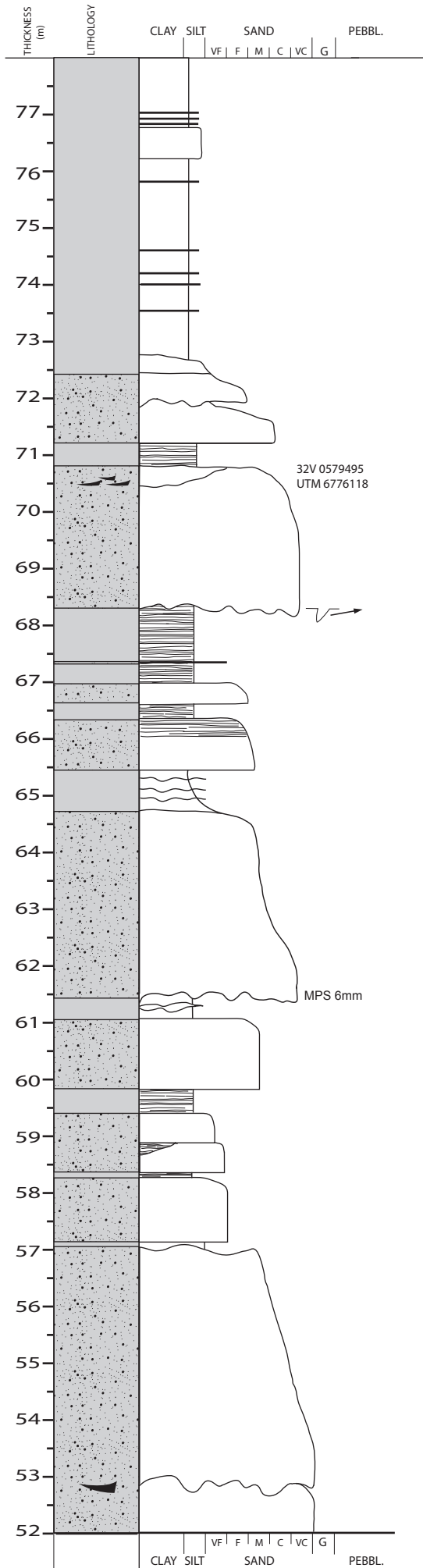
FA 2.1

FA 1.1



FA 2.2 MAIHAUGVEIEN 2/5
 19.05.2005
 1:100

FA 2.1



MAIHAUGVEIEN 3/5
19.05.2005
1:100

FA 1.1

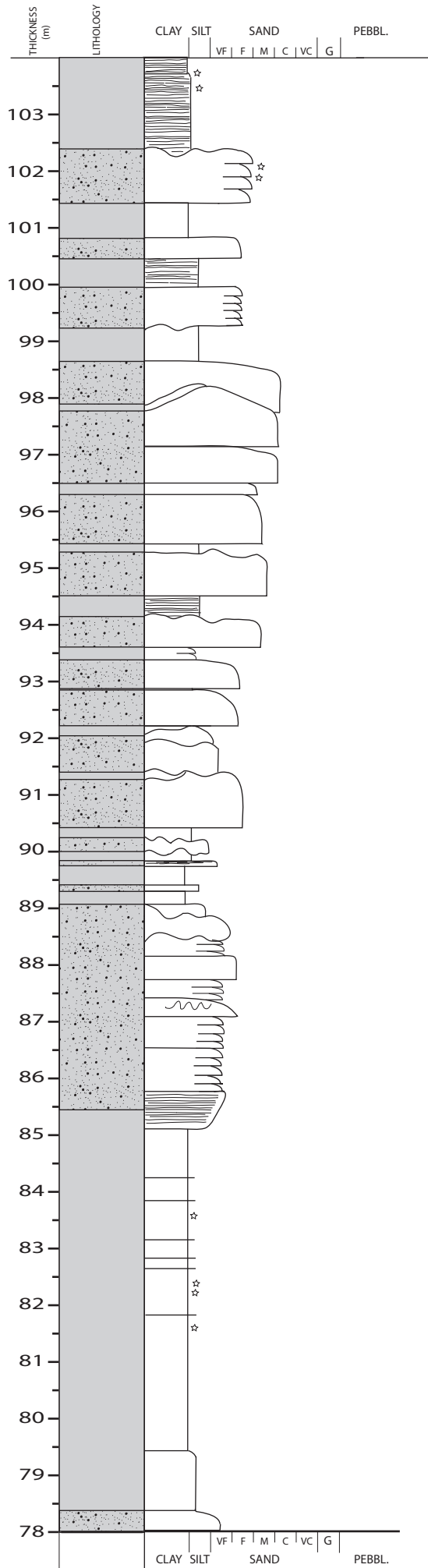
FA 2.2

FA 2.2

FA 2.2

CLAY SILT SAND PEBBL.

VF | F | M | C | VC | G



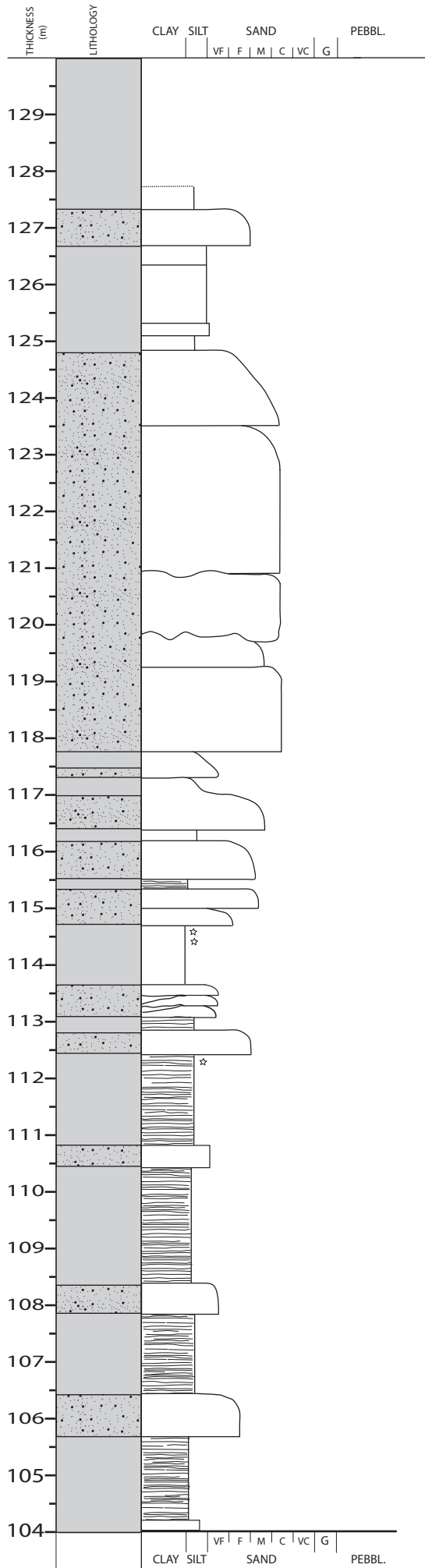
FA 1.1

MAIHAUGVEIEN 4/5
20.05.2005
1:100

FA 2.1

FA 1.2

FA 1.1

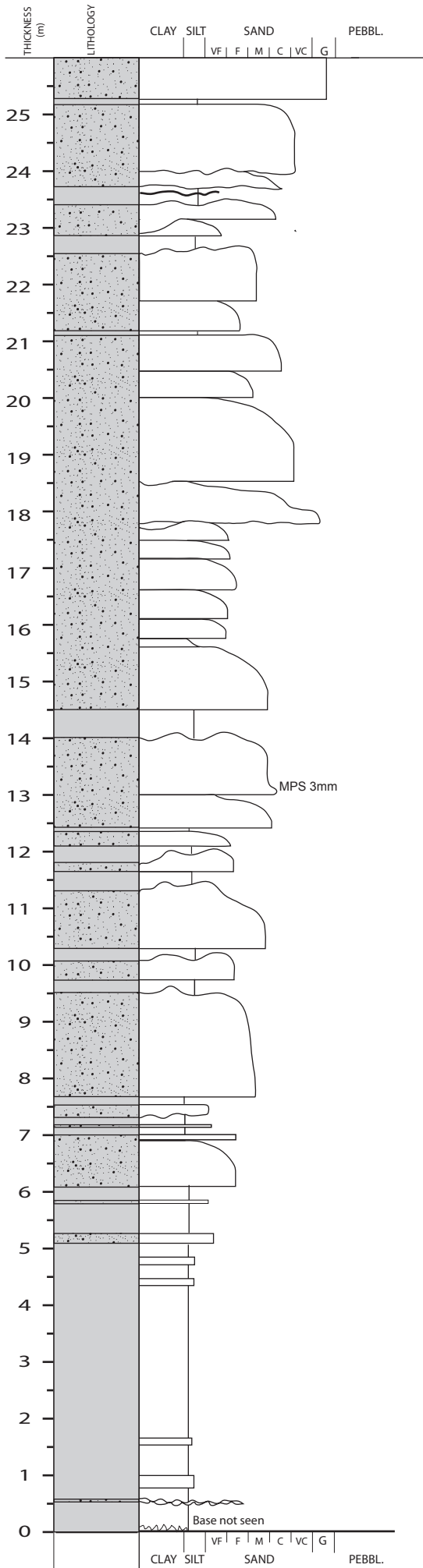


MAIHAUGVEIEN 5/5
 20.05.2005
 1:100

FA 2.2

FA 2.1

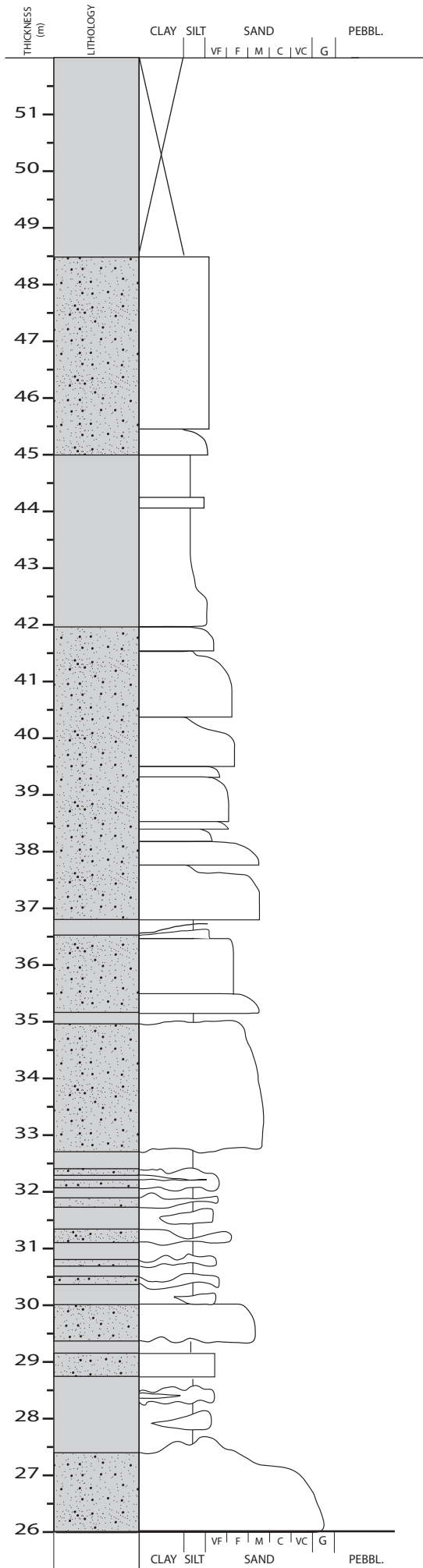
FA 1.1



DAMPSAGVEGEN 1/5
 05.06.2005
 1:100
 32V 0578875
 UTM 6775606

FA 2.1

FA 1.1



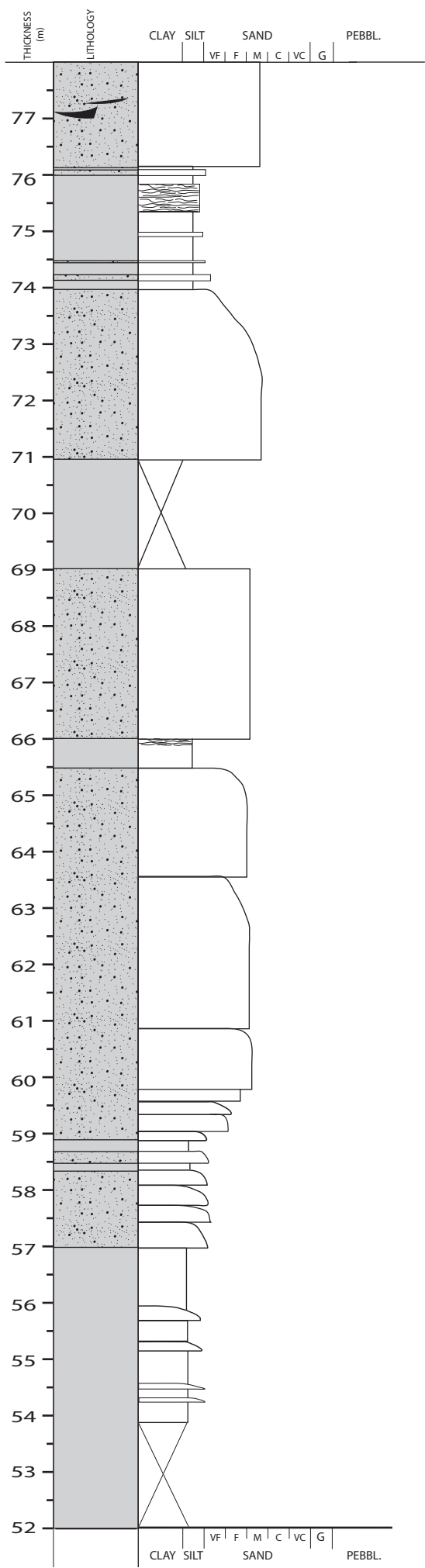
DAMPSAGVEGEN 2/5
 08.06.2005
 1:100

FA 1.1

FA 2.2

FA 5.1

FA 2.1



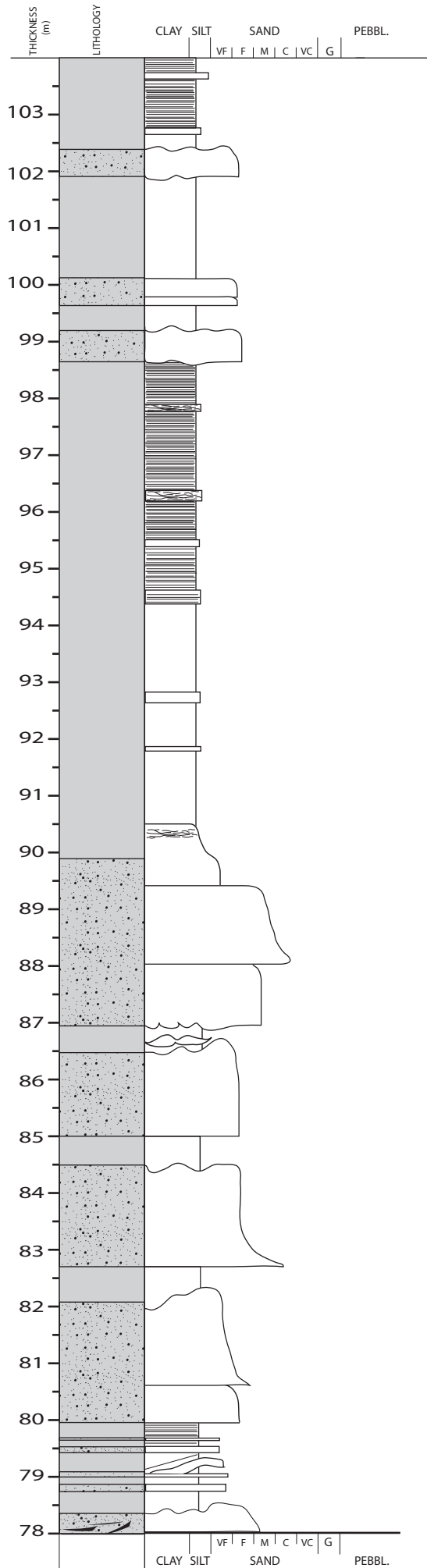
FA 2.1

DAMPSAGVEGEN 3/5
07.06.2005
1:100

FA 1.1

FA 2.1

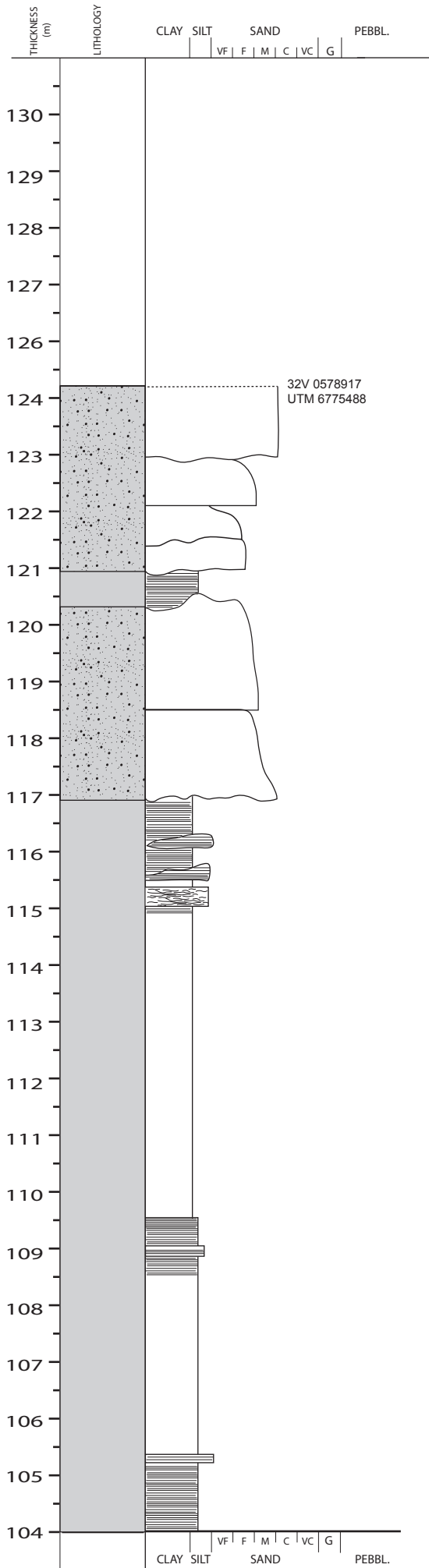
FA 1.1



DAMPSAGVEGEN 4/5
 08.06.2005
 1:100

FA 1.1

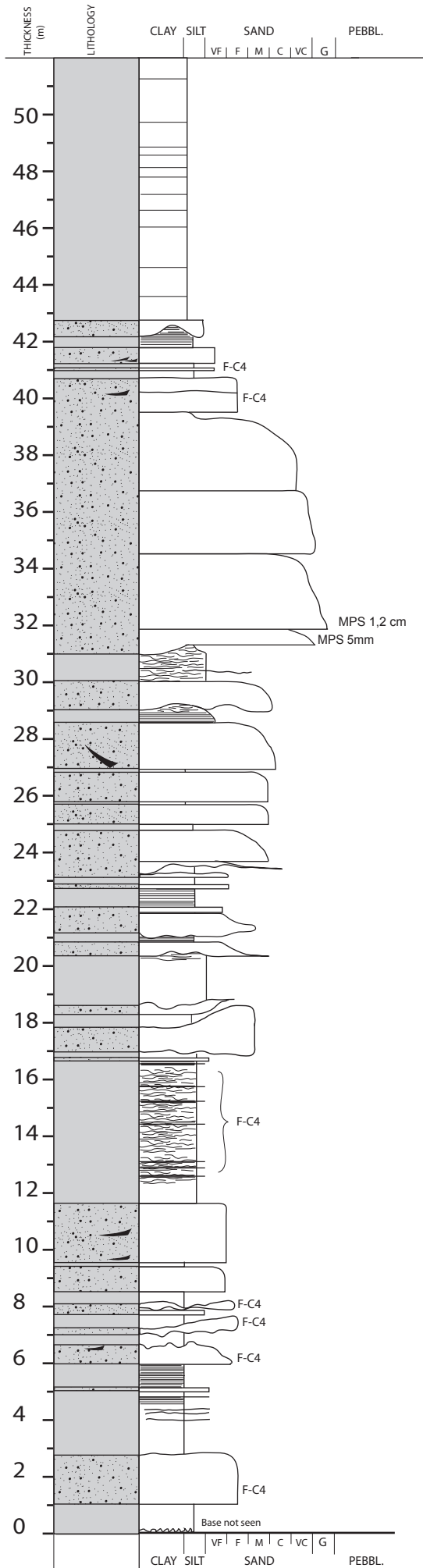
FA 2.1



DAMPSAGVEGEN 5/5
08.06.2005
1:100

FA 3.1

FA 1.1

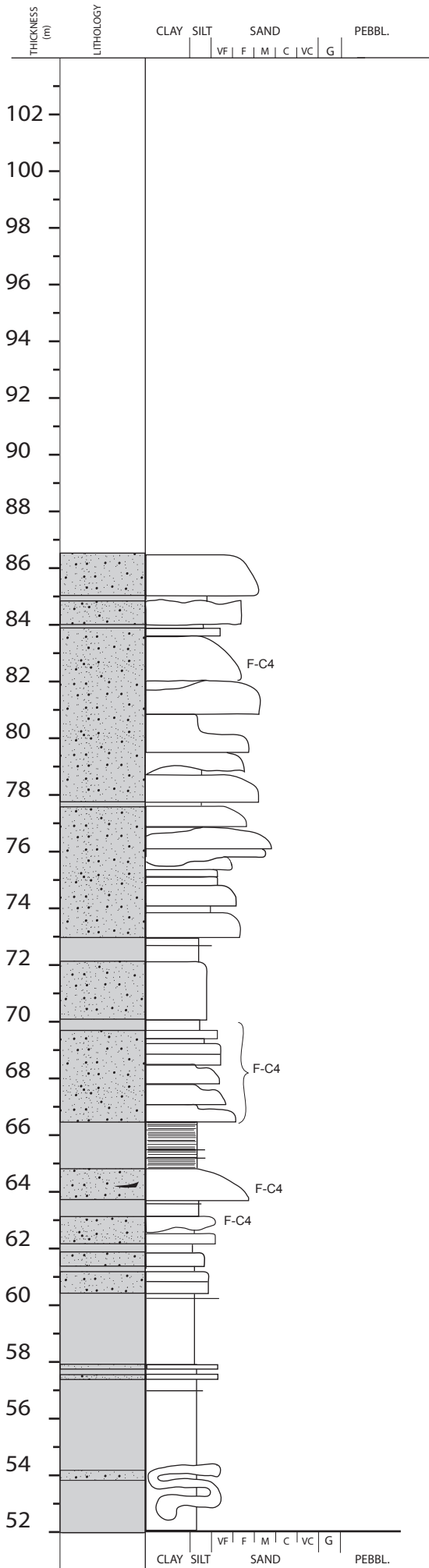


FA 1.1

FA 2.2

FA 2.1

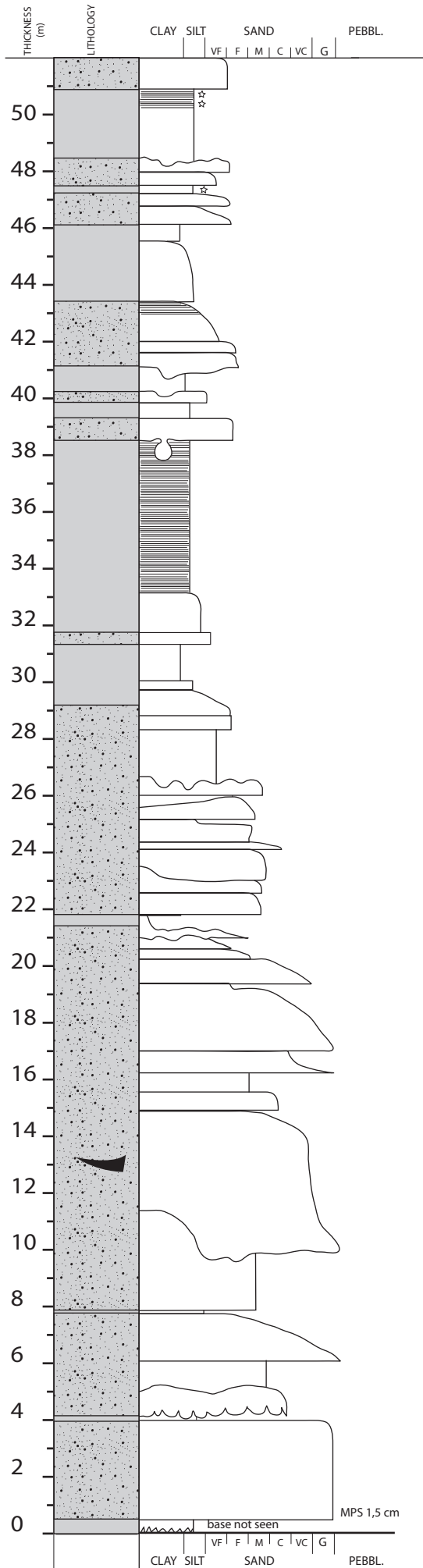
FREDRIK COLLETS VEG 1/2
 11.06.2005
 1:200
 32V 0579911
 UTM 6774232



FREDRIK COLLETS VEG 2/2
 14.06.2005
 1:200

FA 2.1

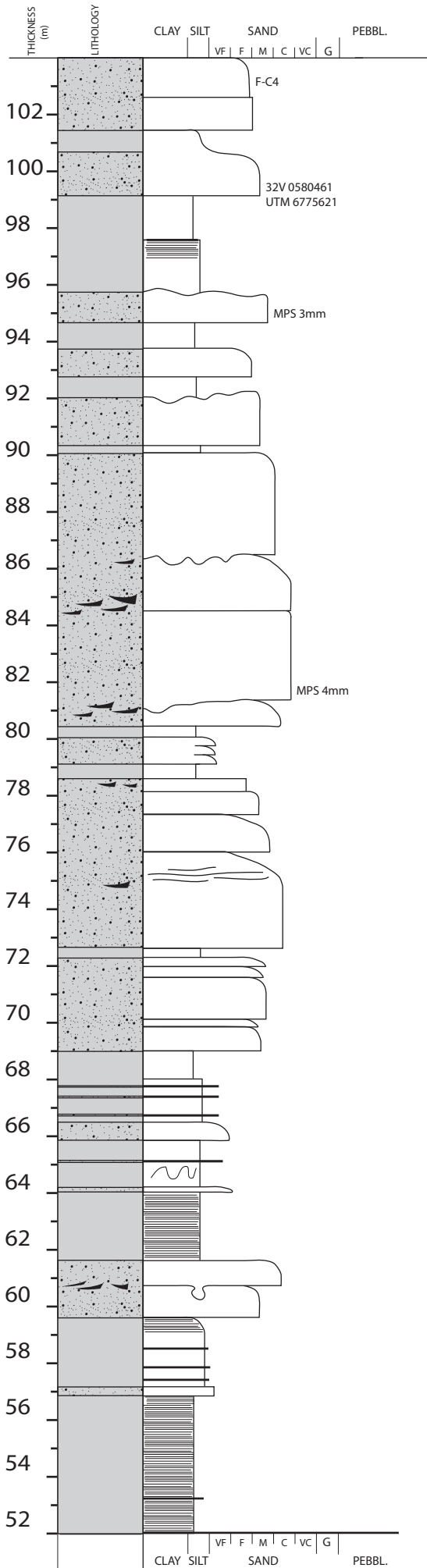
FA 1.1



MESSENLIVEGEN 1/8
 21.05.2005
 1:200
 32V 0580396
 UTM 6775732

FA 1.1

FA 2.2



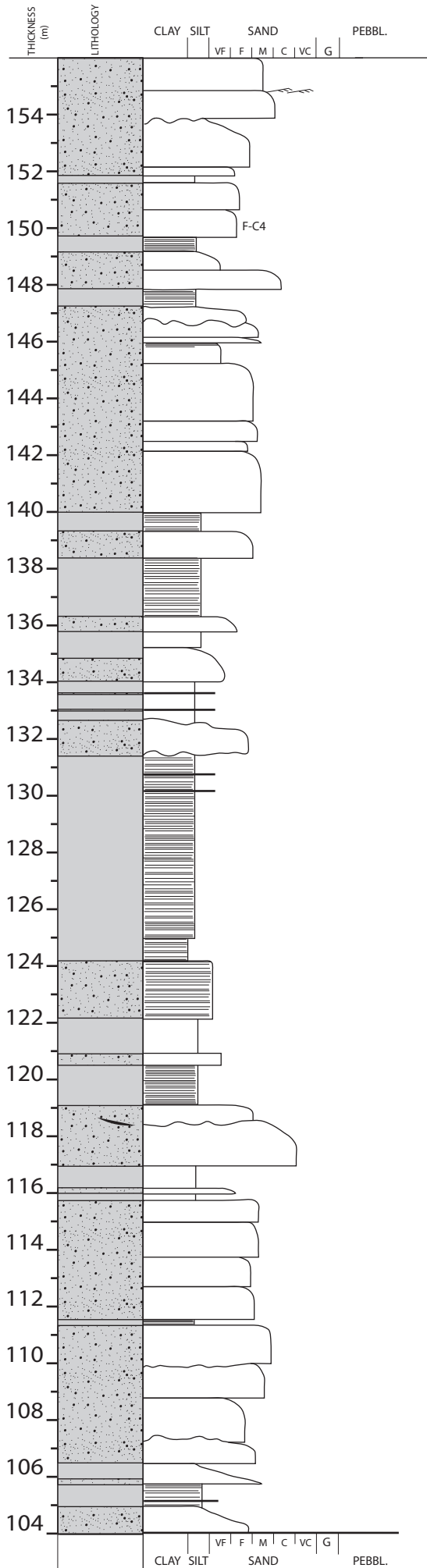
FA 2.1

MESSENLIVEGEN 2/8
21.05.2005
1:200

FA 1.1

FA 2.1

FA 1.1

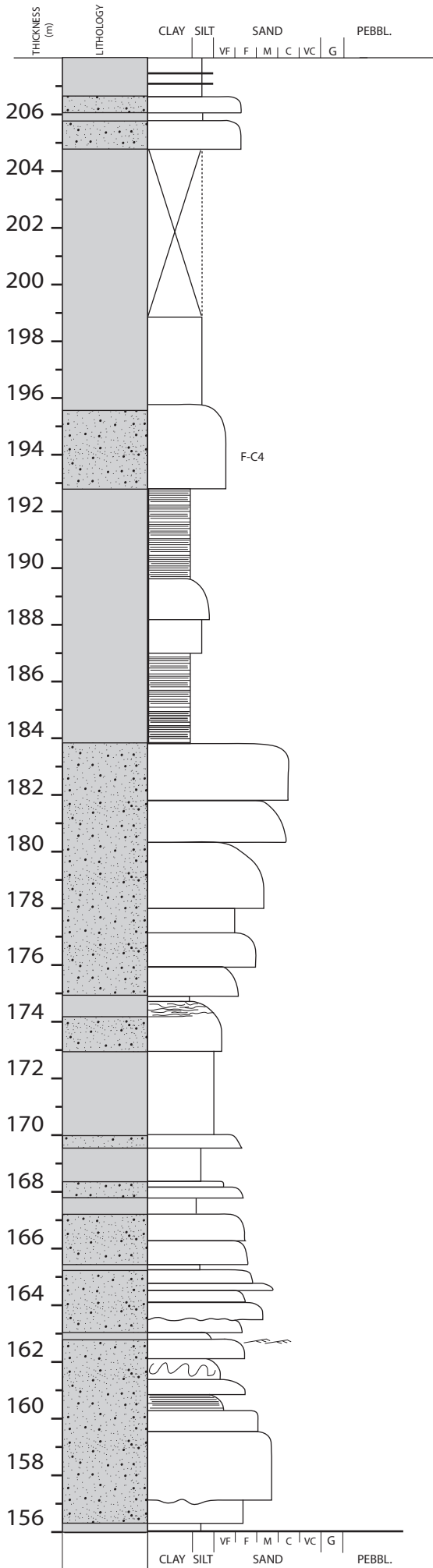


MESSENLIVEGEN 3/8
 21.05.2005
 1:200

FA 2.1

FA 1.1

FA 2.1

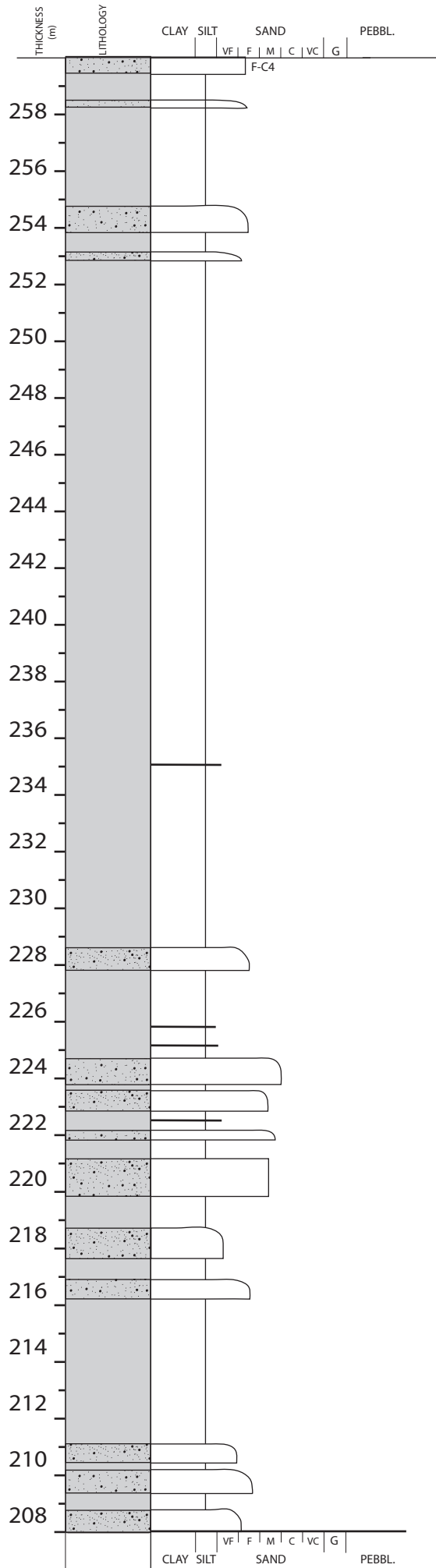


MESSENLIVEGEN 4/8
 21.05.2005
 1:200

FA 1.1

FA 2.1

FA 2.1



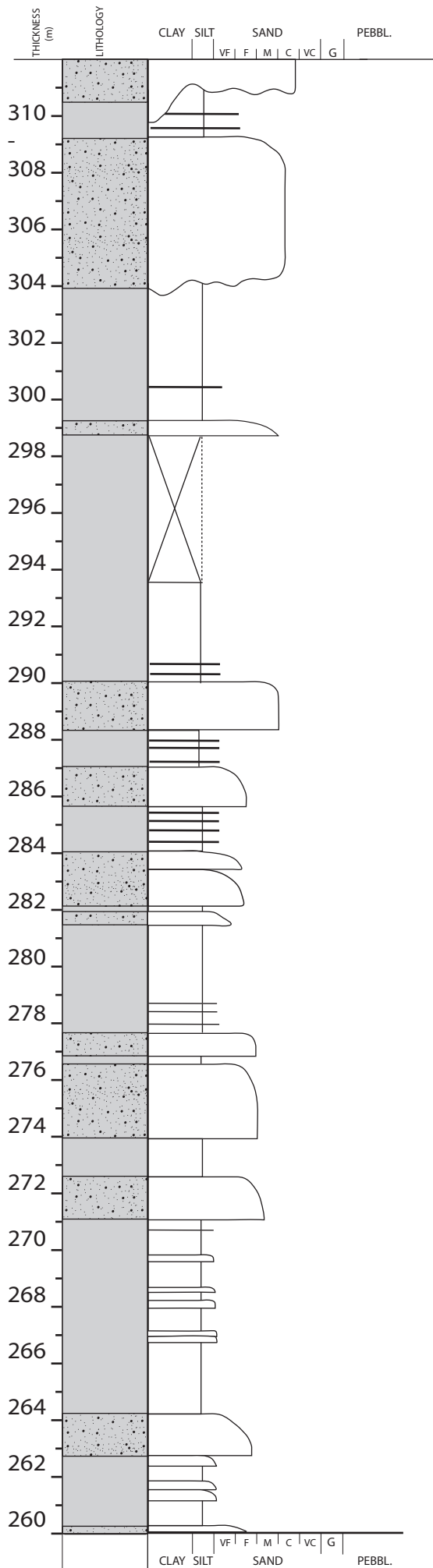
MESSENLIVEGEN 5/8
 22.05.2005
 1:200

FA 2.1

FA 1.1

FA 2.1

Distal lobe



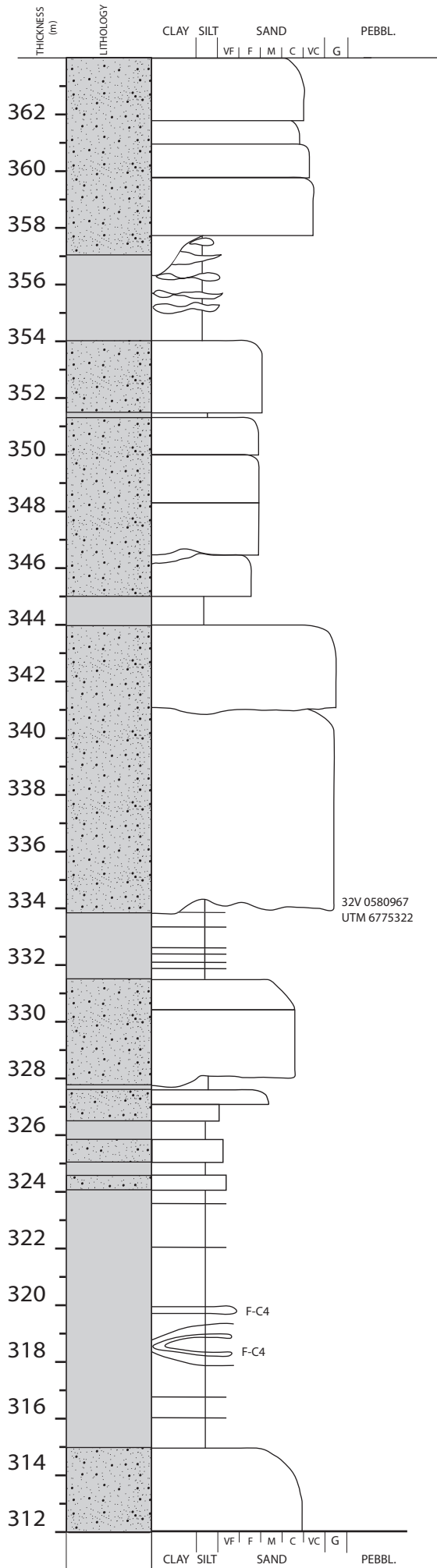
MESSENLIVEGEN 6/8
 22.05.2005
 1:200

FA 4.1

FA 1.1

FA 2.1

Distal lobe



MESSENLIVEGEN 7/8
22.05.2005
1:200

FA 4.1

FA 5.1

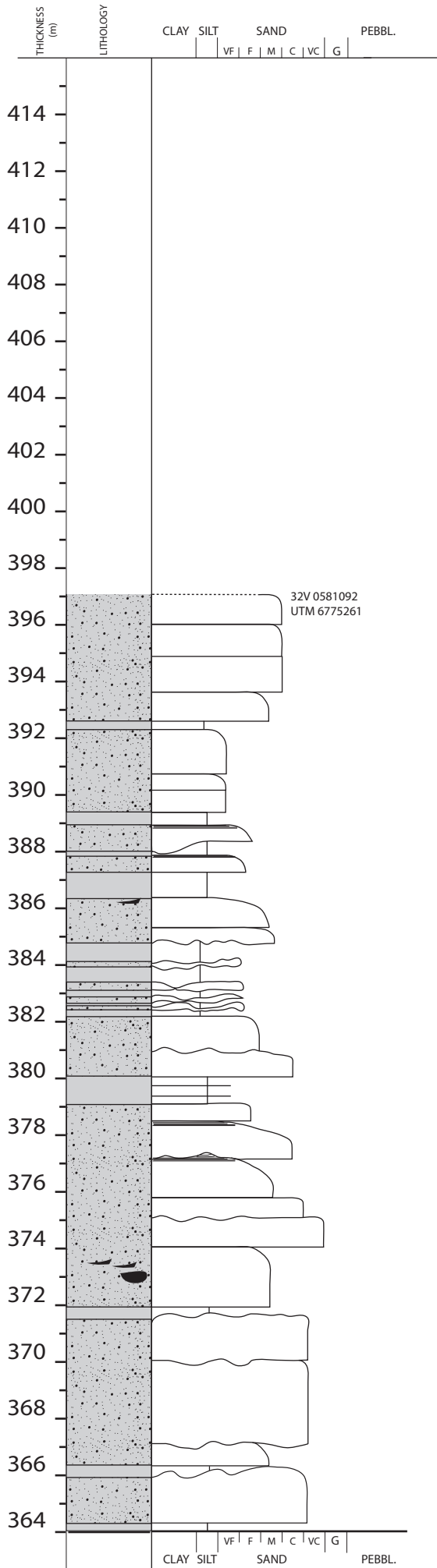
FA 4.1

FA 1.1

FA 4.1

FA 1.1

FA 4.1

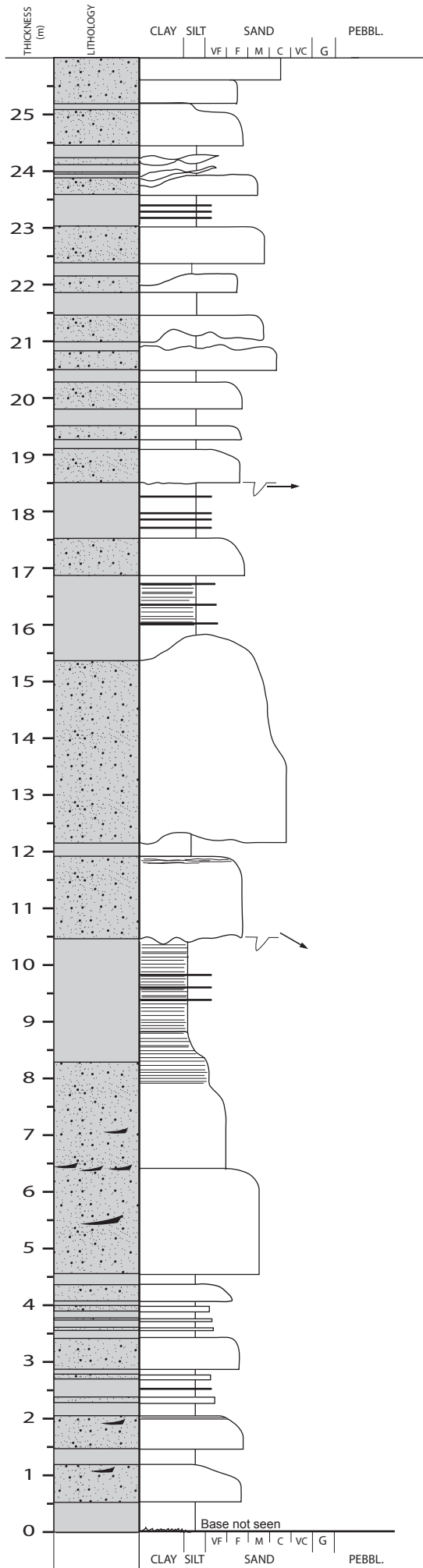


MESSENLIVEGEN 8/8
22.05.2005
1:200

FA 2.1

FA 5.1

FA 4.1

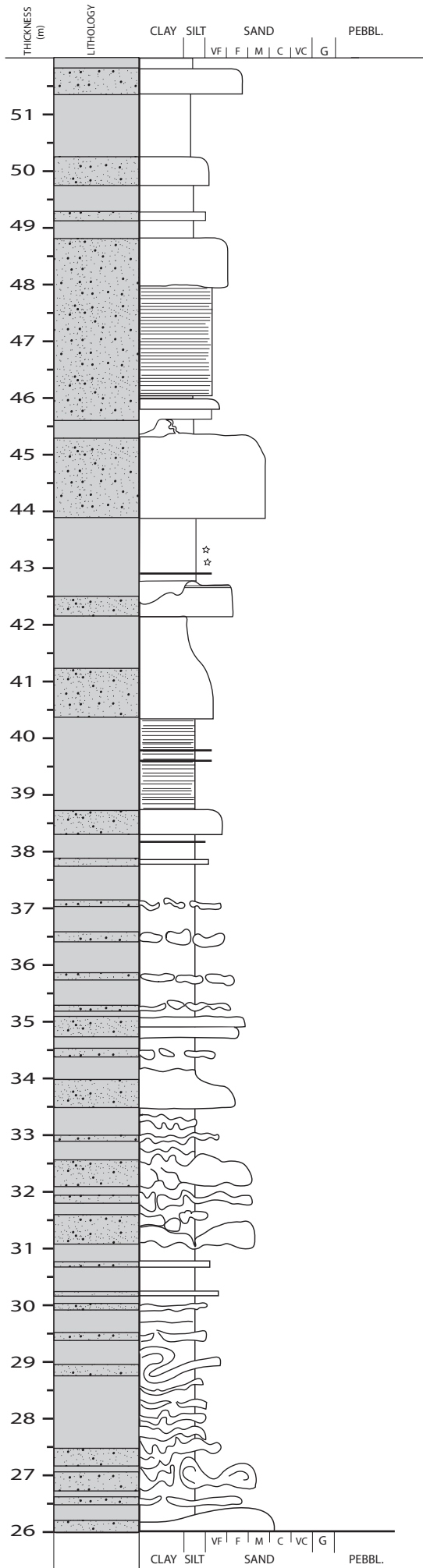


ÅSMARKVEGEN 1 1/3
 23.05.2005
 1:100
 32V 0579969
 UTM 6773814

FA 3.1

FA 1.1

FA 2.2

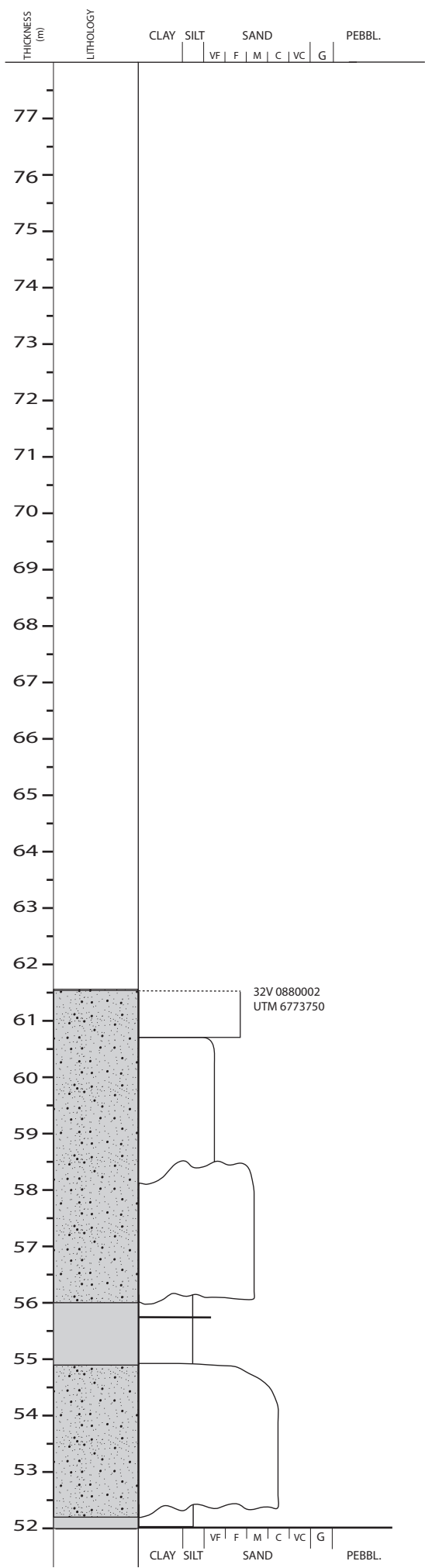


ÅSMARKVEGEN 1 2/3
 23.05.2005
 1:100

FA 5.1

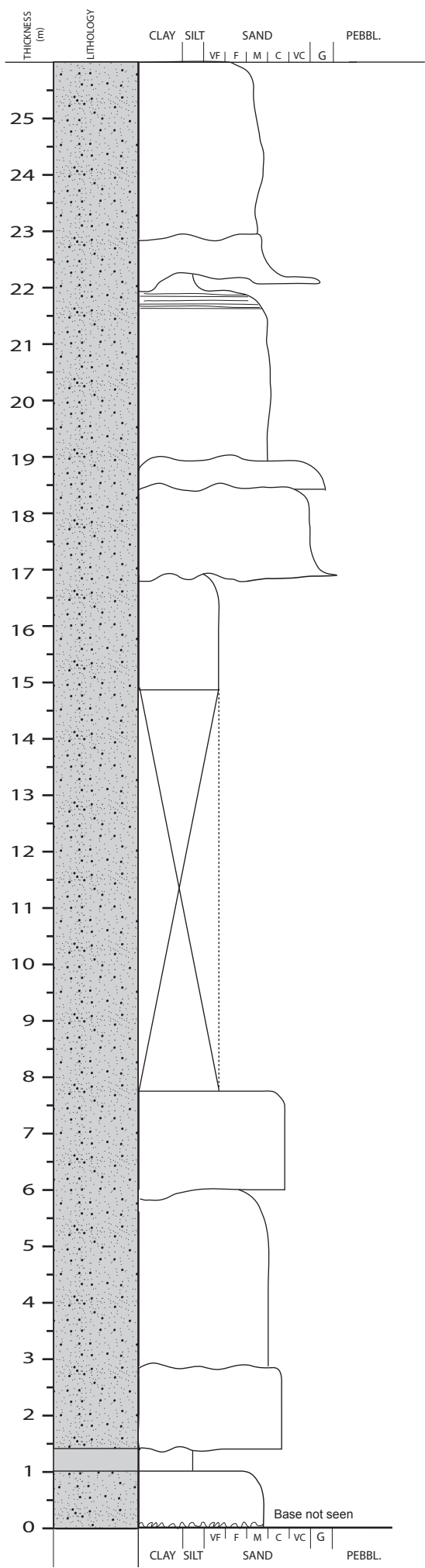
FA 1.1

FA 5.1



ÅSMARKVEGEN 1 3/3
23.05.2005
1:100

FA 3.1



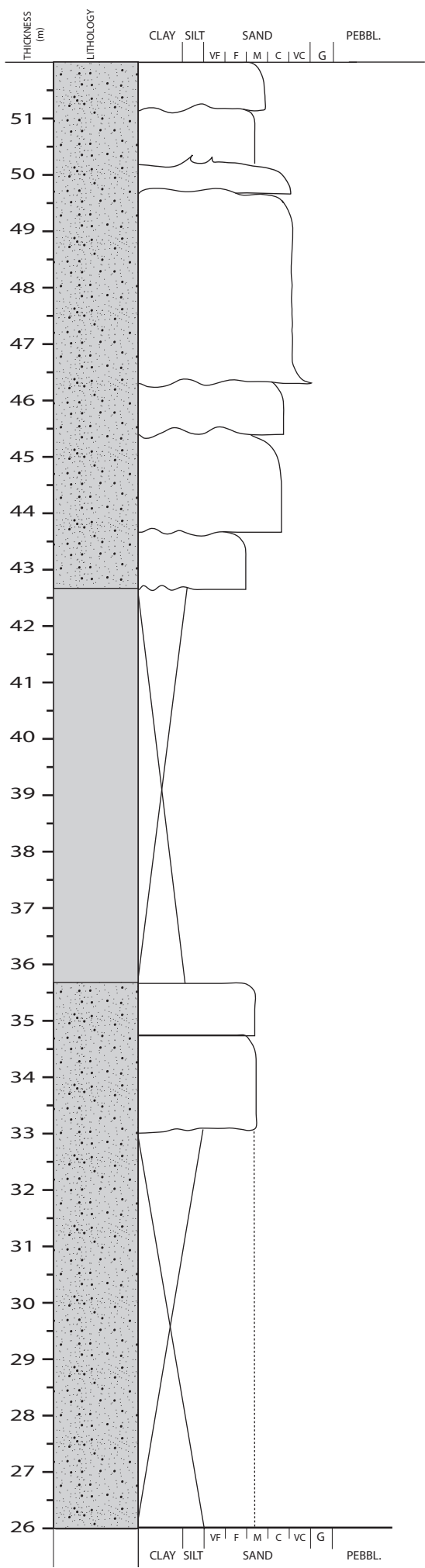
ÅSMARKVEGEN 2 1/3
 24.05.2005
 1:100
 32V 0580019
 UTM 6773632

FA 4.1

FA 4.1

FA 1.1

FA 4.1

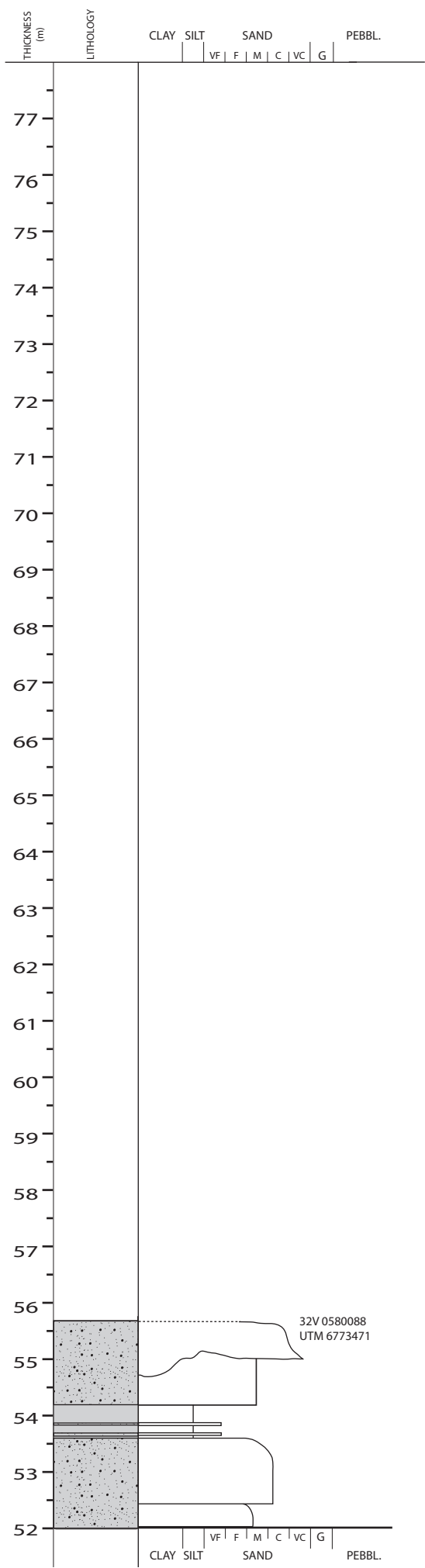


ÅSMARKVEGEN 2 2/3
 24.05.2005
 1:100

FA 4.1

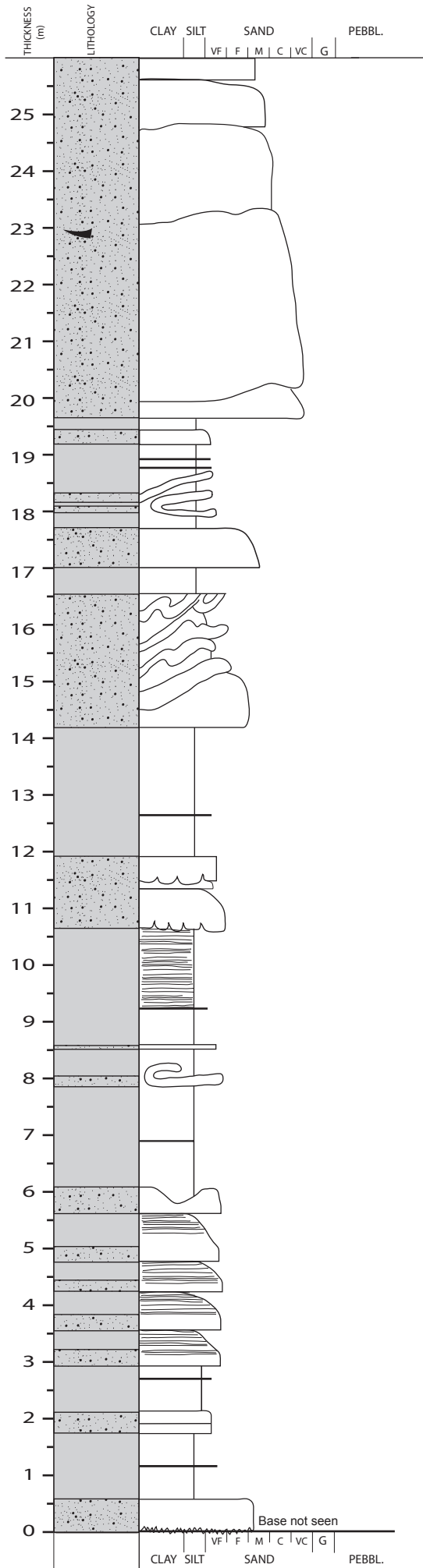
FA 4.1

FA 4.1



ÅSMARKVEGEN 2 3/3
24.05.2005
1:100

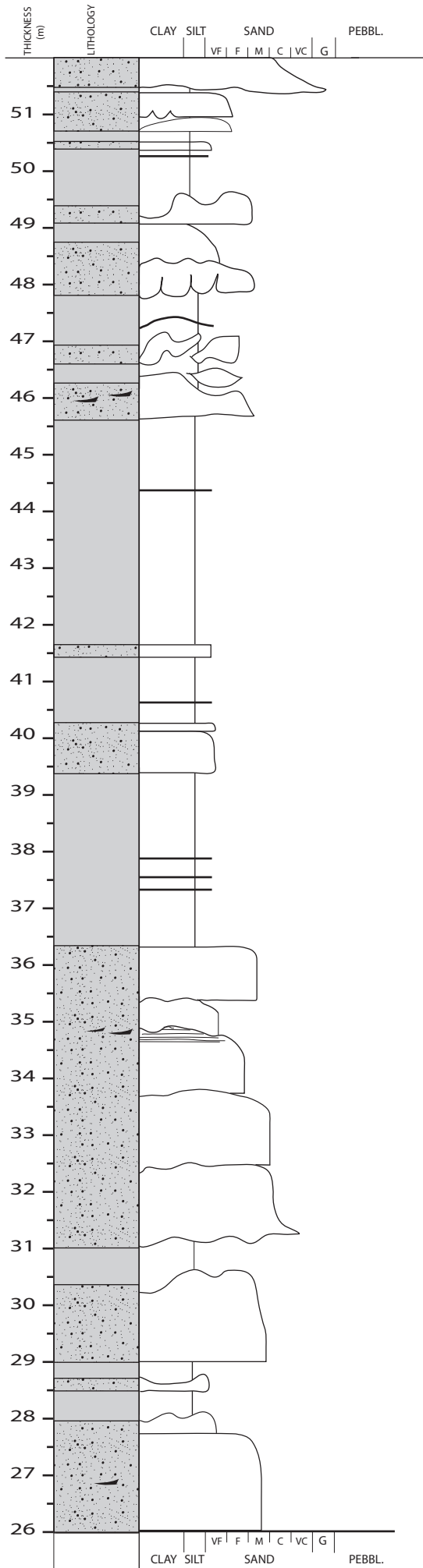
FA 4.1



ÅSMARKVEGEN 3 1/4
 24.05.2005
 1:100
 32V 0580138
 UTM 6773421

FA 4.1

FA 5.1

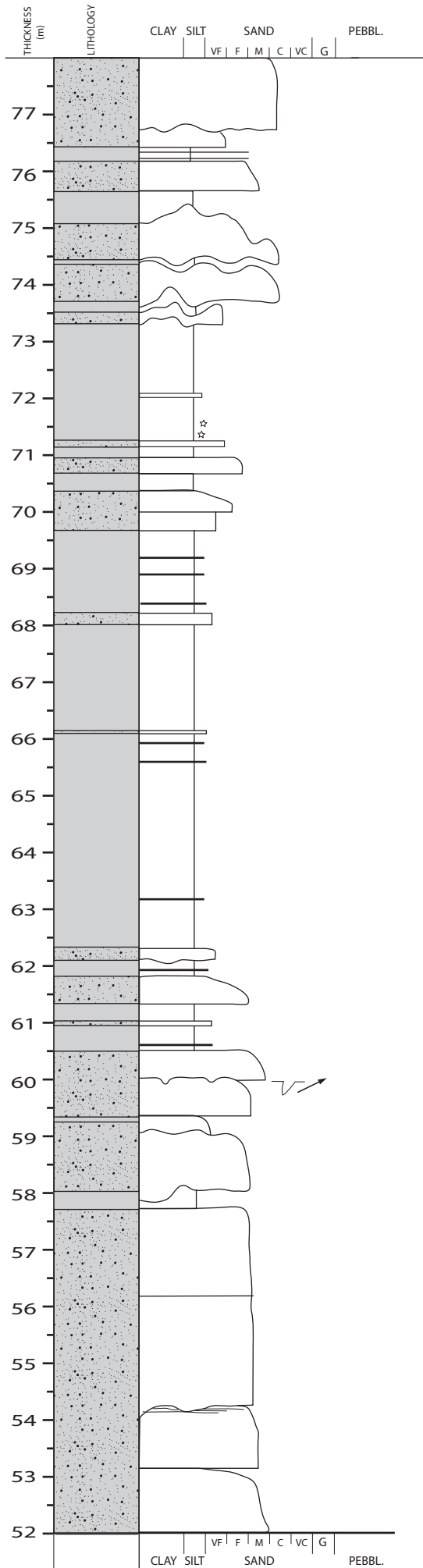


ÅSMARKVEGEN 3 2/4
 25.05.2005
 1:100

FA 5.1

FA 1.1

FA 4.1



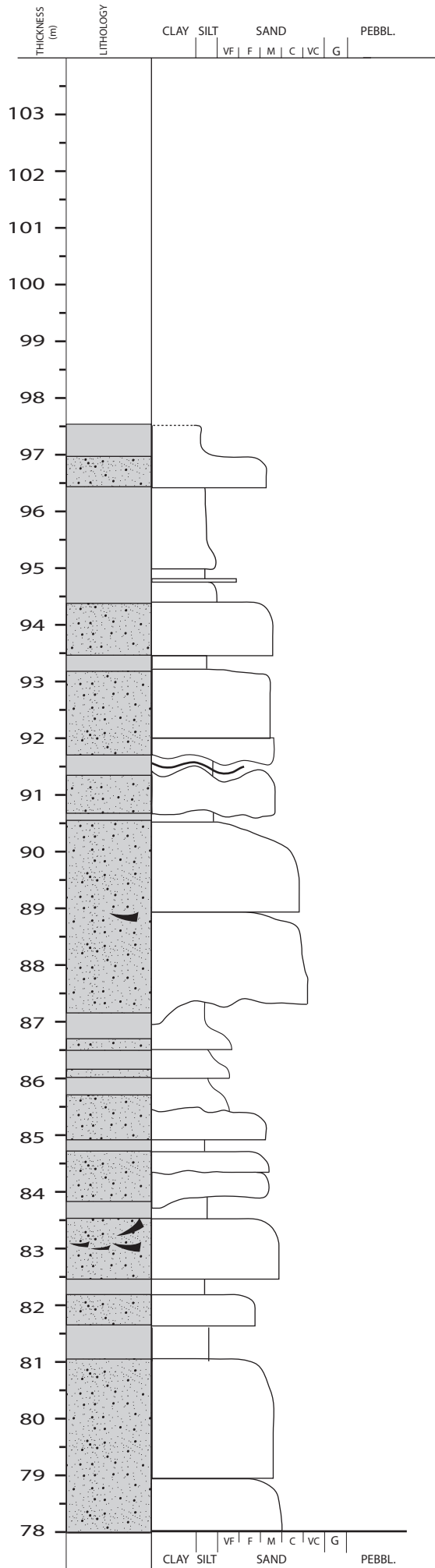
FA 4.1

ÅSMARKVEGEN 3 3/4
25.05.2005
1:100

FA 5.1

FA 1.1

FA 4.1



ÅSMARKVEGEN 3 4/4
 26.05.2005
 1:100

FA 4.1

FA 4.1

